8-2017

Models and Methodologies to Address Emerging Needs in Network and Supply Chain Optimization

Forough Enayaty Ahangar
University of Arkansas, Fayetteville

Models and Methodologies to Address Emerging Needs in Network and Supply Chain Optimization

A dissertation submitted in partial fulfillment
of the requirements for the degree of
Doctor of Philosophy in Engineering with concentration in Industrial Engineering

by

Forough Enayaty Ahangar
Amirkabir University of Technology
Bachelor of Science in Industrial Engineering, 2008
Amirkabir University of Technology
Master of Science in Economical and Social Systems Engineering, 2011

August 2017
University of Arkansas

This dissertation is approved for recommendation to the Graduate Council.

Dr. Chase Rainwater
Dissertation Director

Dr. Edward Pohl Committee Member	Dr. Kelly Sullivan Committee Member

Dr. Thomas Sharkey
Ex-officio Member

Abstract

In this dissertation, we model three different security scenarios and propose solution methodologies to address each problem. Chapter 2 presents a large-scale optimization approach for solving a dynamic bi-level network interdiction problem (NIP) in which interdiction activities must be scheduled in order to minimize the cumulative maximum flow over a finite time horizon. A logic-based decomposition (LBD) approach is proposed that utilizes constraint programming to exploit the scheduling nature of this dynamic NIP.

Chapter 3 considers a set of centers to which content (e.g., data or smuggled items), are assigned to ensure availability. An interdictor (e.g., border security officials) attempts to determine which centers (e.g., border's checkpoints) to interdict in order to minimize the content availability. We present our efforts to model the problem as an Integer Programming formulation and show that the problem is NP-hard. We propose modeling improvements, which, in conjunction with a genetic algorithm is used to obtain quality solutions to the problem quickly. A comparison of the approaches is presented along with future research direction for the problem.

Finally, Chapter 4 pursues a quantitative risk assessment of the complete poultry supply chain in China. This work is supported by collaborators in biological engineering, poultry science and numerous companies and universities throughout China. This effort considers contamination concerns from Salmonella for chicken broilers studied at the production steps in the supply chain as well as offering one of the first attempts to include the transportation, distribution, retail and consumption elements that complete the supply chain. Our quantitative risk assessment model makes use of preliminary data collected from a Chinese poultry company since Fall 2016.

Dedication

To Reza, Maman, and Baba.

Contents

1. **Introduction**

In this dissertation, we model three security scenarios and propose solution methodologies to address each problem. Chapter 2 is a network interdiction study focused on the allocation of resources in a manner that disrupts an illegal drug supply chain. Chapter 3 seeks to eliminate access to collections of content via interdictions. Chapter 4 diverges from traditional defense-based security to consider models related to food security. This effort focuses on the development of a risk assessment models used to quantify microbial poultry contamination across the food supply chain in China.

Chapter 2 details the creation of a large-scale optimization approach for solving an application of a dynamic bilevel network interdiction problem (NIP). In this class of multi-period NIP, interdiction activities must be scheduled in order to minimize the cumulative maximum flow over a finite time horizon. A logic-based decomposition (LBD) approach is proposed that utilizes constraint programming to exploit the scheduling nature of this dynamic NIP. Computational results comparing solutions obtained using the proposed approach versus traditional mixed-integer programming approach suggest that the LBD approach is more efficient in finding solutions for medium to large problem instances.

Chapter 3 details the creation of an optimization approach for solving an interdiction problem in which an attacker attempts to disrupt clusters of content distributed across a collection of resources. We refer to this as the Clustered Content Interdiction Problem (CCIP). CCIP considers groups of content dispersed across a collection of centers. In this problem, different content is assigned to the centers to ensure availability. Given a content assignment across a collection of available centers, an interdictor (attacker) attempts to determine which centers to interdict (attack) in order to maximize the service disruption or minimize the content availability. After the attacks, content will be available if it is assigned to at least one non-interdicted center. Also, content can be divided into multiple portions which means the content is assumed to be available if all the portions are assigned to at least one non-interdicted center. An integer program (IP) is formulated to model the problem, which is proven to be NP-complete. Then, a modified IP formulation is proposed to solve larger problems more efficiently. We add symmetry breaking and other valid inequality constraints, custom branchings and propose a genetic algorithm as a method to generate a quality solution efficiently. Computational results comparing the IP and the enhanced model are presented.

Chapter 4 details the creation of a Quantitative Risk Assessment Model (QRAM) of all phases of poultry supply chain in China. We consider contamination concerns from *Salmonella* for chickens studied at the breeder and production steps in the supply chain destined for human consumption. To our knowledge, all the other QRAMs (e.g., Oscar 1998 and Oscar 2004) regarding *Salmonella* in poultry, specifically chicken broiler, consider a pathway after retail or after it is purchased by a consumer, but in this research we consider all the unit operations of the production and the distribution. This work is supported by researchers in biological engineering, poultry science, and numerous companies and universities throughout China. The quantitative risk assessment offered in this chapter is informed by data collected from Chinese poultry producers since Fall 2016, published data, and predictive models for growth/reduction of *Salmonella*. The model makes use of @Risk that is used to simulate 1,000,000 iterations representing 1,000,000 chickens. Beyond the production, other components of the pathway to consumption (distribution, retail, transportation, handling, preparation and serving, and consumption) are considered to estimate the final *Salmonella* extent in each chicken. A dose-response (DSR) model is then applied to predict the number of *Salmonellosis* cases. Results shows that the number of *Salmonellosis* cases per 100,000 consumers is 1.70. This value is 4 times more than the value obtained in Oscar (2004). Although, 95.6% of the *Salmonellosis* cases are caused by consumers mishandling during the chicken preparation and serving, we demonstrate that by improving the production operations and the transportation and distribution parameters, the extent of contamination can be reduced which translates into a reduction of the final illness occurrence value.

Finally, Chapter 5 summarizes all of our efforts and findings of the three research topics and discusses future work for each chapter.

Bibliography

Oscar, T. (1998). The development of a risk assessment model for use in the poultry industry. *Journal of food safety*, 18(4):371–381.

Oscar, T. P. (2004). A quantitative risk assessment model for salmonella and whole chickens. *International journal of food microbiology*, 93(2):231–247.

2. **A Decomposition Approach for Dynamic Network Interdiction Models**

2.1 Introduction

Wood (1993) considers a Maximum Flow Network Interdiction Problem (MFNIP) formulated as a directed and capacitated *s*-*t* network in which each arc has a deletion cost. The objective of the MFNIP is to minimize the maximum flow between the source node (s) and the sink node (t) by deleting a subset of arcs. MFNIP is known to be NP-complete (Wood, 1993). Applications of this problem include disabling military supply lines, disrupting pipe systems (Phillips, 1993), combating drug trafficking (Wood, 1993), and controlling infections in a hospital (Assimakopoulos, 1987).

Malaviya et al. (2012) utilize a dynamic version of MFNIP to model the flow of illegal drugs within a network. The model is motivated by a homeland security problem in which enforcement officials are seeking to disrupt the flow of drugs in a trafficking network. The law enforcement officials' task is to monitor and arrest individuals. Officer resource allocation decisions are made in each period. Therefore, the structure of the network is modified at each period and the remaining criminals transport the maximum amount of drugs through the remaining network. The law enforcement officials objective is to minimize the total maximum flow over the horizon of the problem while not utilizing more than the available officers in each period for their activities. The problem is best described in two layers as follows:

Outer problem: The law enforcement officials monitor (target) and remove (interdict/arrest) the individuals in order to reduce the illegal drug trafficking flow.

Inner problem: The individuals (criminals) deliver the maximum drugs from the source to the users in each period.

A drug network defined by Malaviya et al. (2012) is assumed to have multiple levels organized in a hierarchical manner. Drugs enter the system through the source nodes and flow through the safehouses. Safehouses pass the drugs to the dealers who sell them to users. An example of a small drug network with 15 criminals is shown in Figure 2.1-a. The capacity of each criminal is given as the number next to its associated node. In Figure 2.1-b, the value on each arc represents the flow in a maximum flow solution. Flows on dashed arcs are equal to zero. For this example, the total flow is 900 in a single period.

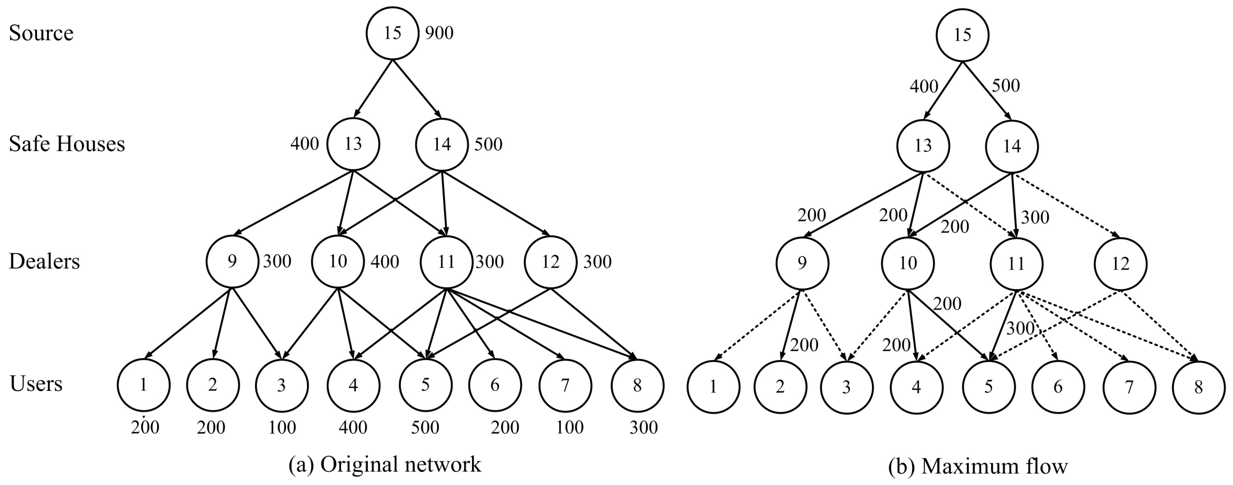

Figure 2.1: A drug network example and its maximum flow

Interdiction of an individual requires a number of law enforcement officials to target the individual over multiple time periods and then arrest them only after targeting is finished. Both targeting and arresting activities require resources. The law enforcement officials are tasked with deciding which criminals to monitor and arrest and when these activities should occur considering a limited budget (officers) in each period. In Figure 2.1-b, you can see that the maximum flow in period *t*, when some of the criminals (4, 5, 8, 11, and 12) had been interdicted in the previous periods is equal to 500.

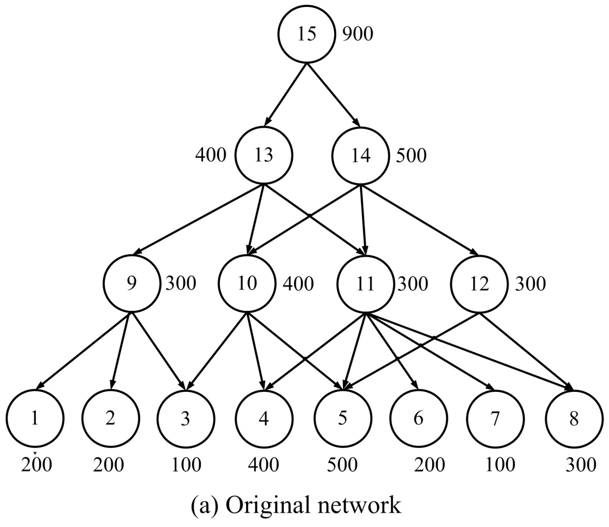

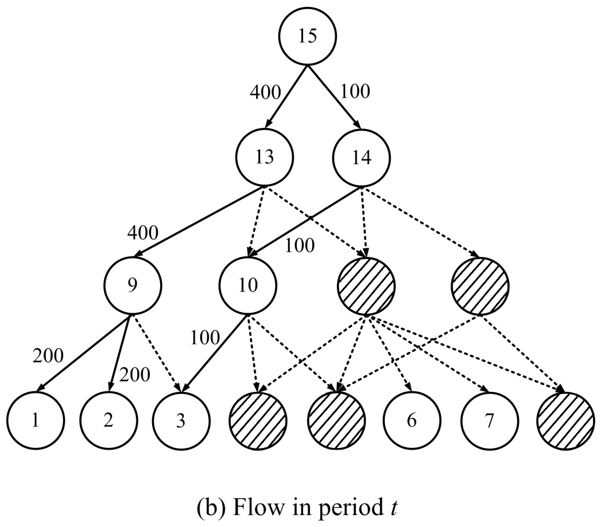

Figure 2.2: Maximum flow in period t

In Malaviya et al. (2012), it is assumed that the connections between the criminals are known, but it is not possible to invest the resources to delete an individual at an upper-level of the hierarchical structure without building a case against that individual; therefore, to remove the upper-level criminal it is necessary to have enough arrested lower-level criminals connected to him. This restriction is called "climbing the ladder" constraint by Malaviya et al. (2012).

The results of Malaviya et al. (2012) suggest that solving a mixed-integer programming formulation using a commercial solver is only viable for small problem size. Like many problems for which time-dependent decisions are made, the number of binary variables required by the model is significant. The largest problems considered in Malaviya et al. (2012) have only 60 users, which are considered medium-sized problems in real application. This was sufficient to provide an analysis for a city with a population of about 50,000 people. However, the problems with 60 users were not often solved to optimality within 10 hours. To expand the problem base for which the dynamic MFNIP can be used to solve more realistic instances, we propose an alternative exact decomposition method which is shown to be effective in solving medium and larger instances. While motivated by the problem proposed in Malaviya et al. (2012), the proposed approach is applicable to any application which is best modeled in a network interdiction framework over a time-expanded planning horizon.

2.1.1 Constraint Programming (CP)

The targeting and interdiction activities in a dynamic MFNIP lend themselves to constraint programming (CP) since CP has been shown to be efficient for solving general scheduling problems (e.g. parallel machine scheduling (Gedik et al., 2016), sports scheduling (Trick and Yildiz, 2011), time-tabling (Topaloglu and Ozkarahan, 2011). Constraint programming is a technique that originated in the computer science community and was inspired by Constraint Satisfaction Problems (CSP) in the 1970s. A CSP is a feasibility problem in which there is no objective function (OF). A solution to the CSP is defined to be a set of variables that are within specified domains while not violating constraints (Lustig and Puget, 2001). However, there are some methods by which CP can be applied to combinatorial optimization problems. According to Focacci et al. (2002), after a feasible solution is found in a CSP, a *bounding constraint* can be applied to the new feasibility problem indicating the next feasible solution should have a better objective function value (OFV). The addition of subsequent constraints allows CSP to as act as an optimization procedure. However, in the decomposition approach proposed in this work, CP is only used in solving a feasibility problem.

There are differences between CP and mathematical programming approaches such as mixed integer programming (MIP). Variables in MIP are defined as real, integer or binary while CP allows Boolean (True/False), symbolic (e.g. green) or intervals representing an activity with a specific length (Heipcke, 1999). The interval variable type is particularly useful in modeling scheduling problems within a constraint programming framework as done by Hooker (2007) in his logic-based Benders decomposition algorithm.

In MIP, constraints are restricted to be linear equality and inequality constraints. However, some nonlinear constraints such as certain logical operations ($\vee, \Rightarrow$) can be transformed to multiple linear constraints with the consideration of additional 0-1 variables. On the other hand, CP allows for a larger variety of constraints including arithmetic ($=$, $<$, $\neq$, etc) and *global* (symbolic) constraints. In the latter, all algebraic constructions are allowed (Heipcke, 1999). *allDifferent* and *cumulative* constraints are two examples of global constraints. An allDifferent constraint makes certain a set of variables take different values (Focacci et al. 2002 and Harjunkoski and Grossmann 2002). The cumulative constraint will be explained in Section 2.3.2. In general, CP offers a very flexible modeling framework (Jain and Grossmann, 2001).

2.1.2 Benders Decomposition (BD) Approach

The MIP formulations of scheduling problems often require a significant number of binary variables in order to model the sequencing decisions, which pose challenges for the application of classic Benders decomposition. It is applied for a toll control application of NIP in Borndörfer et al. (2016). Rad and Kakhki (2013) also utilize a BD to solve a dynamic MFNIP in which an intruder tries to interrupt the flow of a single commodity through the network by using limited budget within a given time limit. In contrast with our problem, Rad and Kakhki (2013) consider only a single determination of interdictions. They apply a BD along with a heuristic algorithm to generate an initial solution with promising results.

However, there are hybrid models in the literature that take advantage of both MIP and CP. This work offers promising results compared to pure CP or pure IP methods (Gedik et al. 2016, Edis and Ozkarahan 2011, and Jain and Grossmann 2001). Therefore, we pursue a logic-based decomposition approach which is inspired by Benders decomposition approach and designed to exploit CP's more efficient time-based variable representation for the scheduling aspects of the problem and the MIP formulations for the NIP considerations.

Hooker (2007) states that the classical Benders decomposition is not suitable for scheduling problems since it requires the subproblem (SP) to be a continuous linear or nonlinear programming problem while most scheduling problems do not take this form. However, a *logic-based* form of decomposition algorithm has recently been applied to such problems for which subproblems are discrete feasibility problems that add feasibility cuts in order to eliminate infeasible solutions obtained in the master problems (Gedik et al., 2016). In our problem, the SP contains some portion of the binary variables and the constraints which does not make the classic BD a reasonable approach since the dual of the SP cannot be taken for BD's feasibility and optimality cuts. However, based on the structure of the problem, our SP can be formulated in a CP language which will be described in Section 2.3.2 and this allows us to add feasibility cuts that will cut any infeasible solution from the MP.

In a *simple* LBD approach, as shown in Figure 2.3, the algorithm starts by solving a master problem (MP) containing a subset of the problem's constraints and variables. If there is no solution to the MP, it means the original problem is infeasible and the solution procedure terminates. If there exists an optimal solution (OS) to the MP, it will be passed to the SP to be evaluated for feasibility according to remainder of constraints not considered in MP. If there is a feasible solution for the SP, that means the MP's OS is the OS for the original problem. If there is no feasible solution for the SP, a new constraint will be added to the MP to eliminate that solution from the feasible region for the next iteration. Note that this constraint is similar to the feasibly cuts of the BD approach but it is logically obtained and not taken from solving the dual of the SP. This iterative process continues until an OS of the MP is feasible to the subproblem, which means it is the original problem's OS.

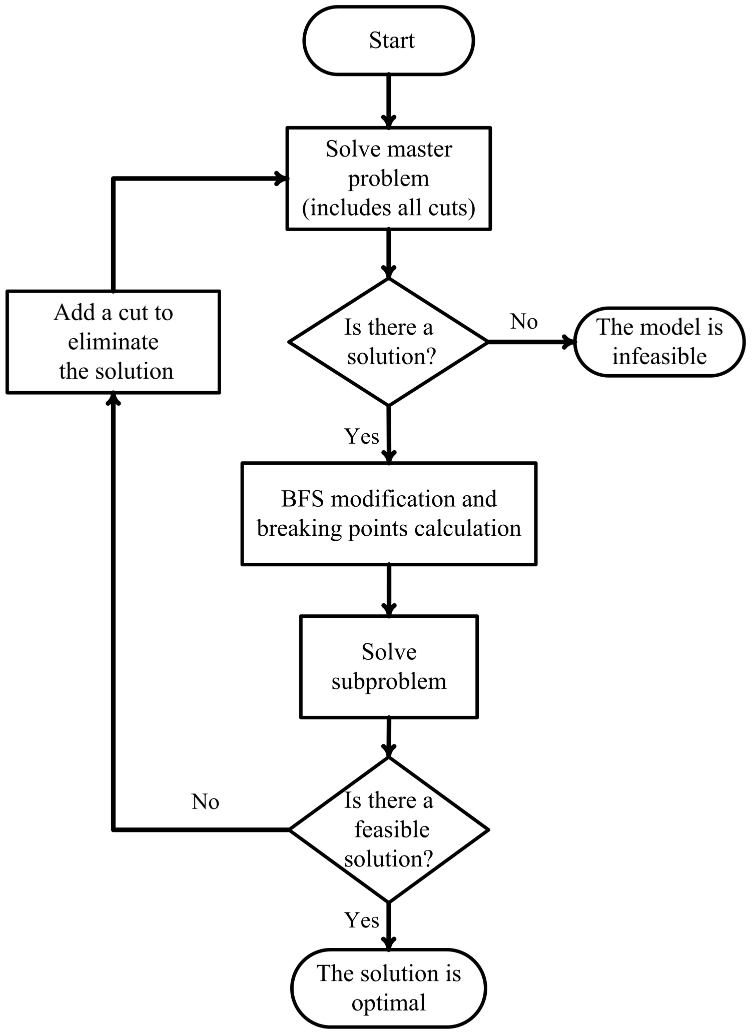
Start
Solve master problem (includes all cuts)
Is there a solution?
No
The model is infeasible
Yes
Add a cut to eliminate the solution
BFS modification and breaking points calculation
Solve subproblem
Is there a feasible solution?
No
Yes
The solution is optimal

Figure 2.3: A simple logic-based decomposition approach

In the remainder of the chapter, we formally define the problem in Section 2.2. Our CP -based decomposition solution approach is described in Section 2.3. Computational results are presented in Section 2.4 and conclusions in Section 2.5.

2.2 Problem Definition

The problem used in this work, the dynamic MFNIP, consists of a directed network, $G = (N, A)$. Without loss of generality, Malaviya et al. (2012) assume the network has one super source, $\alpha \in N$, one super sink, $\omega \in N$, and an arc, $(\omega, \alpha) \in A$, connecting them with a large capacity. There is an upper bound on the amount of flow along each arc. Each actor i is represented by two nodes connected by one arc with a capacity equal to the capacity of the actor (bold arcs in Figure 4). Arcs connecting different criminals are uncapacitated. Since monitoring an actor in our model is assumed to happen in $\tau_{ii'}$ consecutive periods, we define an additional set of binary variables h_{ijt} compared to the model in Malaviya et al. (2012). Note that N, A, and the remaining parameters for MFNIP are defined in Table 1.

Figure 2.4 represents an example of how a network is represented in Malaviya et al. (2012). Assume there is a 2-level network as shown in the left side of Figure 2.4 with only 2 actors in level 1 and 1 actor in level 2. An equivalent network is shown on the right hand side, with only one node representing the super source, one node for the super sink and two nodes for each of the remaining actors.

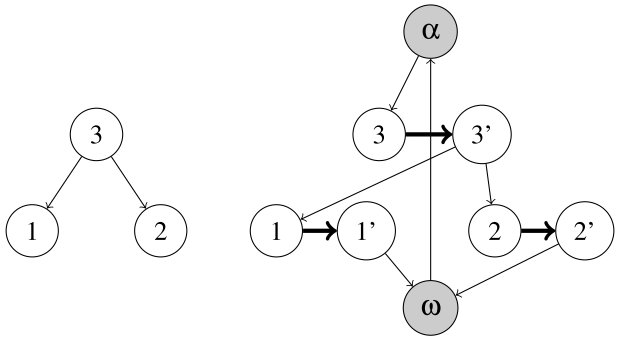

Figure 2.4: Network structure example

Table 2.1: Notation definitions of the dynamic MFNIP adapted from Malaviya et al. (2012)

Sets

N	set of nodes, $i \in N$
A	set of arcs, $(i,j) \in A$
$A(i)$	set of node adjacency list of node i

Parameters

T	time horizon
B	number of available officers (resources) in each period
τ_{ij}	number of periods that arc (i,j) must be monitored before it can be interdicted
a_{ij}	number of resources required to remove arc (i,j)
b_{ij}	number of resources required to monitor arc (i,j)
u_{ij}	flow capacity of arc (i,j)
$\mu_{ii'}$	number of criminals connected to i that must be arrested prior to monitoring actor i

Variables

y_{ijt}	1 if arc (i,j) is monitored in period t, 0 otherwise
w_{ijt}	1 if arc (i,j) is removed in period t, 0 otherwise
z_{ijt}	1 if arc (i,j) is available in period t, 0 otherwise
h_{ijt}	1 if arc (i,j) is monitored for τ_{ij} consecutive periods prior to period t, 0 otherwise
x_{ijt}	amount of flow on the arc (i,j) in period t

2.2.1 Dynamic MFNIP (P)

The inner problem proposed by Malaviya et al. (2012) for period t is as follows:

$$max\ x_{\omega\alpha t} \tag{2.1}$$

Subject to

$$\sum_{j \in A(i)} x_{ijt} - \sum_{j:i \in A(j)} x_{jit} = 0 \qquad \text{for } i \in N \tag{2.2}$$

$$0 \leq x_{ijt} \leq u_{ij} z_{ijt} \qquad \text{for } (i,j) \in A \tag{2.3}$$

As shown in (2.1), the objective function of the inner problem is to maximize the flow between the super sink, ω, and the super source, α, in period t. Constraints (2.2) are flow balance constraints and (2.3) applies lower and upper bounds on the amount of flow through an actor. Note that arcs connecting two actors are uncapacitated and only those arcs representing actors have finite capacities. Since the network is known to the actors who make decisions in the inner problem, z_{ijt}s are considered to be known and act as parameters. However, when looking at the whole problem, they should act as variables. In the following formulation we present the complete problem which includes the inner problem inside the outer problem.

Let $X(z_{.t})$ denote constraints (2.2-2.3) where $z_{.t}$ is the actors' availabilities in period t. Then, the variant of the model proposed by Malaviya et al. (2012) that is solved in this work is as follows:

$$(P) \quad min \sum_{t=1}^{T} \max_{x_{.t} \in X(z_{.t})} x_{\omega\alpha t} \tag{2.4}$$

Subject to

$$\sum_{(i,j)\in A} (a_{ij} w_{ijt} + b_{ij} y_{ijt}) \leq B \qquad \text{for } t = 1,...,T \tag{2.5}$$

$$\sum_{t'=max\{1,t-\tau_{ij}+1\}}^{t} y_{ijt'} - \tau_{ij} h_{ijt} \geq 0 \qquad \text{for } (i,j) \in A,\ t = 1,...,T-1 \tag{2.6}$$

$$\sum_{t'=1}^{t-1} h_{ijt'} - w_{ijt} \geq 0 \qquad \text{for } (i,j) \in A,\ t = 1,...,T \tag{2.7}$$

$$(1 - z_{ijt}) \leq (1 - z_{ij,t-1}) + w_{ijt} \qquad \text{for } (i,j) \in A,\ t = 1,...,T \tag{2.8}$$

$$\sum_{j:j\in A(i')} (1 - z_{jj't}) \geq \mu_{ii'} y_{ii't} \qquad \text{for } i \in N,\ t = 1,...,T \tag{2.9}$$

$$z_{ijt}, y_{ijt}, w_{ijt}, h_{ijt} \in \{0,1\} \qquad \text{for } (i,j) \in A,\ t = 1,...,T \tag{2.10}$$

Where, $x_{.t}$ is the amount of flow that passes through actors in period t. As shown in (2.4), the objective function of the problem (P) is to minimize the cumulative maximum flow over T periods. Constraints (2.5), resource allocation constraints, ensures the total usage for monitoring and removing the actors in each period does not exceed the total number of available interdiction resources. Note that if all the monitoring variables in (2.6) between period $\max\{1, t - \tau_{ij} + 1\}$ and t are equal to one, then h_{ijt} may be 1 and (2.7) ensures that the arc representing the actor can be interdicted in period t. Based on constraints (2.8), if an arc (i,j) is not available in period t ($z_{ijt} = 0$), then either it is removed in period t ($w_{ijt} = 1$) or it was unavailable in the previous period ($z_{ij,t-1} = 0$). Constraints (2.9) are the so-called climbing the ladder constraint by Malaviya et al. (2012). These restrict the time in which monitoring an actor begins to be after the period in which $\mu_{ii'}$ connected lower level actors are interdicted.

As you can see, the problem (P) is a min-max problem which is difficult to solve directly. However, Malaviya et al. (2012) shows that in the inner problem x_{ijt} variables can be relaxed so that by taking the dual of the inner problem, we are left with a minimization problem. The required dual variables of the inner problem are shown in Table 2.2.

Table 2.2: Dual variables

π_{it}	dual variable associated with node i in period t, (constraint (2.2))
θ_{ijt}	dual variable associated with arc (i,j) in period t, (constraints (2.3))
ν_{ijt}	variable representing the linearization of $z_{ijt} * \theta_{ijt}$

By considering z_{ijt}s as decision variables in the problem (P), the dual of the inner problem for fixed z_{ijt}s is non-linear. In Malaviya et al. (2012), the authors show that there exists a binary optimal solution to the dual of the inner problem. A standard linearization technique is then applied to the problem. They introduce a variable v_{ijt} that represents the product of two variables θ_{ijt} and z_{ijt} and add the following constraint to the dual problem:

$$\theta_{ijt} + z_{ijt} - \nu_{ijt} \leq 1 \qquad \text{for } (i,j) \in A,\ t = 1,...,T \qquad (2.11)$$

Then model P can be written equivalently as follows:

$$min \sum_{t=1}^{T} \sum_{(i,j) \in A} u_{ij} \nu_{ijt} \tag{2.12}$$

Subject to

$$\pi_{it} - \pi_{jt} + \theta_{ijt} \geq 0 \qquad \text{for } (i,j) \in A \setminus (\omega, \alpha),\ t = 1, ..., T \tag{2.13}$$

$$\pi_{\omega t} - \pi_{\alpha t} + \theta_{(\omega,\alpha),t} \geq 1 \qquad \text{for } t = 1, ..., T \tag{2.14}$$

$$\theta_{ijt} + z_{ijt} - \nu_{ijt} \leq 1 \qquad \text{for } (i,j) \in A,\ t = 1, ..., T \tag{2.15}$$

$$\sum_{(i,j) \in A} (a_{ij} w_{ijt} + b_{ij} y_{ijt}) \leq B \qquad \text{for } t = 1, ..., T \tag{2.16}$$

$$\sum_{t'=max\{1, t-\tau_{ij}+1\}}^{t} y_{ijt'} - \tau_{ij} h_{ijt} \geq 0 \qquad \text{for } (i,j) \in A,\ t = 1, ..., T-1 \tag{2.17}$$

$$\sum_{t'=1}^{t-1} h_{ijt'} - w_{ijt} \geq 0 \qquad \text{for } (i,j) \in A,\ t = 1, ..., T \tag{2.18}$$

$$(1 - z_{ijt}) \leq (1 - z_{ij,t-1}) + w_{ijt} \qquad \text{for } (i,j) \in A,\ t = 1, ..., T \tag{2.19}$$

$$\sum_{j: j \in A(i')} (1 - z_{jj't}) \geq \mu_{ii'} y_{ii't} \qquad \text{for } i \in N,\ t = 1, ..., T \tag{2.20}$$

$$z_{ijt}, y_{ijt}, w_{ijt}, h_{ijt} \in \{0, 1\} \qquad \text{for } (i,j) \in A,\ t = 1, ..., T \tag{2.21}$$

$$\theta_{ijt},\ \nu_{ijt} \geq 0 \qquad \text{for } (i,j) \in A,\ t = 1, ..., T \tag{2.22}$$

(2.12) is the new OF while constraints (2.13-2.14) are associated with the dual of the inner problem (the maximum flow problem). Constraints (2.15) are responsible for the standard linearization technique. Constraints (2.16-2.20) are the repetition of the scheduling constraints (2.5-2.9) that will be exploited in our decomposition approach using CP. The variables' type constraints are stated in constraints (2.21-2.22).

2.3 Logic-based Decomposition (LBD) Approach

In this section, a decomposition approach that utilizes both MIP and CP is presented. Based on the hierarchical structure of the model, the problem is divided into two parts: (i) constraints (2.13-2.15) with the OF and (ii) constraints (2.16-2.20) from which the interdiction decisions are determined. The first set of constraints is a series of unrestricted maximum flow interdiction problems that do not consider any restrictions on the interdiction activities, while the second includes the set of scheduling constraints impacting the interdiction activities. If solved separately, the first can be solved as a MIP and the second with a CP formulation. In our proposed LBD approach we refer to the first problem as a MP (see Section 2.3.1 and the second problem, which only considers feasibility, as a SP (see Section 2.3.2).

As mentioned in Section 2.1, in a *simple* LBD approach, the iterative MPs are solved. Then the SP runs to validate the feasibility of the MP's OS. The first time the SP reaches to a feasible solution, that solution is the OS to the original problem. However, in our proposed LBD approach, as shown in Figure 2.5, each time CPLEX gets an incumbent/feasible solution in the MP, it calls upon the SP (implemented through a Lazy Constraint Callback). The SP can result in either of two outcomes: (i) the MP's incumbent solution is infeasible, therefore, a new cut is generated to eliminate that solution, which is added to the MP without restarting the search or (ii) the MP's incumbent solution is feasible, so the MP continues the search. Note that if a MP solution is deemed feasible by the SP, then it is a feasible solution to the original problem (not necessarily the optimal solution). This gives a valid upper bound on the original problem. CPLEX continues searching the tree (along the way calling upon SP to validate potential incumbent solutions that are identified). This process continues until the best feasible solution to the original problem is within an optimality tolerance of the best lower bound found in the search tree.

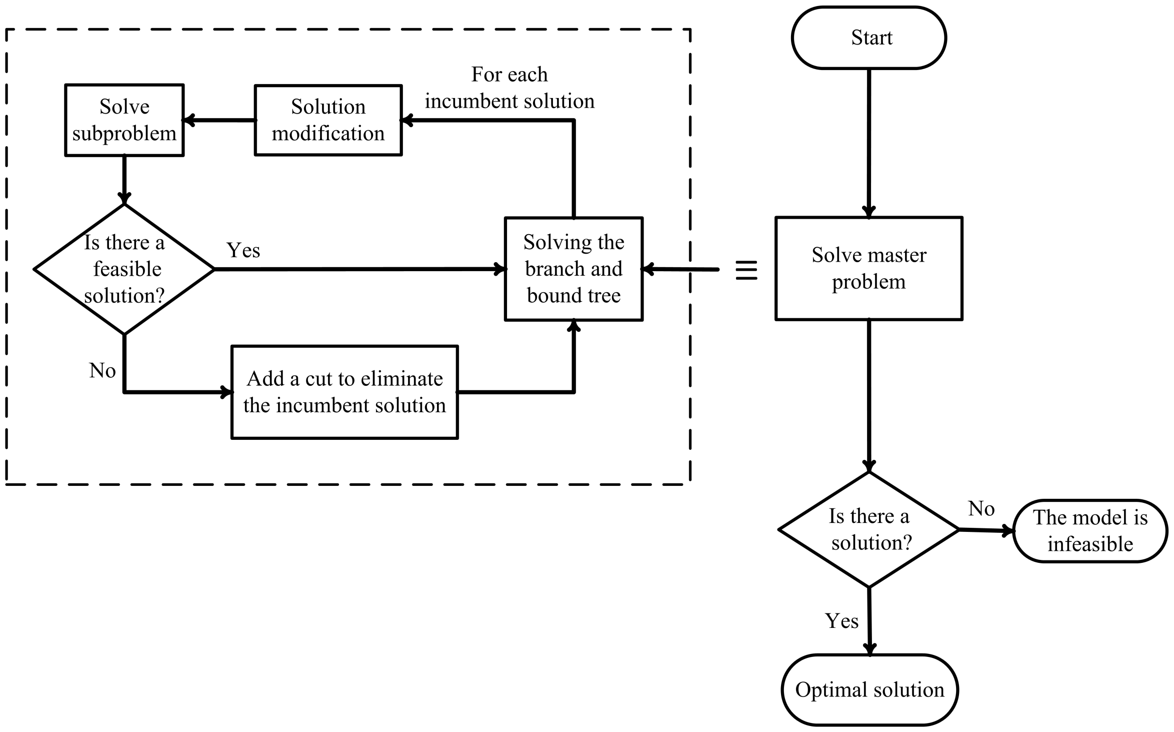

For each incumbent solution
Solve subproblem
Solution modification
Is there a feasible solution?
Yes
Solving the branch and bound tree
No
Add a cut to eliminate the incumbent solution
≡
Start
Solve master problem
Is there a solution?
No
The model is infeasible
Yes
Optimal solution

Figure 2.5: Overview of algorithm framework to solve *P*

2.3.1 Master Problem (MP)

In the following master problem, the objective function in (2.23) is the same as (2.12). Constraints (2.24-2.26) are the same as MIP's constraints (2.13-2.15). Constraints (2.27) is added to the MP to ensure an interdicted actor is not available after the period in which it is removed. We also have the variables type constraints in (2.28-2.29).

$$min \sum_{t=1}^{T} \sum_{(i,j)\in A} u_{ij}\nu_{ijt} \tag{2.23}$$

Subject to

$$\pi_{it} - \pi_{jt} + \theta_{ijt} \geq 0 \qquad \text{for } (i,j) \in A \setminus (\omega,\alpha),\ t = 1,...,T \tag{2.24}$$

$$\pi_{\omega t} - \pi_{\alpha t} + \theta_{(\omega,\alpha),t} \geq 1 \qquad \text{for } t = 1,...,T \tag{2.25}$$

$$\theta_{ijt} + z_{ijt} - \nu_{ijt} \leq 1 \qquad \text{for } (i,j) \in A,\ t = 1,...,T \tag{2.26}$$

$$z_{ijt} \leq z_{ij,t-1} \qquad \text{for } (i,j) \in A,\ t = 1,...,T \tag{2.27}$$

$$z_{ijt} \in \{0,1\} \qquad \text{for } (i,j) \in A,\ t = 1,...,T \tag{2.28}$$

$$\theta_{ijt},\ \nu_{ijt} \geq 0 \qquad \text{for } (i,j) \in A,\ t = 1,...,T \tag{2.29}$$

When solving the MP, incumbent solution data gets passed to a Callback Function (CBF) for feasibility validation. This happens by a set of parameters, each representing a breaking point, BP_i, that is defined to be the first period that arc (i,i') is no longer in the network (i.e., the minimum t such that $z_{ii't} = 0$). Note that if an actor is not removed at all from the network, its BP will be equal to $T+1$, which means it is always available in the planning horizon (see the first phase of Algorithm 1). BPs are only defined for arc (i,i')s since those arcs are capacitated and represent actors.

After calculating the breaking points, the flow for each period is calculated from period 1 to T to determine the first period that it is equal to zero. This calculation utilizes u_{ij} and ν_{ijt} values provided in the candidate solution generated in the MP (see the second phase of Algorithm 1). In the last phase of Algorithm 1, which we refer to as *BP modification*, if there is a period before period T with flow equal to 0, then all the breaking points that are greater than that period will be equal to $T+1$. This is equivalent to forcing the associated actors to be available during the planning horizon. The motivation behind the modification is that if flow is already zero, there is no need to use more resources to interdict more actors. This procedure is intended to prevent other similar solutions with the same OFV from being generated.

```
input  : incumbent solution's $z_{ijt}$ values
output: set of $BP_i$ for the SP
                                                    ▷ First phase: BPs' calculations
for $i \leftarrow 1$ to $|N|$ do
    Set $BP_i = T+1$;
    for $t \leftarrow 1$ to $T$ do
        if $z_{ii't} = 0$ then
            $BP_i = t$;
            break;
        end
    end
end
                                      ▷ Second phase: firstzeroflow period calculation
Set $firstzeroflow = T+1$
for $t \leftarrow 1$ to $T$ do
    Set $flow = 0$;
    for $arc\ (i,j) \in A$ do
        $flow \leftarrow flow + u_{ij} * \nu_{ijt}$ ;
    end
    if $flow = 0$ then
        $firstzeroflow$ = t;
        break;
    end
end
                                                    ▷ Third phase: BP modifications
if $firstzeroflow < T$ then
    for $i \leftarrow 1$ to $|N|$ do
        if $BP_i > firstzeroflow$ then
            $BP_i \leftarrow T+1$;
        end
    end
end
```

Algorithm 1: Breaking points calculation and modification

2.3.2 Subproblem (SP)

The dynamic MFNIP considers two primary activities: actor monitoring and removal. Both of these decisions can be modeled using so-called interval in a CP implementation. According to IBM Corporation, “an interval decision variable represents an unknown of a scheduling problem, in particular an interval of time during which something happens (an activity is carried out) whose position in time is unknown". Modeling monitoring and removal decisions using $2|N|$ interval variables instead of the $2T|A|$ binary variables of w_{ijt} and y_{ijt} allows us to represent our feasibility SP within a CP framework.

An interval variable can be *optional* which means it can be *absent* or *present* in a solution. Being present means the activity does happen in the problem horizon and it has both start and end times. Being absent means the activity does not happen in the planning horizon and both of the values are equal to 0 (IBM Corporation). Since both cases are possible in our problem, all interval variables are defined as optional. For each interval decision, a *requirement* number and a *length* number should be declared, which are equal to $a_{ii'}$ and $\tau_{ii'}$ for monitoring an actor i and $b_{ii'}$ and 1 for removing that actor.

Table 2.3: SP variables

Variables	
ycp_i	optional interval variable associated with monitoring actor i (requirement = $b_{ii'}$, duration = $\tau_{ii'}$)
wcp_i	optional interval variable associated with removing actor i (requirement = $a_{ii'}$, duration = 1)

The constraint programming formulation for the SP which is just a feasibility problem is as follows:

Solution satisfying:

$$ycp_i.StartMin = 1,\ ycp_i.EndMax = T+1 \qquad \text{for } i = 1,...,|N| \qquad (2.30)$$

$$wcp_i.StartMin = 1,\ wcp_i.EndMax = T+1 \qquad \text{for } i = 1,...,|N| \qquad (2.31)$$

$$\text{IfThen }((BP_i \leq T), \text{EndOf}(wcp_i) = BP_i + 1) \qquad \text{for } i = 1,...,|N| \qquad (2.32)$$

$$\text{IfThen }((BP_i = T+1), \text{EndOf}(wcp_i) = 0) \qquad \text{for } i = 1,...,|N| \qquad (2.33)$$

$$\text{IfThen }((BP_i = T+1), \text{EndOf}(ycp_i) = 0) \qquad \text{for } i = 1,...,|N| \qquad (2.34)$$

$$\text{cumulative }((ycp_i, \tau_{ii'}, b_{ii'}), (wcp_i, 1, a_{ii'}); B) \qquad (2.35)$$

$$\text{IfThen (isPresent}(wcp_i), \text{isPresent}(ycp_i)) \qquad \text{for } i = 1,...,|N| \qquad (2.36)$$

$$\text{IfThen (isPresent}(wcp_i), \text{EndOf}(ycp_i) \leq \text{StartOf}(wcp_i)) \qquad \text{for } i = 1,...,|N| \qquad (2.37)$$

$$\text{IfThen (isPresent}(ycp_i), \text{StartOf}(ycp_i) \geq Tmin_i) \qquad \text{for } i = 1,...,|N| \qquad (2.38)$$

As shown in the model above, SP is a feasibility problem. Constraints (2.30-2.31) set the minimum start time and maximum end time of all interval variables to be equal to 1 and $T+1$, respectively. Constraints (2.32-2.34) contain information from the incumbent solution taken from the MP and connect the modified BP_is to the interval variables. If a criminal is arrested at some period ($BP_i \leq T$), constraint (2.32) ensures that the end of its arresting interval variable happens exactly one period after its BP_i. This means the removal activity happens in the period BP_i. If a BP_i is equal to $T+1$, the end of the interval variable wcp_i is equal to 0 (i.e., it is absent). This relationship is modeled in constraint (2.33). If an actor is not removed, there is no need for it to be monitored since it will have no impact on the objective function value. Therefore, the monitoring interval variable may be absent. This situation occurs in constraint (2.34).

To represent constraints (2.19) in the SP, we use a so-called cumulative function that accounts for the total resource usage of multiple activities. Activities may make use a resource in different ways. There are some activities that exhaust a resource at their start time, without releasing any of the resource until completion of a task. There are other activities that increase the cumulative usage functions for a source at their start time and decrease it at their end time

(IBM Corporation). For the latter, a $pulsefunction$ should be used in the cumulative function. The monitoring and removing activities in our problem act the same, which means they consume resources at their start time and release all of them at the end. Constraints (2.35) ensure that at each period the total resource usage of all monitoring and removal activities do not exceed B.

Constraints (2.36-2.37) enforce that the presence of a monitoring interval variable is dependent on the presence of the removal interval variable and there should be no overlap between the intervals. All of this can be reformulated by a *precedence constraint* in CP Optimizer. We include an *IfThen* type constraint to ensure the start time of each removal variable is at least equal to the end of monitoring variable, if the removal interval variable is present.

In order to transform the climbing the ladder constraint (2.20), an integer parameter, $Tmin_i$, is defined for each actor i. Actor i's $Tmin_i$ is the minimum period at which monitoring can be started and it is calculated based on the number of removed lower level actors connected to it. Because all the availabilities and connections are known in the subproblem, $Tmin_i$ can be calculated and used in the precedence constraint (2.38). This ensures that each present monitoring interval occurs after the associated $Tmin_i$. The procedure of calculating $Tmin_i$ is presented in Algorithm 2. At each period, for each actor i with a positive $\mu_{ii'}$, the number of removed lower level actors is counted. If there are enough removed actors, then $Tmin_i$ is less than or equal to the period, else it will be greater than the period. At the end, $Tmin_i$ will be equal to the first period in which there are enough removed lower level actors.

```
input  : $BP_i$ values
output: $Tmin_i$ values
for $t \leftarrow 1$ to $T$ do
    for $i \leftarrow 1$ to $|N|$ do
        if $\mu_{ii'} > 0$ then
            $counter = 0$
            for $j \in A(i')$ do
                if $t \geq BP_j$ then
                    $counter \leftarrow counter + 1$ ;
                end
            end
            if $counter < \mu_{ii'}$ then
                $Tmin_i > t$
            end
            if $counter \geq \mu_{ii'}$ then
                $Tmin_i \leq t$
            end
        end
        else
            $Tmin_i = 1$
        end
    end
end
```

Algorithm 2: $Tmin$ calculations

2.3.3 Subproblem Feasibility Cuts

After running SP for an incumbent solution in the CBF, if the incumbent solution is not feasible to the SP, a new constraint must be added to the MP to eliminate the infeasible solution from MP. In order to eliminate the current solution, at least one actor needs to be removed one period after or one period before (if removed at least at period 2) than the period in which it is currently being removed. Note that the second part is necessary since for some instances there are actors who can wait to be removed later in the planning horizon without affecting the OFV. Therefore, the cut generated is as follows:

$$\sum_{i \in S} z_{ii',BP_i} + \sum_{i \in S'} (1 - z_{ii',BP_i - 1}) \geq 1 \tag{2.39}$$

Here, $S = \{i = 1,...,|N| \,|\, BP_i \leq T\}$ and $S' = \{i = 1,...,|N| \,|\, 2 \leq BP_i \leq T\}$. In the first summation we have the actor availability variables, $z_{ii't}$, for the periods at which the actors are removed, BP_i. In the second summation we have items representing the actors' absence, $1 - z_{ii't}$, in the period before BP_i. This means at least one actor needs to be available in the period that it is currently removed or at least one actor should be removed one period before its BP_i. For the example shown in Table 2.4, 4 out of 6 actors are removed at some points in time based on the $z_{ii't}$ values.

Table 2.4: Cut example

t	$z_{11't}$	$z_{22't}$	$z_{33't}$	$z_{44't}$	$z_{55't}$	$z_{66't}$
4	1	0	**0**	0	0	1
3	1	0	**1**	0	**0**	1
2	1	0	1	**0**	**1**	1
1	1	**0**	1	**1**	1	1
i	1	2	3	4	5	6

The following constraint is the feasibility cut that will eliminate the solution represented in Table 2.4. Note that the bold zeros in the table are the first period that the individual are removed and the bold ones are the last periods the individuals were available (if arrested after period 1).

$$z_{22'1} + z_{33'4} + z_{44'2} + z_{55'3} + (1 - z_{33'3}) + (1 - z_{44'1}) + (1 - z_{55'2}) \geq 1$$

2.3.4 Master Problem Tightening Constraints

The MP will have numerous OSs which are not feasible to SP. For example, one possible solution to MP is to remove all actors in the first period so the flow is zero for all the periods. In realistic instances, this solution will not be feasible since there are finite resources available for actor removal. In order to eliminate similar infeasible solutions, four sets of constraints are added to MP. The first set of constraints are:

$$z_{ii',\underline{t}_i} = 1 \qquad \text{for } i \in N \qquad (2.40)$$

An actor i will need to have at least $\mu_{ii'}$ actors connected to it to be removed before it can be monitored. If we were to know the earliest times that each of the connected actors can be removed, then we can determine the time at which $\mu_{ii'}$ or more actors are removed and targeting can begin. We define $\underline{t}_i$ which is the first period the actor i can be removed if we have unlimited resources. It can be calculated based on the actor's input parameters and the structure of the network. For example, in the network shown in Figure 2.6, assuming unlimited resources, all the first-level actors (FLAs) can be removed in the first period. Therefore, because $\tau_{66'} = 2$, monitoring the second-level actors can be started in period 1 and continues until the end of period 2. Therefore, the minimum period that actor 6 can be removed is the next period (i.e., $\underline{t}_{66'} = 3$). The same argument results in $\underline{t}_{77'} = 4$. In order to start monitoring the only safe house in level 3, actor 8, both second-level actors need to be removed since $\mu_{88'} = 2$. So monitoring the safe house can happen in period 4 at the earliest. Thus $\underline{t}_{88'} = 4 + \underline{t}_{88'} + 1 = 9$. These requirements are enforced by constraints (2.40) to ensure that each actor is available until the first period that it may be removed when considering monitoring and hierarchical actor removal requirements.

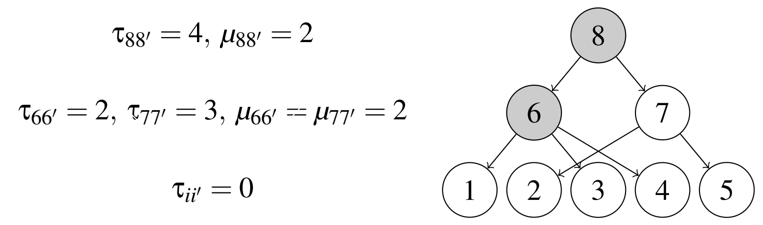
$\tau_{88'} = 4,\ \mu_{88'} = 2$
$\tau_{66'} = 2,\ \tau_{77'} = 3,\ \mu_{66'} = \mu_{77'} = 2$
$\tau_{ii'} = 0$
8
6
7
1
2
3
4
5

Figure 2.6: MP: Eliminating infeasible actor interdiction solutions

We now present another set of constraints:

$$\sum_{i \in N} (a_{ii'}) * (1 - z_{ii'1}) \leq B \tag{2.41}$$

$$\sum_{i \in N} (a_{ii'}) * (z_{ii',t-1} - z_{ii't}) \leq B \qquad \text{for } t = 2, ..., T \tag{2.42}$$

Constraints (2.41-2.42) are responsible for not allowing the amount of resources used for removal activities occurring in time t to exceed the available resources. The difference between two consecutive $z_{ii',t-1}$ and $z_{ii',t}$ variables is 1 if actor ii' is removed at period t. Note that for $t = 0$, $z_{ii'0}$ is assumed to be 1.

The next set of tightening constraints are as follows:

$$\sum_{i \in N} (b_{ii'}\tau_{ii'} + a_{ii'}) * (1 - z_{ii',t-1}) + \sum_{i \in N} (b_{ii'}\tau_{ii'}) * (z_{ii',t-1} - z_{ii',t}) +$$
$$\sum_{i \in N} \sum_{tt=t+1}^{\max\{t+\tau_{ii'}-1,T\}} b_{ii'} * (z_{ii',tt-1} - z_{ii',tt}) * (\tau_{ii'} - (tt - t)) \leq (t-1)B \qquad \text{for } t = 2, ..., T \tag{2.43}$$

The motivation behind constraint (2.43) is that for a specific period t, the total resource usage up to the beginning of period t cannot exceed $(t-1)B$. This includes the resource usage for (i) monitoring and removal actors who are removed at or before period $t-1$; (ii) monitoring actors who are removed at period t; and (iii) partial monitoring of actors who are removed in the next subsequent periods after period t (i.e., periods t through $t + \tau_{ii'} - 1$). If an actor is removed within $\tau_{ii'}$ periods after period t, then we know at least some part of its monitoring needs to happen by period t.

The final set of tightening constraints can be written as:

$$\sum_{j: j \in A(i')} (1 - z_{jj',t}) \geq \mu_{ii'} * (1 - z_{ii',t+\tau_{ii'}}) \qquad \text{for } i \in N, t = 1, ..., T - \tau_{ii'} \tag{2.44}$$

$$\sum_{j: j \in A(i')} (1 - z_{jj',t}) \geq \mu_{ii'} * (1 - z_{ii',T}) \qquad \text{for } i \in N, t = T - \tau_{ii'} + 1, ..., T \tag{2.45}$$

As constraints (2.44) state, if at least $\mu_{ii'}$ destination nodes of actor ii' are removed at period t, then that actor can be removed in period $t + \tau_{ii'}$ (i.e., $z_{ii',t+\tau_{ii'}} = 0$). However, if there is not enough time to remove an actor before period T, that actor should remain available during the time horizon. This is enforced by constraints (2.45).

2.4 Computational Results

In this section we consider a set of experiments designed to assess the effectiveness of the approached described in the preceding sections and compare its performance versus that of commercial solvers. Our instances varied with according to the following network characteristics: (i) number of FLAs; (ii) amount of connections between levels of the network; (iii) number of periods, and (iv) amount of resources available. All other parameters, including the number of levels, were generated based on the experiment scheme described in Malaviya et al. (2012).

As shown in Table 2.5, we have 8 different values for the number of FLAs in our instances. For smaller problems with 25, 50 and 75 FLAs, we have generated 5 different networks for each of these problem sizes. For the large problems, with 200, 400, 600, 800 and 1000 FLAs, we have one network instance for each problem size. In the third column, the range for the total numbers of actors in the networks is presented. For example, for the 5 instances generated with 25 FLAs, the total numbers of actors are either 38 or 39. For small networks, time horizon lengths of 3, 5 and 10 are considered. For large networks, time horizon lengths of 3, 5, 10, 25 and 50 are considered. The various numbers of available resources considered in each problem class for each instance is shown in the last column. All instances were solved with and without presolver in CPLEX for both MIP and LBD. Therefore, in total we have 450 small and 250 large problems. For all problems, LBD's total variables are 25% of the MIP's which often results in a great difference between the size of the MIP's tree and the LBD's tree.

Table 2.5: Instance data

# of FLAs	# of instances	# of nodes	# of arcs	T	B
25	5	38-39	20-29	3, 5, 10	6, 9, 12, 15, 18
50	5	68-78	35-56	3, 5, 10	10, 16, 22, 28, 34
75	5	105-113	51-74	3, 5, 10	10, 20, 30, 40, 50
200	1	259	98	3, 5, 10, 25, 50	5, 15, 25, 50, 75
400	1	508	183	3, 5, 10, 25, 50	5, 25, 50, 75, 100
600	1	751	272	3, 5, 10, 25, 50	5, 25, 50, 100, 150
800	1	998	376	3, 5, 10, 25, 50	5, 25, 50, 100, 200
1000	1	1224	418	3, 5, 10, 25, 50	5, 25, 75, 150, 250

All instances were solved by CPLEX 12.6.3. The time limit is 1 hour for smaller instances and 5 hours for large instance. A stopping gap of 0.1% was used, where

$$\text{gap} = \frac{\text{best integer solution's OFV} - \text{best linear programming relaxation solution's OFV}}{\text{best integer solution's OFV}} * 100$$

The small problems were solved on a 12-core 24 GB computer while the large problems were solved on a 16-core 32 GB computer. For 36 of the problems we were forced to use a computer with larger memory (12-core 96 GB). Note that the consideration of multiple computer architectures was allowed so that we could more consistently retrieve a solution for MIP to compare against LBD. In addition, the MIP and LBD procedures were run on the same architecture for each instance to ensure a fair comparison of performance.

As discussed in Section 2.3, LBD initially generates numerous infeasible solutions. For this reason, the constraints (2.40-2.45) are implemented. In Table 2.6, the results comparing the two LBD are presented; one LBD including the tightening constraints (LBD1) and one without them (LBD2). The comparison is done for 20 instances (10 small and 10 large), which are chosen among the instances for which LBD did relatively better than MIP. All the small instances and one large instance were solved to gap=0.1% by LBD1, while LBD2 could not find a feasible solution in the time limit for all the instances. The portions of time consumed in the CBF and SP in LBD1 are on average 2.1% and 1.3% of the total solving time, respectively, while they are 30.0% and 6.7% for LBD2. This can be explained by the difference in feasible region sizes of LBD1 and LBD2. LBD2 clearly has a larger feasible region, which could result in numerous incumbent solutions during the examination of the search tree. This is also represented by the fact that the average number of cuts is 106.7 for LBD1 and 40332.5 for LBD2. Therefore, it is clear that the tightening constraints have a significant impact on our ability to efficiently solve problems using the LBD approach.

Table 2.6: CBF and SP - with/without tightening constraints

			LBD1 (with the tightening constraints)					LBD2 (without the tightening constraints)				
Prob. #	# of FLAs	Time limit (s)	Solving time (s)	Number of cuts	CBF portion of time (%)	SP portion of time (%)	Gap (%)	Solving time (s)	Number of cuts	CBF portion of time (%)	SP portion of time (%)	Gap (%)
S-006	25	3600	2	18	18.5%	16.0%	**0.1%**	3600	58049	11.4%	4.6%	-
S-036	25	3600	8	3	1.1%	1.0%	**0.1%**	3600	57024	11.4%	4.8%	-
S-116	25	3600	55	39	1.3%	0.7%	**0.1%**	3600	56913	13.9%	6.4%	-
S-146	25	3600	8	10	4.1%	3.5%	**0.1%**	3600	56294	13.9%	6.6%	-
S-216	50	3600	30	49	2.4%	1.6%	**0.1%**	3600	46751	13.6%	5.2%	-
S-276	50	3600	1720	4	0.0%	0.0%	**0.1%**	3600	46457	15.9%	6.1%	-
S-306	75	3600	449	108	0.6%	0.3%	**0.1%**	3600	40773	20.3%	8.1%	-
S-327	75	3600	274	10	0.6%	0.3%	**0.1%**	3600	39248	20.7%	8.9%	-
S-386	75	3600	386	324	4.3%	0.9%	**0.1%**	3600	36210	24.3%	9.8%	-
S-431	75	3600	1086	17	0.1%	0.0%	**0.1%**	3600	38161	23.0%	8.9%	-
L-010	200	18000	2859	0	0.1%	0.0%	**0.1%**	18000	60201	18.0%	4.2%	-
L-036	200	18000	18000	1096	1.4%	0.1%	2.2%	18000	54079	23.6%	5.2%	-
L-062	400	18000	18000	187	0.9%	0.0%	18.7%	18000	35999	35.4%	6.6%	-
L-093	400	18000	18000	39	1.2%	0.1%	13.8%	18000	25002	65.5%	8.5%	-
L-104	600	18000	18000	5	0.1%	0.1%	6.2%	18000	39509	36.3%	6.7%	-
L-134	600	18000	18000	30	0.3%	0.1%	13.3%	18000	31035	42.6%	6.2%	-
L-156	800	18000	18000	53	0.1%	0.0%	0.3%	18000	25662	44.4%	6.9%	-
L-187	800	18000	18000	195	2.2%	0.1%	28.3%	18000	18109	67.1%	6.7%	-
L-209	1000	18000	18000	13	0.2%	0.0%	20.5%	18000	21460	51.3%	7.3%	-
L-233	1000	18000	18000	29	0.4%	0.1%	6.1%	18000	19714	59.8%	6.6%	-

The difference between LBD and MIP for all the 700 problems is summarized in Table 2.7. For each number of FLAs, total number of instances, number of instances not solved to optimality, and the average gap for those unsolved instances are shown for MIP and LBD for two cases: (i) presolver off (PS=0) and (ii) presolver on (PS=1). In the case where presolver is off, LBD was able to obtain more optimal solution than MIP for 50, 75, 600, and 800 FLAs instances while they operated equally for the rest of the problems. In the case with presolver on, LBD also did better for 75, 200, and 1000 FLAs instances, while MIP was better for instances with 400 FLAs. In terms of average gap, except for two cases, with 75 and 800 FLAs with presolver on, the remainder of the problems have smaller average gaps for LBD compared to MIP. Exhaustive information for individual problems can be found in Tables 2.8-2.10. Figures 2.7-2.9 provide visual evidence of LBDs performance when compared with solving the MIP via a commercial solver.

Table 2.7: Problems not solved to optimality in the time limit

Presolver:		Off (PS=0)				On (PS=1)			
		MIP		LBD		MIP		LBD	
# of FLAs	Total # of instances	# of instances not solved to optimality	Ave. gap	# of instances not solved to optimality	Ave. gap	# of instances not solved to optimality	Ave. gap	# of instances not solved to optimality	Ave. gap
25	75	1	3.4%	1	1.6%	1	3.6%	1	**0.3%**
50	75	20	4.7%	**17**	**3.8%**	17	4.2%	17	**3.8%**
75	75	37	8.1%	**34**	**7.9%**	36	**7.4%**	**33**	8.2%
200	25	17	24.7%	17	**15.5%**	17	19.2%	**16**	**15.9%**
400	25	23	32.4%	23	**21.4%**	**22**	27.4%	23	**18.5%**
600	25	24	36.0%	**23**	**32.8%**	22	36.1%	22	**26.4%**
800	25	24	43.6%	**22**	**41.5%**	22	**41.4%**	22	43.0%
1000	25	24	46.2%	24	**41.8%**	24	42.9%	**23**	**39.3%**

In Figure 2.7, LBD's solving time and differences between LBD's and MIP's solving time are shown for 328 (out of 450) small instances that were solved to optimality by both methods. As shown in the upper portion of the figure, all instances were solved in less than 3400 seconds by LBD and the difference of solving time is shown in the lower part. If a point is above 0 in the lower part of the figure then MIP reached a OS in shorter amount of time compared to LBD and if it is below the line that means LBD solved the problem more efficiently. Out of the 328 instances, 54 were solved in the same amount of time by both methods. LBD solved 180 instances more efficiently.

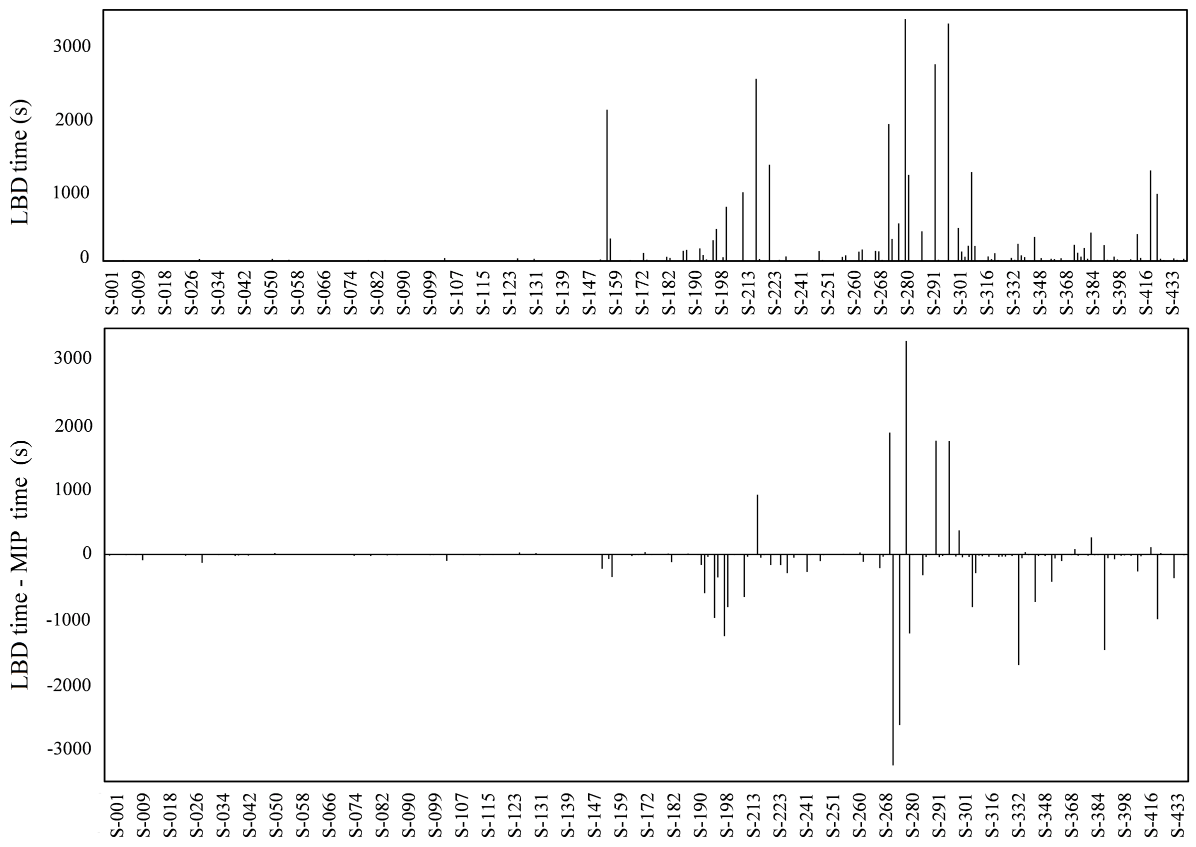

Figure 2.7: Small instances' solving times

In Table 2.8, gaps for 29 small instances for which one method did not solve to optimality are shown. LBD solved the first 19 instances to optimality in an average time of 1160.6 seconds, while MIP reached to an average gap of 1.7% in an hour. The next 10 instances were solved by MIP in an average time of 786.9 seconds while LBD reached an average gap of 1.2% in 3600 seconds.

Table 2.8: Small instances for which one method could not finish solving in 1 hour

					MIP			LBD		
Prob. #	# of FLAs	PS	T	B	IP OFV	IP gap	time	IP OFV	gap	time (s)
S-201	50	0	10	10	41.46	0.16%	3600	41.46	0.10%	342
S-206	50	0	5	10	41.46	0.39%	3600	41.46	0.10%	578
S-208	50	0	10	10	17.73	0.81%	3600	17.73	0.10%	820
S-210	50	0	5	10	16.31	3.35%	3601	16.15	0.10%	1812
S-227	50	0	10	10	26.79	2.62%	3600	26.79	0.10%	3288
S-232	75	0	10	10	26.79	3.64%	3601	26.79	0.10%	1363
S-276	75	0	10	10	41.46	0.43%	3600	41.46	0.10%	702
S-281	75	0	5	10	41.46	0.69%	3600	41.46	0.10%	2772
S-314	75	0	10	10	26.27	2.40%	3600	26.27	0.10%	324
S-321	75	0	5	10	104.03	2.39%	3600	104.03	0.10%	166
S-336	75	0	10	10	69.55	0.54%	3600	69.55	0.10%	2598
S-347	75	0	10	10	31.10	1.85%	3600	31.10	0.10%	541
S-352	75	0	5	10	31.10	1.33%	3600	31.10	0.10%	1783
S-356	75	1	3	20	61.61	3.57%	3600	61.61	0.10%	564
S-386	75	1	5	20	82.27	1.98%	3600	82.27	0.10%	384
S-411	75	1	10	20	69.55	0.58%	3601	69.55	0.10%	1068
S-426	75	1	10	20	60.20	1.20%	3600	60.20	0.10%	222
S-431	75	1	10	20	61.61	4.21%	3601	61.61	0.10%	419
S-436	75	1	10	10	49.10	0.14%	3600	49.10	0.10%	2305
Average						**1.7%**	3600.2		0.1%	**1160.6**
S-154	50	0	3	28	13.64	0.10%	151	13.64	0.18%	3600
S-229	50	1	3	28	13.64	0.10%	361	13.64	0.51%	3601
S-234	50	1	5	28	13.64	0.10%	267	13.64	0.34%	3600
S-239	50	1	10	28	13.64	0.10%	883	13.64	0.14%	3600
S-278	50	1	5	22	17.73	0.10%	31	17.73	0.26%	3600
S-302	75	0	3	20	44.81	0.10%	28	44.81	1.21%	3600
S-312	75	0	10	20	45.82	0.10%	2977	45.82	3.69%	3600
S-371	75	0	10	10	68.66	0.10%	2724	69.42	1.51%	3600
S-377	75	1	3	20	44.81	0.10%	16	44.84	1.34%	3601
S-382	75	1	5	20	45.82	0.10%	431	45.82	3.22%	3600
Average						0.1%	**786.9**		**1.2%**	3600.2

Neither method produced an optimal solution in 1 hour for 93 instances. In Figure 2.8, you can see the gaps for MIP and the difference between LBD and MIP gaps in 1 hour. In the lower part of the figure, if a point is above 0 line then MIP reached to a lower gap compared to LBD while the opposite is true if LBD outperforms MIP. MIP outperformed LBD for 45 instances while LBD was more effective in the remaining 48 instances. From the lower part of the Figure 2.8 we can conclude that the two approaches perform comparably for smaller instances.

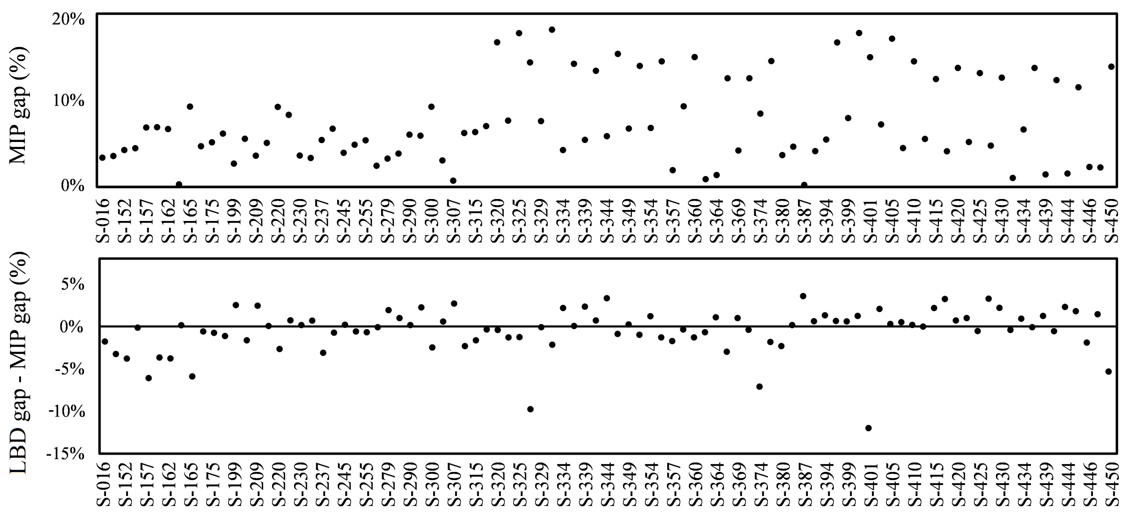

Figure 2.8: Small instances' gaps

In Table 2.9, data for 36 (out of 250) large instances is shown. In each of these 36 instances, at least one of the two approaches solved the problem to optimally within 5 hours. In the first portion of the table there are 9 instances that LBD solved optimally in an average time of 1755.7 seconds while MIP's average solving time is 5240.3 seconds. In the second part, 21 instances that MIP solved faster are presented. MIP and LBD solved them in average times of 650.2 and 2778.0 seconds, respectively. Also, there are 6 instances, shown in the last part of the table, that only one method could solve to optimality within the time limit. It should be noted that most instances for which MIP outperforms LBD are problems in which only 3 or 5 periods are considered. In these cases, the advantages of the LBD formulation are anticipated to be minimized.

Table 2.9: Large instances for which just at least one method finished solving in 5 hours

					MIP			LBD		
Prob. #	# of FLAs	PS	T	B	IP OFV	gap	time (s)	IP OFV	gap	time (s)
L-010	200	0	5	75	60.14	0.10%	612	60.14	0.10%	**528**
L-052	400	0	3	25	385.44	0.10%	2455	385.44	0.10%	**630**
L-077	400	1	3	25	385.44	0.10%	811	385.44	0.10%	**501**
L-127	600	1	3	25	710.71	0.10%	17429	710.71	0.10%	**7441**
L-131	600	1	5	5	1,278.07	0.10%	3436	1278.08	0.10%	**1326**
L-151	800	0	3	5	952.66	0.10%	611	952.66	0.10%	**415**
L-176	800	1	3	5	952.66	0.10%	294	952.66	0.10%	**239**
L-177	800	1	3	25	890.52	0.10%	14952	890.31	0.10%	**1637**
L-181	800	1	5	5	1,568.46	0.10%	6563	1568.46	0.10%	**3084**
Average:							5240.3			**1755.7**

Prob. #	# of FLAs	PS	T	B	IP OFV	gap	time (s)	IP OFV	gap	time (s)
L-001	200	0	3	5	**171.93**	0.10%	34	171.93	0.10%	91
L-002	200	0	3	15	**148.56**	0.10%	42	148.56	0.10%	219
L-005	200	0	3	75	**60.14**	0.10%	209	60.14	0.10%	899
L-006	200	0	5	5	**273.56**	0.10%	191	273.56	0.10%	5643
L-015	200	0	10	75	**60.15**	0.10%	1828	60.14	0.10%	1917
L-020	200	0	25	75	**60.14**	0.10%	2102	60.14	0.10%	2787
L-025	200	0	50	75	**60.14**	0.10%	1621	60.14	0.08%	1928
L-026	200	1	3	5	**171.93**	0.10%	9	171.93	0.10%	26
L-027	200	1	3	15	**148.56**	0.10%	24	148.56	0.10%	49
L-030	200	1	3	75	**60.14**	0.10%	62	60.14	0.10%	523
L-031	200	1	5	5	**273.56**	0.10%	181	273.56	0.07%	17231
L-035	200	1	5	75	**60.14**	0.10%	83	60.14	0.10%	2889
L-040	200	1	10	75	**60.14**	0.10%	142	60.14	0.10%	1653
L-045	200	1	25	75	**60.14**	0.10%	317	60.14	0.10%	2287
L-050	200	1	50	75	**60.14**	0.10%	391	60.14	0.10%	1294
L-051	400	0	3	5	**441.09**	0.10%	291	441.09	0.10%	2517
L-076	400	1	3	5	**441.09**	0.10%	355	441.09	0.10%	556
L-101	600	0	3	5	**780.13**	0.10%	312	780.13	0.10%	804
L-126	600	1	3	5	**780.13**	0.10%	245	780.13	0.10%	1294
L-201	1000	0	3	5	**1,146.38**	0.10%	4293	1146.38	0.10%	12480
L-226	1000	1	3	5	**1,146.38**	0.10%	922	1146.38	0.10%	1251
Average:							650.2			**2778.0**

L-033	200	1	5	25	173.17	7.24%	18001	172.11	0.10%	**8379**
L-106	600	0	5	5	1,279.40	0.90%	18004	1278.08	0.10%	**6917**
L-152	800	0	3	25	893.77	1.18%	18003	890.52	0.10%	**1766**
L-156	800	0	5	5	1,569.59	1.13%	18007	1568.46	0.10%	**6934**
L-231	1000	1	5	5	1,889.60	0.57%	18003	1889.40	0.10%	**12724**
L-078	400	1	3	50	326.25	0.10%	**11937**	326.25	0.11%	18001

However, the results for larger instances are notably different. First, note that 214 (out of 250) of the large instances were not solved optimally by either of the methods. There are 23 instances for which LBD could not find a feasible solution while MIP managed to reach an average gap of 90.81%. For the ease of comparison, we set the LBD gap for those instances to be equal to 100%

(the maximum gap for our problem since OFV cannot be negative and it is a minimization problem). Also, for three instances (L-003, L-028, and L-029), MIP ran out of memory even on the computer with 96 GB memory before the time limit, so the final gaps are considered for comparison. In Figure 2.9, you can see the gaps for MIP and the difference between LBD and MIP gaps in 5 hours. In the lower part of the figure, if a point is above 0 line then MIP reached to a lower gap compared to LBD while the opposite is true if LBD outperforms MIP. It is apparent that LBD's gap are better than MIP's gaps after 5 hours for these problems. LBD outperforms MIP in 174 instances (with 10.0% smaller average gap) while MIP did better for only 40 instances (with 10.6% smaller average gap). Based on Figure 2.9 and Table 2.9 it can be concluded that LBD outperforms MIP for the majority of the large instances.

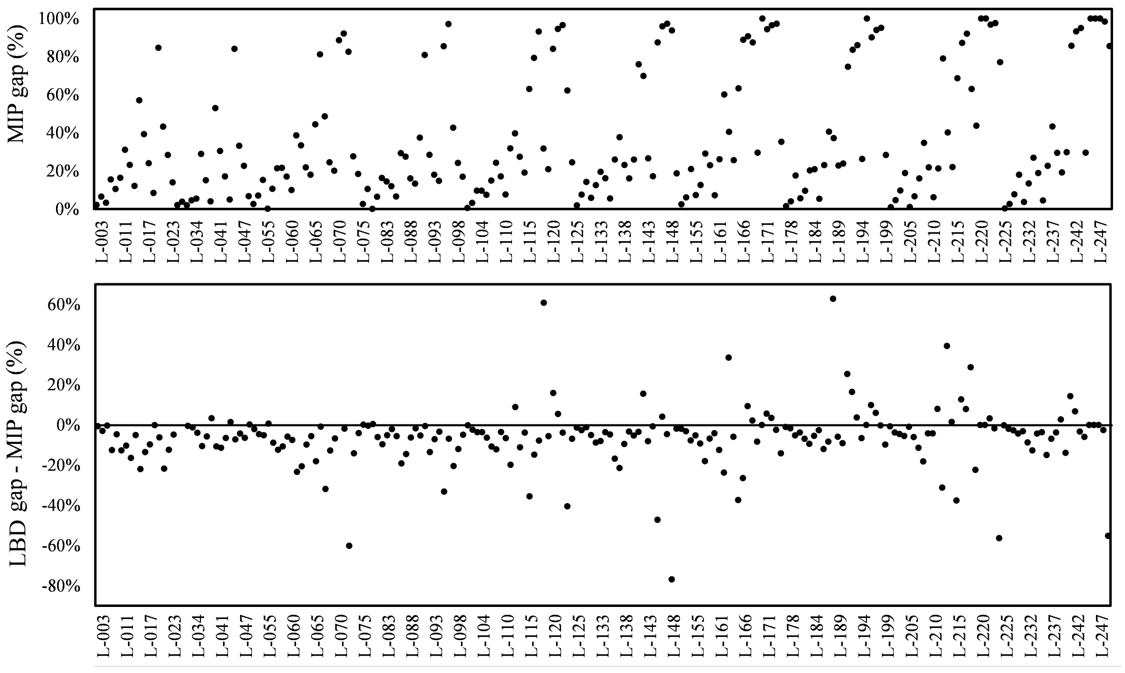

Figure 2.9: Large instances' gaps

Table 2.10 summarizes the results for each method. A method is counted to be better than the other one if when solving a particular instance it terminates in shorter amount of time or with a smaller gap during the time limit. The larger number of each race between LBD and MIP for each row, shown in bold, indicates which method performed better. If presolver is off LBD is better than MIP for any number of FLAs, and when it is on MIP is only better for the cases of 50 and 75 FLAs.

Table 2.10: Number of instances that MIP or LBD performed better

presolver:		off			on		
# of first-level actors	# of instances	MIP performed better	LBD performed better	same	MIP performed better	LBD performed better	same
25	75	11	**45**	19 *	22	**34**	19*
50	75	16	**51**	8 *	**38**	32	5*
75	75	20	**53**	2 *	**42**	32	1*
200	25	7	**18**	-	11	**14**	-
400	25	3	**22**	-	4	**21**	-
600	25	5	**20**	-	3	**22**	-
800	25	5	**20**	-	7	**18**	-
1000	25	10	**15**	-	7	**18**	-

* The two methods solved in same amount of time

2.5 Conclusion and Future Work

This study presented a logic-based decomposition approach for a class of dynamic maximum flow network interdiction problems. We utilize constraint programming to more efficiently formulate scheduling aspects of the problem and integrate that with a mixed integer formulation to form our hybrid decomposition framework.

LBD gets tested on 700 small and large instances that were generated based on real data parameters and compared with a standard mixed-integer programming formulation. Presolver utilization allows MIP to overtake LBD for instances with 50 and 75 FLAs, yet LBD proves to be more efficient to solve larger instances (with 200-1000 FLAs). If presolver is off, LBD can do better than MIP for small and large instances. The benefits of LBD are only amplified by the inclusion of the tightening constraints in its MP. In conclusion, LBD is comparable to MIP for smaller cases but consistently outperforms MIP for the large cases.

One of the challenges for the LBD approach for some instances was reaching the initial feasible solution. Thus, one of the directions to which this work can be extended is to initiate LBD with a given feasible solution that can be generated by forcing LBD to just remove the FLAs. An analysis of the tradeoff between the quality of solution for this special case versus the time required to generate that solution would be an interesting starting place for exploration into heuristic approaches to this problem. While this chapter's proposed approach offers better performance for solving larger and more realistic instances of dynamic interdiction problems, there remain applications for which even larger instances must be solved. Of course, large-scale heuristics might be an appropriate avenue of study for this class of problems, given the availability of this chapter's exact approach to provide solutions for performance comparison. However, it is also important to note that computational gains from the proposed method may be attainable through the use of a custom parallel programming implementation of the CP subproblems. A particular challenge to that research avenue would be the control of constraints generated for MP in parallel and how the feasibility of MP's best feasible solution would be validated.

Acknowledgment

This material is based upon work supported by NSF Contract awards number 1266056 and Arkansas High Performance Computing Center which is funded through multiple National Science Foundation grants and the Arkansas Economic Development Commission.

Bibliography

Assimakopoulos, N. (1987). A network interdiction model for hospital infection control. *Computers in biology and medicine*, 17(6):413–422.

Borndörfer, R., Sagnol, G., and Schwartz, S. (2016). An extended network interdiction problem for optimal toll control. *Electronic Notes in Discrete Mathematics*, 52:301–308.

Edis, E. B. and Ozkarahan, I. (2011). A combined integer/constraint programming approach to a resource-constrained parallel machine scheduling problem with machine eligibility restrictions. *Engineering Optimization*, 43(2):135–157.

Focacci, F., Lodi, A., and Milano, M. (2002). Mathematical programming techniques in constraint programming: A short overview. *Journal of Heuristics*, 8(1):7–17.

Gedik, R., Rainwater, C., Nachtmann, H., and Pohl, E. A. (2016). Analysis of a parallel machine scheduling problem with sequence dependent setup times and job availability intervals. *European Journal of Operational Research*, 251(2):640–650.

Harjunkoski, I. and Grossmann, I. E. (2002). Decomposition techniques for multistage scheduling problems using mixed-integer and constraint programming methods. *Computers & Chemical Engineering*, 26(11):1533–1552.

Heipcke, S. (1999). Comparing constraint programming and mathematical programming approaches to discrete optimisation-the change problem. *Journal of the Operational Research Society*, pages 581–595.

Hooker, J. N. (2007). Planning and scheduling by logic-based benders decomposition. *Operations Research*, 55(3):588–602.

IBM Corporation. IBM ILOG CPLEX optimization studio. http://www.ibm.com/support/knowledgecenter/en/SSSA5P_12.4.0/ilog.odms.cpo.help/CP_Optimizer/User_manual/topics/model_vars_interval.htm. Accessed 2016.10.29.

Jain, V. and Grossmann, I. E. (2001). Algorithms for hybrid milp/cp models for a class of optimization problems. *INFORMS Journal on computing*, 13(4):258–276.

Lustig, I. J. and Puget, J.-F. (2001). Program does not equal program: Constraint programming and its relationship to mathematical programming. *Interfaces*, 31(6):29–53.

Malaviya, A., Rainwater, C., and Sharkey, T. (2012). Multi-period network interdiction problems with applications to city-level drug enforcement. *IIE Transactions*, 44(5):368–380.

Phillips, C. A. (1993). The network inhibition problem. In *Proceedings of the twenty-fifth annual ACM symposium on Theory of computing*, pages 776–785. ACM.

Rad, M. A. and Kakhki, H. T. (2013). Maximum dynamic network flow interdiction problem: new formulation and solution procedures. *Computers & Industrial Engineering*, 65(4):531–536.

Topaloglu, S. and Ozkarahan, I. (2011). A constraint programming-based solution approach for medical resident scheduling problems. *Computers & Operations Research*, 38(1):246–255.

Trick, M. A. and Yildiz, H. (2011). Benders' cuts guided large neighborhood search for the traveling umpire problem. *Naval Research Logistics (NRL)*, 58(8):771–781.

Wood, R. K. (1993). Deterministic network interdiction. *Mathematical and Computer Modelling*, 17(2):1–18.

Appendix

2.A Certification of Student Work

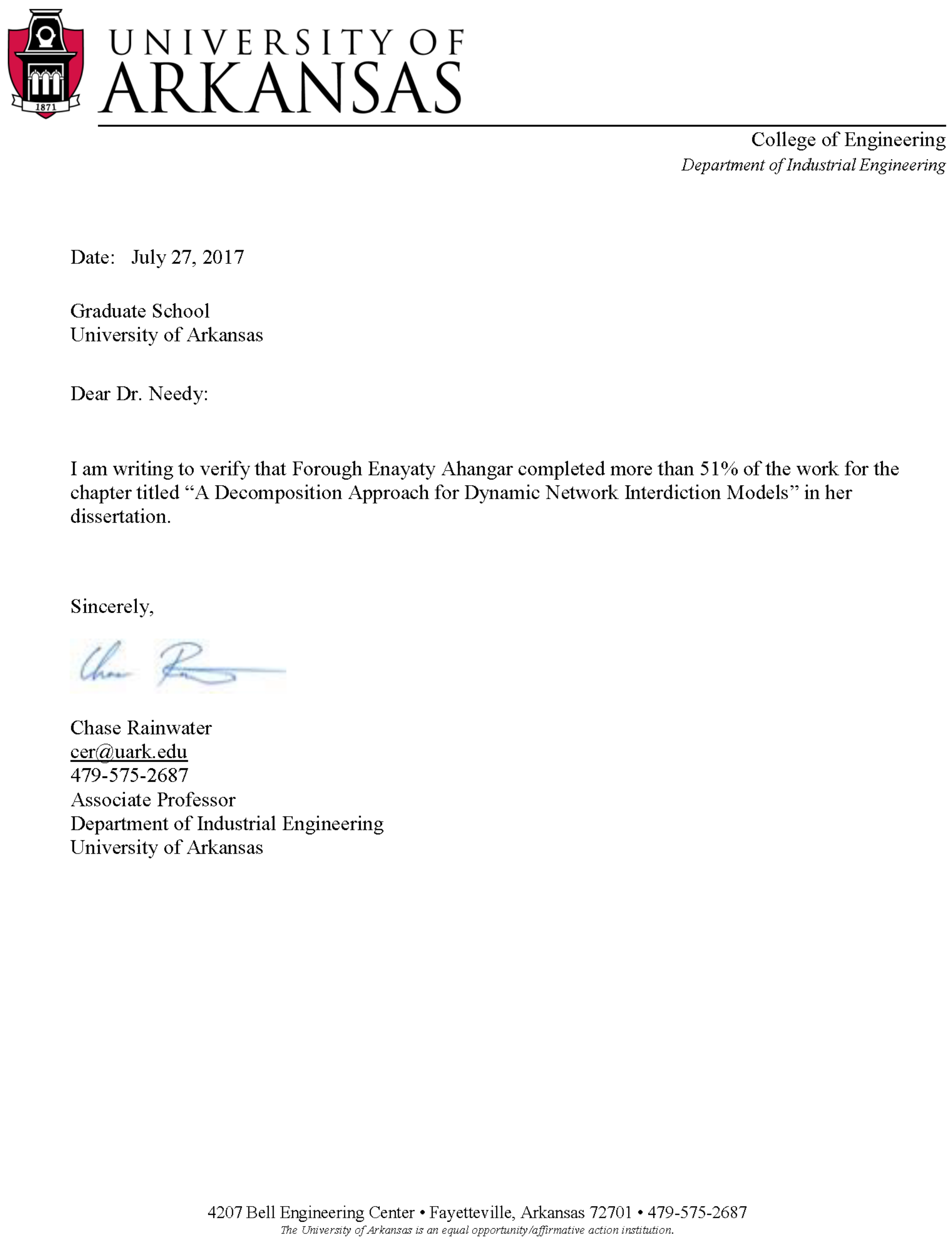

UNIVERSITY OF ARKANSAS

College of Engineering
Department of Industrial Engineering

Date: July 27, 2017

Graduate School
University of Arkansas

Dear Dr. Needy:

I am writing to verify that Forough Enayaty Ahangar completed more than 51% of the work for the chapter titled "A Decomposition Approach for Dynamic Network Interdiction Models" in her dissertation.

Sincerely,

[illegible]

Chase Rainwater
cer@uark.edu
479-575-2687
Associate Professor
Department of Industrial Engineering
University of Arkansas

4207 Bell Engineering Center • Fayetteville, Arkansas 72701 • 479-575-2687
The University of Arkansas is an equal opportunity/affirmative action institution.

3. **Interdicting Content Clusters Across a Distributed Resource System**

3.1 Introduction

Interdiction problems have become an active topic since the Vietnam War in 1970s when a model was developed to minimize the maximum flow of enemy troops with supplies (McMasters and Mustin 1970 and Ghare et al. 1971). An interdiction problem can be viewed as a Stackelberg game on one network in which two competitors compete with each other with an objective function in two opposite directions (Pan and Kasiviswanathan, 2010). Multiple applications for this topic have been extended during the past few decades that include disabling military supply lines, disrupting pipe systems (Phillips, 1993), combating drug trafficking (Wood (1993), Altner et al. (2010), and Malaviya et al. (2012)), and controlling infections (Assimakopoulos, 1987) or respiratory pathogens in a hospital (Pourbohloul et al., 2005), disruption of terrorist networks (Memon and Larsen, 2006), and illegal drugs or nuclear material threats by smugglers (Morton et al., 2007).

Based on the objective of each application, a different model is developed. Some models attempt to remove arcs or nodes to minimize the maximum flow between a source node and a sink node (McMasters and Mustin 1970, Ghare et al. 1971, and Malaviya et al. 2012), while some others consider removing edges or nodes to maximize the length of the shortest path between a source node and a sink node (Fulkerson and Harding 1977 and Israeli and Wood 2002).

The increase in information and technology has resulted in a highly-connected digital world. With a reliance on cyber systems comes new threats. According to Infosecurity Magazine (2013), data breach, malware, distributed denial of service (DDoS), mobile threats, and industrialization of fraud are known to be the most significant threats to IT cybersecurity. Unfortunately, protection strategies lag far behind the evolution of security technology development (Benzel, 2011). Therefore, engineers, scientists, and researchers are being called upon for rapid advancements in the cybersecurity domain (Von Solms and Van Niekerk, 2013).

In 2013, L. Columbus predicted public clouds will be used for more than half of organizations data storage by the end of this decade, suggesting that cloud storage solutions have become growingly attractive to service providers. A cloud is a network of computing resources providing applications and/or data storage to a population of users. An individual piece of content is an application and/or data element that relies on the cloud for transmission or processing. In addition, a data center is often referred to as the hardware that function as a storage in the cloud. One of the advantages of cloud storage is ease of access, however, it creates vulnerability to cyber threats such as data breach and DDoS.

In cybersecurity, a data breach occurs when confidentiality of content is compromised (i.e., an unauthorized user is able to access the content). A DDoS occurs when the content is not available to its authorized user(s) because it is not available due the attacks on centers containing it.

Content mirroring is one strategy to mitigate against the loss of access to content on a cloud service. It is implemented when the content is duplicated across multiple data centers within the cloud framework. On one hand, mirroring increases the content's availability and makes it more resilient to DDoS. However, it decreases its confidentiality because the content is more accessible and susceptible to data breach. Content portioning is a way to resolve that issue by reducing content accessibility to data breach. In portioning, each content can be divided into multiple portions that are assigned on different data centers. In order for the content to be available after the attacks, all of its portions must be available (i.e., if one portion is not available, then the whole content is unavailable).

This increased reliance on cloud-supported computing platforms only amplifies those at risk from cybersecurity threats. For this reason we study a generic content/cloud cyber system in which information and/or services are stored/hosted on one (or many) cloud platforms. The focus of this research is to study how these attacks can disrupt content availability given the assignment of the content. We introduce a new class of interdiction models which we call the Clustered Content Interdiction Problem (CCIP). CCIP is an interdiction problem in which an attacker attempts to disrupt clusters of content distributed across a collection of resources.

In this chapter, we detail the creation of an optimization approach for solving CCIP. Section 3.2 provides details of the problem studied. Our proposed enhancements to the problem formulation and approaches to better solve it are explained in Section 3.3. Our proposed genetic algorithm is discussed in Section 3.4 followed by other attempetd methods in Section 3.5. Computational results and conclusions follow in Sections 3.6 and 3.7, respectively.

3.2 Problem Overview

CCIP considers groups of content dispersed across a collection of centers. In this problem, content (e.g., smuggled items or data) should be assigned to centers to ensure availability. Given a content assignment across a collection of centers, an interdictor (e.g., a border security) attempts to determine which centers to interdict (attack) in order to maximize the service disruption or minimize the content availability. Content is considered to be available if it is assigned to at least one non-interdicted center after the interdictions occur. In this section, an integer programming (IP) formulation is presented to model the problem.

Let I denote the set of centers and J the set of content types. All content are assigned to at least one center. Replication across multiple centers and partitioning are considered for all content. $n_j \geq 1$ denotes the number of portions for content j. We consider the protection against worst-case interdiction on B servers where it denotes the number of interdictions an interdictor completes. This value reflects the power of the potential interdictor and is considered to be determined in our problem.

A content is considered to be unavailable if after the interdictions it is not available on any of the non-interdicted centers. Denial of service (DoS) of content j after the interdictions is considered to have a cost (value) equal to c_j. A portion of content is known to be unavailable if all the centers containing it have been interdicted. Content $j \in j$ is considered to be disrupted if at least one portion of it is unavailable. The objective function of the problem is to determine which centers to interdict in order to maximum the summation of content's DoS's costs.

An example of our problem framework of a cybersecurity application is depicted in Figure 3.1. In this illustration, a cloud is a collection of 4 centers connected to a single network (e.g., the internet). Within the cloud, different content (e.g., costumers' data) is stored amongst the 4 data centers. We assume data centers are autonomous and an interdiction on one of them has no direct effect on the others. Each content, represented by individually colored circles, can be replicated among different centers. Note that in Figure 3.1 the number of partitions, n_j, equals to 1 for all content.

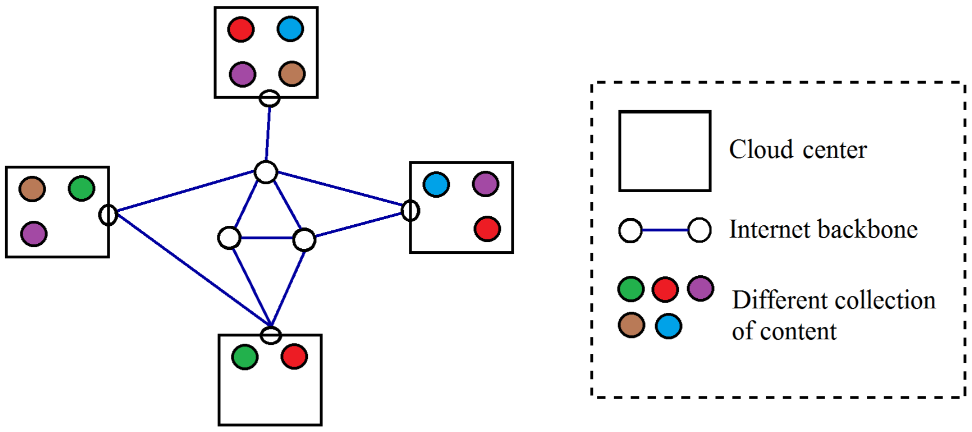

Figure 3.1: A model of the cloud representing a cybersecurity application

If the problem represents a smuggling problem, then the network will look like Figure 3.2. In this example 5 pieces of content attempt to pass through 3 centers and reach the destination node, t. All content in this example is also considered to be single-portioned.

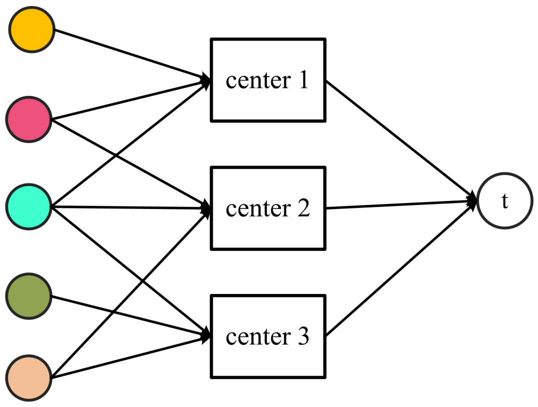

Figure 3.2: A model of a network representing a smuggling application

3.2.1 Problem Formulation

Table 3.1: Notation definitions of CCIP

Sets

I	set of centers, $i \in I$
J	set of content, $j \in J$

Parameters

B	number of interdictions an interdictor completes
n_j	number of partitions of content j, $k \in \{1, \ldots, n_j\}$
c_j	cost of available content j
$x^i_{jk} =$	$\begin{cases} 1 & \text{if } k^{th} \text{ portion of content } j \text{ is assigned to center } i \\ 0 & \text{otherwise} \end{cases}$

Variables

$z_i =$	$\begin{cases} 1 & \text{if center } i \text{ is interdicted} \\ 0 & \text{otherwise} \end{cases}$
$y_{j0} =$	$\begin{cases} 1 & \text{if content } j \text{ remains available through the network} \\ 0 & \text{otherwise} \end{cases}$
$y_{jk} =$	$\begin{cases} 1 & \text{if } k^{\text{th}} \text{ portion of content } j \text{ is unavailable, } k = 1, \ldots, n_j \\ 0 & \text{otherwise} \end{cases}$

Let $x \in X$ represent the current content assignment, then the problem's formulation is as follows:

Model (P):

$$\min \sum_{j \in J} c_j y_{j0} \tag{3.1}$$

Subject to

$$1 - y_{jk} \geq x^i_{jk} - z_i \qquad \text{for } i \in I,\ j \in J,\ k \in \{1, \ldots, n_j\} \tag{3.2}$$

$$\sum_{k=0}^{n_j} y_{jk} = 1 \qquad \text{for } j \in J \tag{3.3}$$

$$\sum_{i \in I} z_i = B \tag{3.4}$$

$$y_{jk} \in \{0,1\} \qquad \text{for } j \in J,\ k \in \{0, 1, \ldots, n_j\} \tag{3.5}$$

$$z_i \in \{0,1\} \qquad \text{for } i \in I \tag{3.6}$$

In the objective function, (3.1), we need to make sure that $y_{j0} = \min\limits_{k=1,\ldots,n_j} \max\limits_{i \in I} \{x^i_{jk}(1 - z_i)\}$ which means if at least one portion is not available (i.e., $\max\limits_{i \in I}\{x^i_{jk}(1 - z_i)\} = 0$), then the content is unavailable (i.e., $y_{j0} = 0$). This will be done by defining auxiliary variables of y_{jk} such that $1 - y_{jk}$ are equal to $\max\limits_{i \in I}\{x^i_{jk}(1 - z_i)\}$ for $k = 1, \ldots, n_j$. Based on constraint (3.2), if center i containing portion k of content j ($x^i_{jk} = 1$) is not interdicted ($z_i = 0$), then y^k_j should be equal to 0, which means portion k of content j is available. This constraint can also be written as $y_{jk} \leq z_i$ for all the k where $x^i_{jk} = 1$ since when $x^i_{jk} = 0$ the constraint imposes no restriction. Constraint (3.3) guarantees $y_{j0} = \mathop{min}\limits_{k \in \{1,\ldots,n_j\}} (1 - y_{jk})$. Note that in constraint (3.3) instead of equality sign we could use $\geq$, however, having only one unavailable portion is enough to have an unavailable content. Therefore, the relation between y_{j0} and the rest of the y_{jk} for each content j can be written as $y_{0k} + (y_{j1} + \ldots + y_{jn_j}) = 1$ which means either content j is available (i.e., $y_{j0} = 1$) after the interdictions or we can identify one portion k that is unavailable (i.e., $y_{jk} = 1$). Constraint (3.5) ensures exactly B centers get interdicted by the interdictor. Finally, we have variables' types in constraint (3.6).

Figure 3.3 represents a content assignment in a network containing 4 centers and 10 different content with known numbers of portions. As shown in Figure 3.3, content 1 has 3 portions, $1a$, $1b$, and $1c$, and content 9 has only 1 portion, $9a$. The second portion of content 1, $1b$, is assigned to centers 1 and 2, while the only portion of content 9 is assigned to centers 1 and 4.

Content		1			2		3			4		5		6			7	8	9	10		
Portion		1a	1b	1c	2a	2b	3a	3b	3c	4a	4b	5a	5b	6a	6b	6c	7a	8a	9a	10a	10b	10c
Centers	1	1	1	1	0	1	0	0	1	0	0	1	0	1	0	0	0	1	1	1	0	1
	2	0	1	0	1	0	0	1	0	1	1	0	1	0	0	1	0	0	0	1	1	0
	3	0	0	1	0	0	1	1	1	0	0	1	0	0	1	0	1	1	0	0	1	1
	4	1	0	0	0	1	1	0	0	1	0	0	1	1	1	0	1	0	1	1	1	0

Figure 3.3: An example of content assignment before the interdictions

The feasible solution of the problem depicted in Figure 3.4, indicates 2 interdictions to centers 1 and 3. After the interdictions, the third portion of content 1 is not available since it cannot be found on any of the non-interdicted centers, thus content 1 is unavailable. However, the set of content {2, 4, 6, 7, 9} remains available resulting in an objective function value (OFV) equal to $c_2 + c_4 + c_6 + c_7 + c_9$.

Content		1			2		3			4		5		6			7	8	9	10		
Portion		1a	1b	1c	2a	2b	3a	3b	3c	4a	4b	5a	5b	6a	6b	6c	7a	8a	9a	10a	10b	10c
Centers	~~1~~	~~1~~	~~1~~	~~1~~	~~0~~	~~1~~	~~0~~	~~0~~	~~1~~	~~0~~	~~0~~	~~1~~	~~0~~	~~1~~	~~0~~	~~0~~	~~0~~	~~1~~	~~1~~	~~1~~	~~0~~	~~1~~
	2	0	1	0	1	0	0	1	0	1	1	0	1	0	0	1	0	0	0	1	1	0
	~~3~~	~~0~~	~~0~~	~~1~~	~~0~~	~~0~~	~~1~~	~~1~~	~~1~~	~~0~~	~~0~~	~~1~~	~~0~~	~~0~~	~~1~~	~~0~~	~~1~~	~~1~~	~~0~~	~~0~~	~~1~~	~~1~~
	4	1	0	0	0	1	1	0	0	1	0	0	1	1	1	0	1	0	1	1	1	0
Available?					✓					✓				✓			✓		✓			

Figure 3.4: Content availability after the interdictions

Smuggling Network Problem

CCIP can also be related to the smuggling network problem in which a smuggler tries to travel on a path through a network in a way that maximizes his probability of evading some detections (Morton et al., 2007). The detections are installed by an interdictor that tries to minimize the probability. The interdictor attempts to install detectors/sensors on specific locations (i.e., checkpoints which can be considered to be at borders crossing of a country). The network defined for this problem can be represented as a bipartite network where nodes can be divided into two sets, one containing all the smuggled items and the other containing all the checkpoints. All the edges connect nodes from the two sets. CCIP can also be seen as a bipartite network in which content owners (the first set of nodes) attempt to find a path through the centers (the second set of nodes) installed in the network in a way to maximize their availability after some of centers are interdicted. The smuggling interdiction problem assumes that there are different paths for each content (e.g., a smuggled item) with specific probabilities between 0 and 1. Each path connects a node of the first set to a node of the second set and the smuggler will only choose one path based on the probability matrix. CCIP, on the other hand, allows content (e.g., a smuggled item) to be passed through multiple centers (e.g., checkpoints). Finally, instead of a matrix containing fractional values (i.e., probabilities), the matrix of CCIP contains 0 or 1 values. 0 represents that the content is not assigned to that center while 1 represents that it is. Thus a single-portioned CCIP problem is equivalent to the smuggling problem in which all probabilities in the matrix are either 0 or 1. However, in general, neither of those are a special case of the other.

Matrix Interdiction Problem

A special case of CCIP can be related to *matrix interdiction problem* defined by Pan and Kasiviswanathan (2010). The problem is motivated by security applications such as smuggled weapon and its objective is to remove K columns of a matrix in a way that the summation of the largest values in rows is minimized. Our single-portion problem also tries to remove centers in a way that all content is rendered unavailable. We can let each column and row in the corresponding matrix represent a center and content, respectively. Then, each row of the matrix is filled with values of 1 and 0 indicating whether or not the content is assigned to a center (column). In this scenario, our problem can be viewed as a matrix interdiction problem whose matrix can have values other than 0 and 1. The matrix interdiction problem with 0/1 values is proven to be NP-hard

(Pan and Kasiviswanathan, 2010). Since a single-portioned CCIP is equivalent to matrix interdiction problem, it can be concluded that CCIP is also an NP-hard problem. .

3.3 Proposed Enhancements to *P*

To improve the solving time and lower bound to P, we introduce multiple enhancements that are aimed to better enabling us to solve larger instances. Multiple combinations of these enhancements are to be discussed in Section 3.6. In the following sections, each of the enhancement is described.

3.3.1 Tightening Constraints

We introduce multiple constraints to reduce the size of feasible region. Three of them showing improvements when individually added to P are selected for the final enhanced models. In the following sections, each of them are described.

3.3.1.1 Content Availability Constraint

Let $\hat{I}_j$ be the minimum number of centers to which a portion of content j is assigned (i.e., the minimum number of interdictions required to make content j unavailable) and $\bar{I}_{ji}$ a parameter representing whether ($\bar{I}_{ji} = 1$) or not ($\bar{I}_{ji} = 0$) any portion of content j is assigned to center i. These two parameters can be calculated as follows:

$$\hat{I}_j = \min_{k=1,\dots,n_j} \sum_{i \in I} x^i_{jk} \qquad \forall j \in J \tag{3.7}$$

$$\bar{I}_{ji} = 1 \quad \text{if} \sum_{k=1,\dots,n_j} x^i_{jk} \geq 1, \quad 0, \text{ otherwise} \quad \forall j \in J, \forall i \in I \tag{3.8}$$

Constraint (3.9) requires the content to be available if all of its portions are assigned to more than B centers since none of the portions can be unavailable after attacking B centers. Constraint (3.10), on the other hand, forces $\hat{I}_j$ centers from all the centers containing content j to be interdicted when content j can be unavailable (i.e., $y_{j0} = 0$).

$$y_{j0} = 1 \qquad \forall j \in J, \hat{I}_j > B \tag{3.9}$$

$$\sum_{i \in I, \bar{I}_{ji}=1} z_i - \hat{I}_j * (1 - y_{j0}) \geq 0 \qquad \forall j \in J, \hat{I}_j \leq B \tag{3.10}$$

3.3.1.2 Portion Availability Constraint

Constraint (3.11) forces each y_{jk} to be equal to 0 if the portion is assigned to more than B centers. This means no matter which centers are interdicted, the portion is still available after the interdictions.

$$y_{jk} = 0 \qquad \forall j \in J, \forall k = 1, ..., n_j,\ \hat{I}_j > B \tag{3.11}$$

3.3.1.3 Symmetry Removing Constraint

As described in constraint (3.3), only one portion must be unavailable in order to make the content unavailable. In cases where there are multiple portions unavailable, there will be multiple solutions with the same OFV. In order to eliminate symmetrical solutions, we propose the following constraint:

$$y_j^k \leq \sum_{i \in I} x^i_{jk'}(1 - x^i_{jk})(1 - z_i), \qquad \forall j \in J,\ k \in \{2, \ldots, n_j\},\ k' \in \{1, \ldots, k-1\}. \tag{3.12}$$

Constraint 3.5 will ensure that the portion (k) whose value of y_{jk} is equal to 1 in constraint (3.3) is the first unavailable portion. For all those available portions before portion k, we know that y is equal to 0, thus this constraint impose no restrictions (the right hand side of the inequality will be a non-zero integer value). We also know that this constraint does not impose any restrictions on the first unavailable portion (e.g., k^1), since on the right hand side of the inequality there is always an available center for which a portion k', $k' < k^1$ is available and we know that $x^i_{jk^1}$ for those centers are 0 (since portion k is unavailable). The main purpose of this constraint occurs for the portions after the first unavailable portion. If a portion k, $k > k^1$ is not the first unavailable portion, this constraint will be $y_{jk} \leq 0$ because of the restriction imposed by the first unavailable portion (i.e., k^1) since any time z_i is 0, $x^i_{jk^1}$ is 0.

3.3.2 Modified Objective Function

The inclusion of constraint (3.12) results in a much larger problem. Therefore, we consider a second approach to remove the symmetry in the problem. However, we test both of these methods in Section 3.6

Consider the two models of P_1 and P_2 with the same feasible region as model P. Model P_1 is exactly the same as model P while model P_2 has one difference in the OF as shown below. We denote the difference in the OFs, α, which is equal to $(\sum_{j\in J}\sum_{k=1}^{n_j}\frac{ky_{jk}}{n_j+1})/|J|$.

Model P_1

$$\min \sum_{j\in J} c_j y_{j0} \tag{3.13}$$

Model P_2

$$\min \sum_{j\in J} c_j y_{j0} + \frac{\sum_{j\in J}\sum_{k=1}^{n_j}\frac{ky_{jk}}{n_j+1}}{|J|} \tag{3.14}$$

Theorem 1 *If there exists an optimal solution (OS) to P_2, the solution is also optimal to P_1 and the optimal OFV of P_1 is the floor of the optimal OFV of P_2.*

Proof. Let $s^* = (z^*, y^*)$ be the OS of P_2 with $OFV_{P_2}(s^*)$. It is also a feasible solution to P_1 since both problems have the same feasible region. Assume s^* is not optimal for P_1 and there exists a feasible solution s' which has a better OFV for P_1 than s^* does. Without of loss of generality all the c_j are assumed to be integer valued, therefore, the minimum positive difference between each pair of c_j is greater than or equal to 1. So:

$$OFV_{P_1}(s') \leq OFV_{P_1}(s^*) - 1 \tag{3.15}$$

We also know that s' is feasible to P_2 with an $OFV_{P_2}(s') = OFV_{P_1}(s') + \alpha_{s'}$ where $\alpha_{s'} = (\sum_{j \in J} \sum_{k=1}^{n_j} \frac{ky'_{jk}}{n_j+1})/|J|$ for s' solution. Since constraint (3.3) indicates at most one of the y_{jk} variables in this summation is equal to one, we have that $\sum_{k=1}^{n_j} ky_{jk}/(n_j+1) < 1$, hence it is concluded that $0 \leq \alpha_{s'} < 1$. Now we have:

$$\begin{aligned} &OFV_{P_2}(s') = OFV_{P_1}(s') + \alpha_{s'} \leq OFV_{P_1}(s^*) - 1 + \alpha_{s'} < \\ &OFV_{P_1}(s^*) \leq OFV_{P_1}(s^*) + \alpha_{s^*} = OFV_{P_2}(s^*) \end{aligned} \tag{3.16}$$

This means s' is a better solution than s^* for P_2 (i.e., $OFV_{P_2}(s') < OFV_{P_2}(s^*)$), which contradicts the optimality of s^* for P_2. □

The theorem proves that if the α part of the objective function in P_2 is added to the OF of model P it will not affect the optimal OFV and the floor of the OS's OFV_{P_2} is the same as OFV_{P_1}. This part in the OF lets the model to choose the first unavailable portion, which has the smallest k, for each content to have the value of 1 for its y_{jk} variable. Therefore, based on the fact that the problem is a minimization one, all the other solutions in which a $y_{k'j} = 1$ where k' is not the first unavailable portion will not be considered.

3.3.3 Relaxing Problem *P*

It can be proven that if all y_{jk} variables are binary and the interdiction decision variables are relaxed (i.e., $z_i \in [0,1]$), then a solution in which all variables are binary still exists. The proof is available in Appendix 3.A. Since the number of z-variables is smaller than the number of y-variables, we propose a theorem in which it shows that if z-variables are binary, then all the y-variables can be relaxed without changing the problem's OFV.

Theorem 2 *If all y_{jk} variables are relaxed in problem P (i.e., $y_{jk} \in [0,1]$), it will not change the optimal OFV. Also all y_{j0} will be binary valued in the optimal solution and the solution can be modified so that all other y variable are also binary valued. The modified solution is also an optimal solution to problem P.*

Proof. Let problem P_3 be the same as problem P but with relaxed y-variables. Assume $s^* = (z^*, y^*)$ is an OS of problem P_3 and it contains some fractional y-values. Note that the OFs of both problems are the same and problem P_3's feasible region contains problem P's feasible region. If we find a solution for problem P which has the optimal OFV of problem P_3, we know it is an OS of problem P.

Since the interdiction of each content is purely dependent on the values of z_i variables and independent of other content and also in the modification, we only change the y-variables (and not the z), without loss of generality we can assume that we only have one content in our problem. There can be 4 cases defined for y values in s^* as follows:

1- All y^*_{jk}, $\forall k \geq 0$ are binary valued

2- y^*_{j0} is binary valued and at least one of the y^*_{jk}, $\forall k \geq 1$ has a fractional value

3- y^*_{j0} has a fractional value and all the other y^*_{jk}, $\forall k \geq 1$ are either 0 or 1

4- y^*_{j0} and at least one of y^*_{jk}, $\forall k \geq 1$ have fractional values

Case 1: If all the y^*_{jk} variables are binary valued for content j, then there is nothing required to be done to modify the solution and it is an OS to problem P.

Case 2: Having a binary value for y^*_{j0} means the the solution can be modified to a solution which is also feasible to problem P. Since there are some fractional values for y^*_{jk}, $\forall k \geq 1$, based on constraint (3.3) it can be concluded that y^*_{j0} cannot be 1, hence it is 0. Constraint (3.2) is the only constraint that includes y-variables for portions. Depending on the binary values of z^*_i variables, constraint (3.2) can be equal to: $y^*_{jk} \leq 0$ or $y^*_{jk} \leq 1$, $\forall k \geq 1$. If there is at least one k' for which $y^*_{jk'}$ has a fractional value, it means for none of the centers, constraint (3.2) became $y^*_{jk'} \leq 0$ and that is why $y^*_{jk'}$ can have a fractional value. If so, all the other possible fractional values of y^*_{jk},

$\forall k = 1, ..., n_j,\ k \neq k'$ can be reduced to 0, so that $y^*_{jk'}$ can become 1. Constraint (3.3) will remain satisfied and since y^*_{j0} has still the same value, 0, the OFV will not change. This means the modified solution is also feasible to problem P (it is still satisfying other constraint since they do not include $y^*_{jk}, \forall k \geq 1$) and has the same OFV as s^*.

Case 3: This case cannot occur because of constraint (3.3).

Case 4: If there is at least one portion k' with fractional value, for all centers i containing this portion, constraint (3.2) under fixed z^* reduces to $y^*_{jk'} \leq 1$. This means by increasing the value of $y^*_{jk'}$ to 1 and setting all the other $y^*_{jk}, \forall k = 1, ..., n_j,\ k \neq k'$ to 0 (whether they are already 0 or they have fractional values), y^*_{j0} can be equal to 0. This means the OFV can be reduced by the product of c_j and the previous fractional value of y^*_{j0} which contradicts with the optimality of the solution s^*. So this case cannot occur. □

Note that in a case with multiple content, the modification can occur for each one of them independently. So any OS of P_3 can be modified to a solution that is also feasible and optimal to problem P. We also know that all the values of y^*_{j0} are binary in the OS of P_3 and we just need to modify the values of y for portions.

3.3.4 Custom Branching

Theorem 2 showed that y variables can be relaxed if all the z variables are forced to be binary valued. Also, in the GA (Section 3.4) each solution is just represented by a chromosome containing z values and then y values can be calculated based on them. These motivated us to generate a custom variable selection rule to control branching in the CPLEX branch-and-bound solver. Three of the considered branching rules will be explained in the following two sections.

3.3.4.1 Branching on z-variables

In this custom branching, at each fractional-valued node, z variables' values will be checked according to the order described in the next paragraph. Then, the first z variable (e.g., z_i) with fractional value will be selected to be branched. Therefore, one of the two nodes derived from the current node on the branch will have $z_i = 1$ as a new constraint and the other will have $z_i = 0$.

In a preprocessing step prior to beginning the solution algorithm, all centers will be sorted based on the *"worth"* of all content portions assigned to them. The worth of each center can be calculated based on the total value of content portions assigned to it. If it is a single-portioned problem, the worth of center j is equal to the summation of c_j-values of all content assigned to it (i.e., $\sum_{j\in J}\sum_{k=1}^{n_j} x_{jk}c_j$). If it is a multiple-portioned problem, depending on the number of content j's portions assigned to a center, only a fraction of c_j will be considered in this value (i.e., $\sum_{j\in J}\sum_{k=1}^{n_j}(x_{jk}/n_j)c_j$). For example if content j has 3 portions and value of c_j and center i contains two of them, worth of center i will be contain the value of $\frac{2}{3}c_j$. After each center's worth is calculated, they will be sorted in an decreasing order. For instance, in Figure 3.1 the 3 values for centers 1, 2, and 3 are calculated as follows:

$$\text{center 1: } (2/2)c_1 + (2/3)c_2 + (3/4)c_3 = 50 + 40 + 75 = 165$$
$$\text{center 2: } (1/2)c_1 + (1/3)c_2 + (1/4)c_3 = 25 + 20 + 25 = 70$$
$$\text{center 3: } (1/2)c_1 + (1/3)c_2 + (2/4)c_3 = 25 + 20 + 50 = 95$$

Therefore, the decreasing order of centers is: center 1 - center 3 - center 2. This order will be used in Sections 3.3.4 and 3.4.

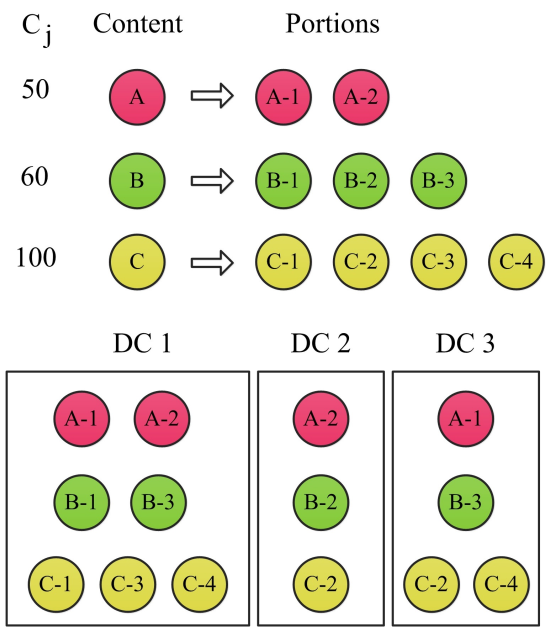

Figure 3.1: An example for preprocessing

3.3.4.2 Branching on $\mathbf{y_{j0}}$-variables

Testing the first custom branching motivated us to do the same for y variables. Since an important y variable is y_{j0}, we attempt to force branching on y_{j0} according to an order. Each y_{j0} will be assigned a value, called w_j. Each w_j parameter indicates *worth* of the associated y_{j0} variable and is determined by (3.17). A w_j is more if its c_j value is higher and it is assigned to less number of centers which makes it easier to be unavailable.

$$w_j = \frac{c_j}{\sum_{i \in I} x^i_{jk}} \qquad \forall j \in J \tag{3.17}$$

However, the *worth* of each content is better to be dynamically calculated during the branch and bound procedure when values (including fractional values) of z variables are known for each node. Then, the w parameters are calculated by (3.18).

$$w_j = \frac{c_j}{\sum_{i \in I,\, z_i = 0} x^i_{jk}} \qquad \forall j \in J \tag{3.18}$$

(3.18) differs from the order in (3.17) since it considers how hard it is for the content to be unavailable now that some of the z_i variables are known (i.e., interdiction decisions for the associated centers are made). Then, the same procedure as Section 3.3.4.1 is performed when branching only occurs on y_{j0} variables according to the order described in (3.18).

3.3.4.3 Branching on z-variables and $\mathbf{y_{j0}}$-variables

We also consider a mixed branching. In this branching, an initial parameter is determined at the beginning of solving IP. Then, for each node a discrete Uniform variable between $[1,100]$ is generated. If the value of the generated variable is less than the parameter, then the next branch is performed on the first z variable according to order described in 3.3.4.1 that has a fractional value; otherwise it is performed on the first y_{j0} according to order (3.18) with a fractional value.

Note that if the parameter is 0, the branching is equal to the one explained in Section 3.3.4.2 and if it is equal to 100, the branching discussed in Section 3.3.4.1 is performed.

3.4 Genetic Algorithm (GA)

Since solving time of the IP model for large sized problems is high, we developed a GA whose solution in a short amount of time can assist IP as an initial solution to reduce its solving time. The steps of the proposed GA are described as follows:

Step 1. An initial population is randomly generated.

Step 2. The fitness of each individual is computed.

Step 3. At each generation the first two individuals are the two elites, taken from the last generation, and the remaining population size - 2 individuals are selected using a tournament of size of two.

Step 4. If possible, a crossover is then applied on each pair of parents, except for the first two.

Step 5. Two rounds of mutations with fixed probabilities are applied on offspring, except for the first two offspring.

Step 6. If none of the termination criteria is met, return to step 3.

In the following sections, each of the steps will be explained.

3.4.1 Encoding a Chromosome

Given the results from Theorem 2, we define each chromosome only based on the z-variables. Each chromosome, representing a solution, has one part containing $|I|$ (number of centers) genes. A gene is equal to 1, if the corresponding center is interdicted and 0, if it is not interdicted.

In Figure 3.4.1, a chromosome representation of one feasible solution is presented. This chromosome represents a problem in which there are 7 centers and 3 (2, 3, and 7) of them are assumed to be interdicted in the inner problem.

centers	1	2	3	4	5	6	7
attacked or not?	0	1	1	0	0	0	1

Figure 3.1: Representation of a chromosome

3.4.2 Initial Population

The fist chromosome in the first population is based on order calculated in preprocessing part. The first B centers according to the order will be equal to 1 and the rest of the genes will be equal to 0. This follows the same greedy algorithm developed in Pan and Kasiviswanathan (2010). To generate the rest of the population, for each chromosome B centers are randomly chosen to be interdicted and their genes become 1, then the rest of the genes will be equal to 0. This occurs until population size, PS, chromosomes are generated. Multiple PSes were tested with different combination of other parameters. PS=50 showed to be the most effectiveness for all sizes (small to large). Larger PSs (e.g.,100) cause each generation to take more time for larger instances and eventually affected the best fitness. On the other hand, smaller PSes (e.g., 20), made improvement between iterations slower and were not as effective as PS=50.

3.4.3 Fitness Calculation

To calculate the fitness of each chromosome, each content's portion gets checked to see that it is available on at least one of the centers which are not interdicted. If there is at least one portion which is not available on any of the unattached centers, it means the content is unavailable and this will not affect the fitness value. If, however, a content is available, its c_j will be added to the fitness value. The first population of chromosomes will be the children who will generate the first set of parents at iteration 1.

3.4.4 Selection

At each iteration the first two parents of each population will be the two elites of the last population. Other parents are selected using a tournament of size of two which means two random parents will be chosen among all the parents and the one with lower fitness will be selected as the next parent until we have *PS* parents. Note that at each iteration the best child will be replaced by the global best chromosome if its fitness is less than the global best chromosome's fitness.

3.4.5 Crossover

At each iteration, one single point crossover is used to generate offspring for all pairs of parents except for the first two. The one point crossover may occur at a point before which both parents have the same number of genes equal to 1, so that both of the children after the crossover still have B numbers of genes equal to 1.

Starting from the 3rd parent, a crossover occurs for each pair of parents. In order to do a crossover on the parents, a crossover point needs to be designated. The initial value for this point is $\lfloor |I|/2 \rfloor$. To determine if the crossover can occur for this point, the total number of genes equaled to one from the first gene up to the candidate point are counted. If the numbers are equal for both parents, then a crossover is performed; otherwise, in an iterative process, points before and after the initial point will be considered respectively. For example, if the two parents have

$|I| = 20$ genes, point 10 is initially the candidate of the crossover. If the crossover cannot be performed, then point 9 (and then 11) are the candidate. The numbers that will be considered will be in this order: 10, 9 , 11, 8, 12, 7, 13, 6, 14, etc. The search stops if it reaches to a point for which the crossover can be performed or it reaches to the first or the last center since even if the crossover is performed, no difference will result between the children and the parents.

For example, in Figure 3.2, the first candidate point for the crossover is 4. The first parent has 2 genes equal to 1 (genes 2 and 3) before the point while the second parent has only one gene equal to 1 (gene 1). Therefore, the crossover cannot occur at point 4. The next point to be considered is point 3. There are two genes of parent 1 equal to 1 and 1 gene of parent 2, so point 5 will be considered next. Still the numbers of ones before the point 5 are not equal. The next point to be considered is point 2 before which both parents have the same numbers of genes equal to 1. Therefore, the crossover occur at point 2.

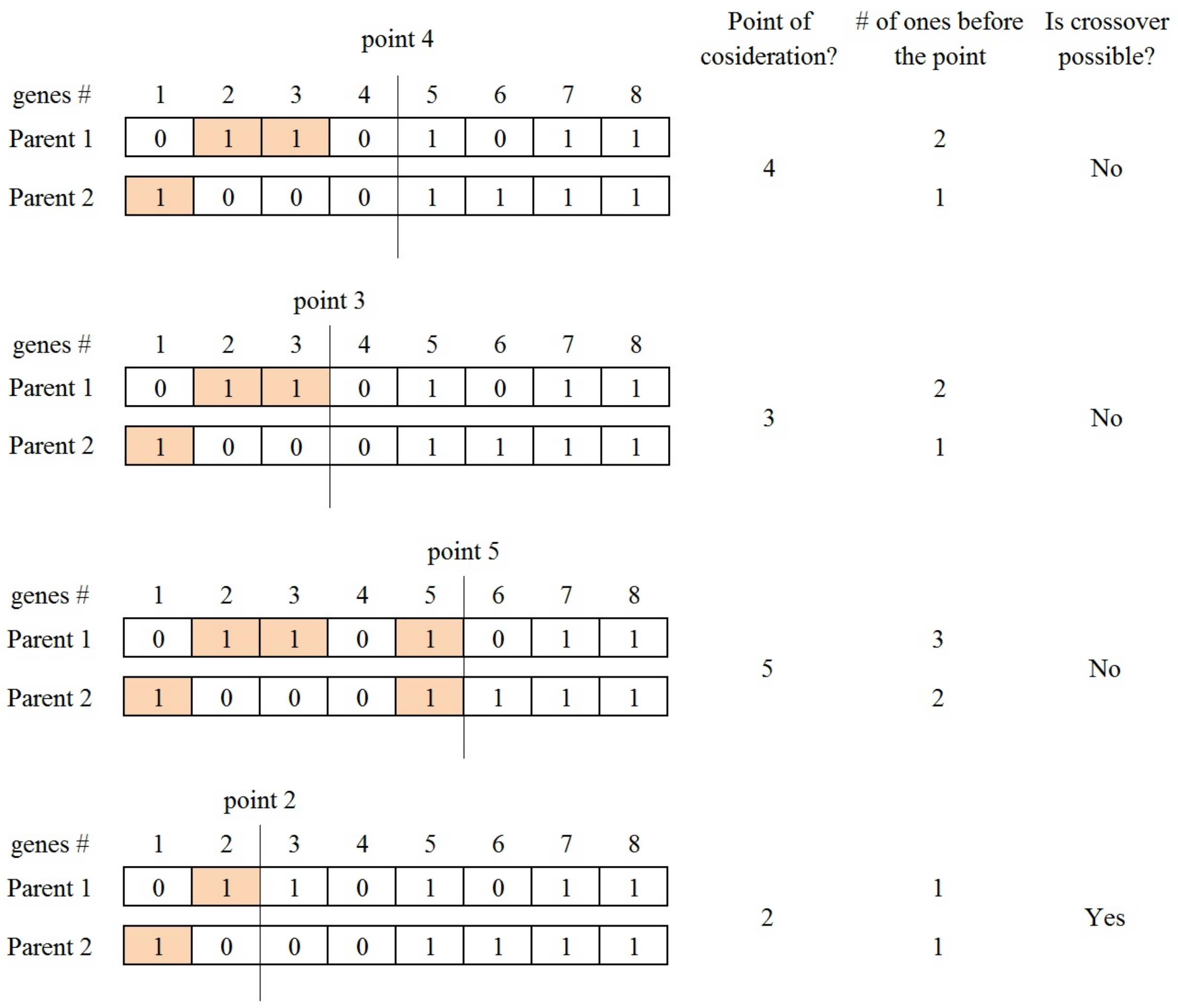

Figure 3.2: Selection of a point for a crossover

As shown in Figure 3.3, child 1 inherits the first two genes of parent 2 and the others from parent 1 and child 2 inherits the first two genes from parent 1 and the others from parent 2.

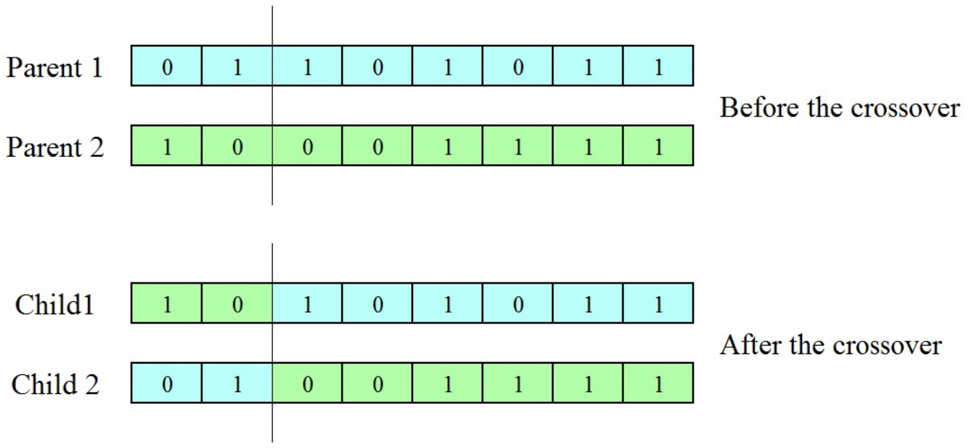

Figure 3.3: Representation of the crossover

In general, for each crossover, this process continues between points on the left side and then right side consecutively until the first or the last centers. Note that our search does not start from the first gene because the goal of our crossover is that both offspring inherit the most from both parents. Thus, it is desirable for the crossover to happen at a point closer to the middle gene. However, based on the chromosome structure, the crossover cannot occur for all pairs of parents. The lower the number of the centers, the smaller chance there is to find a point at which the crossover can happen. Also, by increasing the number of centers, the chance of finding such point will be high and as a result the crossover will occur for almost all the pairs of parents. Therefore, a maximum rate of crossover is enforced to prevent a crossover from occurring between all pairs. After testing multiple values, 60% was chosen since it showed the most rapid improvement for various problem sizes.

3.4.6 Mutation

After generating *PS* children, two consecutive rounds of single point mutations are applied on each child by probabilities of 0.25. This means there is a 0.0625 (0.26*0.25) chance that a child has two single point mutations. The probability of the first mutation is equal to 0.5 for problems with 5000 content or more, but the second mutation's probability remains 0.25. In order to do a mutation, two different genes with different values will be chosen and their values will be swapped. As shown in Figure 3.4, gene 3 and 4 switch their values after mutation.

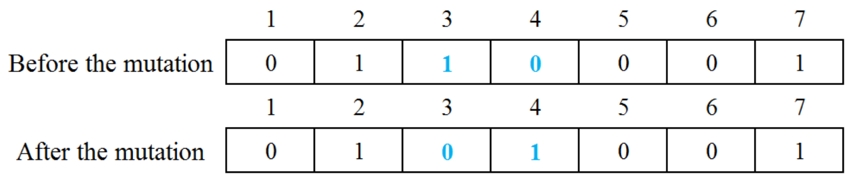

Figure 3.4: Mutation Representation

After the mutation, all children's fitnesses will be calculated and the best of them will replace the global best solution if it has a lower fitness. All children will be then considered as candidates to be parents for the next iteration.

3.4.7 Stopping Criteria

This process continues until one of the stopping criteria according to 3.1 is met. For instances with 4000 content they are: 1- 1000 total iterations, 2- 100 iterations without improvement in the best chromosome's fitness, 3- 120 seconds time limit. These values have been fixed after multiple runs of tests to make sure there is enough time for improvement while not spend extra time when the chance of getting better solution is low.

Table 3.1: GA's stopping criteria

# of content	time limit (sec)	maximum iterations	maximum iterations without improvement
1-99	30	1000	25
100-999	60	1000	50
1000-4999	120	1000	100
5000-9999	300	1000	300
10000-19999	600	1000	400
20000^{+}	1200	1000	500

3.5 Other Attempted Methods

Given that the problem is NP-hard, different exact large-scale solution methods have been tested. In the following paragraphs the ones which did not outperform the original model will be briefly described.

Reformulation-Linearization Technique (RLT): Two sets of first level RLT (Sherali and Adams, 1998) were tested on multiple instances (single and multiple portioned content) to see if it can reduce the solving time of the problem or generate a good lower bound for the P formulation in a shorter amount of time. Although it managed to reach to the optimal solution for most of the single portioned instances, the efforts did not last due to the number of variables and constraints added to the formulation which caused memory loss. Also, solving time in almost all the instances were not comparable with P's.

Benders Decomposition: Given that z variables can be relaxed, we attempted to solve the problem with a Benders decomposition (BD) approach. BD requires its subproblem (SP) to be a continuous linear or nonlinear programming problem, so that the dual of the SP can be used to obtain optimality and feasibly cuts. All the variables and constraints containing the relaxed z variables were moved to the subproblem. Since coefficients of all z variables in the original problem's OF is 0, only feasibility cuts were applied to the master problem (MP) after each iteration. Two BD approaches were implemented, the traditional iterative BD and BD with application of Lazy Constraint Callback which was described in section **??**. Unfortunately, none of the approaches could outperform the P even for small instances.

Logic-based Decomposition: We also pursued a logic-based decomposition approach which is inspired by Benders decomposition approach. Same approach with application of Lazy Constraint Callback, as described in Chapter 2 and shown in Figure 2.5, was applied for this problem. The difference with the BD described in the previous paragraph was that instead of solving the dual of the SP, the original SP was solved and a newly defined feasibility cut, which was responsible to cut the current node was applied. Again, the solving time could not outperform the P

solving time.

3.6 Computational Results

100 different instances with 10 to 30000 content and 3 to 300 centers were generated. The data of different instances are presented in Table 3.1. There are two types of problems, single portioned (S) and multiple-portioned (M). In all the M instances, the number of portions is randomly chosen to be between 3 to 7. There are 50 single portioned problems (S1-S50) and 50 multiple ones (M1-M50). c_js are randomly generated between 10 to 40.

Table 3.1: Single and multiple portioned instances data

Single instance #	Multiple instance #	# of content	# of servers	# of interdictions	Single instance #	Multiple instance #	# of content	# of servers	# of interdictions
S1	M1	10	3	1	S26	M26	4000	50	45
S2	M2	10	3	2	S27	M27	7000	70	5
S3	M3	20	4	1	S28	M28	7000	70	10
S4	M4	20	4	3	S29	M29	7000	70	35
S5	M5	50	6	2	S30	M30	7000	70	60
S6	M6	50	6	4	S31	M31	10000	100	5
S7	M7	100	10	2	S32	M32	10000	100	10
S8	M8	100	10	7	S33	M33	10000	100	20
S9	M9	200	15	3	S34	M34	10000	100	50
S10	M10	200	15	7	S35	M35	10000	100	90
S11	M11	200	15	12	S36	M36	15000	150	10
S12	M12	400	20	4	S37	M37	15000	150	20
S13	M13	400	20	10	S38	M38	15000	150	30
S14	M14	400	20	16	S39	M39	15000	150	75
S15	M15	800	25	5	S40	M40	15000	150	120
S16	M16	800	25	12	S41	M41	20000	200	10
S17	M17	800	25	22	S42	M42	20000	200	20
S18	M18	1000	30	5	S43	M43	20000	200	40
S19	M19	1000	30	15	S44	M44	20000	200	100
S20	M20	1000	30	25	S45	M45	20000	200	150
S21	M21	2000	40	5	S46	M46	30000	300	15
S22	M22	2000	40	20	S47	M47	30000	300	30
S23	M23	2000	40	35	S48	M48	30000	300	60
S24	M24	4000	50	5	S49	M49	30000	300	150
S25	M25	4000	50	25	S50	M50	30000	300	250

As shown in Table 3.1, each content number has multiple instances with different values of B (e.g., problems S1 and S2). Note that the problems with the same letter (S or M) and number of content have same assignments such as problems S3 and S4 whose only difference is the number of B. All instances were solved by CPLEX 12.6.3 on a 12-core 12 GB computer. Time limit for each instance is shown in Table 3.2. A stopping gap of 0.001% was used, where

$$\text{gap} = \frac{\text{best integer solution's OFV} - \text{best linear programming relaxation solution's OFV}}{\text{best integer solution's OFV}} * 100$$

Table 3.2: Time limit

Problem #	Time limit (min)
S1-S30	30
S31-S40	60
S41-S50	120
M1-M30	60
M31-M40	120
M41-M50	180

Each enhancement described in Section 3.3 was individually run on a subset of the S and M instances. Then, combinations show to improve either on solving time, objective function value, or lower bound (LB) in the assigned time limit were pursued. Figure 3.1 presents the implementation that incorporates multiple enhancements. Initially, the preprocessing occurs which sort centers based on the order described in Section 3.3.4.1. Then, the GA is run and its best solution is used as an initial solution to an enhanced version of *P* which exploits a custom branching. Both solving time or gap will be our base of comparison between *P* solved with default CPLEX and the enhanced version of *P* that also makes use of the proposed genetic algorithm.

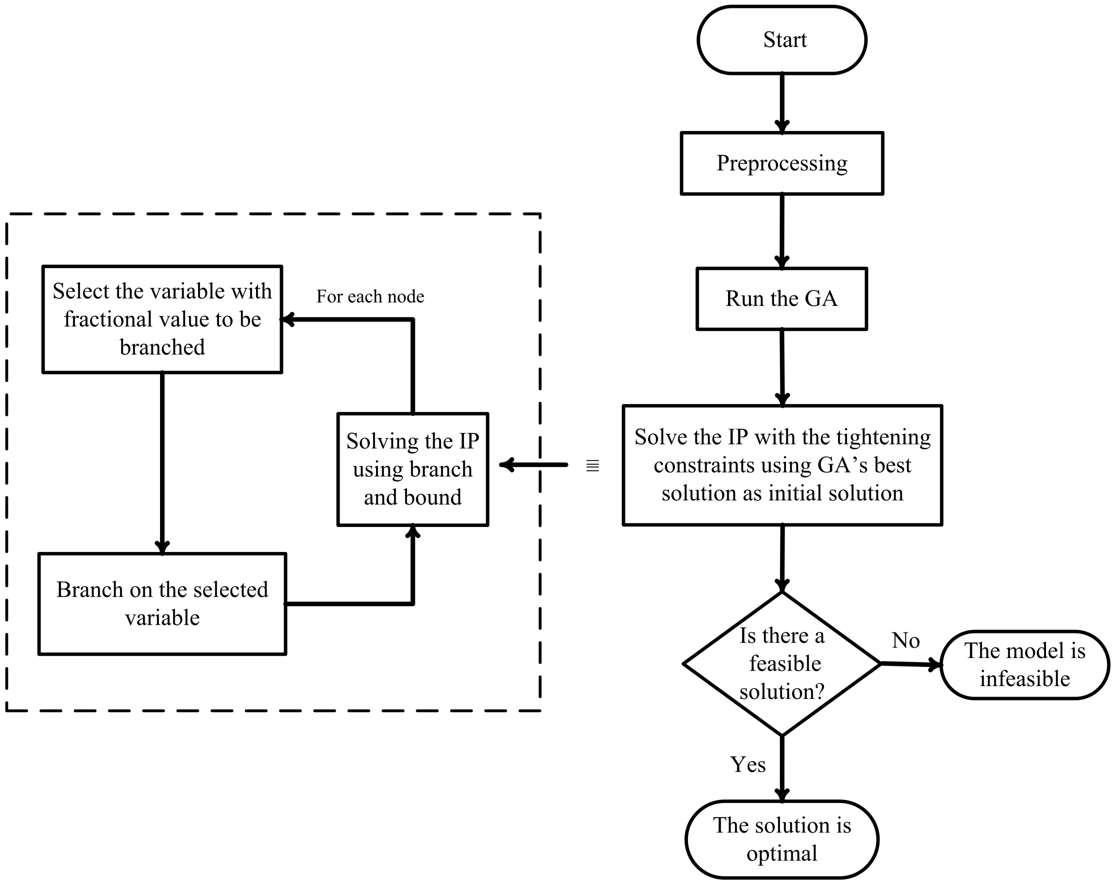
Start
Preprocessing
Run the GA
Solve the IP with the tightening constraints using GA's best solution as initial solution
Is there a feasible solution?
No
The model is infeasible
Yes
The solution is optimal
≡
Select the variable with fractional value to be branched
For each node
Solving the IP using branch and bound
Branch on the selected variable

Figure 3.1: An illustration of using multiple enhancements in a model

3.6.1 Different IP Formulations for Solving Single-Portioned (S) Instances

After attempting multiple combinations of the implementation features, the three best were considered in a full comparison with P solved by a standard IP solver. The implementations considered are defined as follows:

- P, which is the original IP
- P_1^S, in which y variables are binary. It includes constraints (3.9), (3.10), and (3.11), and utilizes GA and branching on z variables as discussed in Section (3.3.4.1).
- P_2^S, in which y variables are continuous. It includes constraints (3.9), (3.10), and (3.11), and utilizes GA and branching on z variables as discussed in Section (3.3.4.1).
- P_3^S, in which y variables are binary. It includes constraints (3.9), (3.10), and (3.11), and utilizes GA and branching on z and y_{j0} variables as discussed in Section (3.3.4.3) with the parameter of 50.

Table 3.3 contains all the data regarding the enhancements used in the 4 IP models used to solve S instances.

Table 3.3: Implementations to solve S problems

IP model	Binary y variables	Continuous y variables	GA	Constraint (3.9)	Constraint (3.10)	Constraint (3.11)	Branch on z	Branch on y and z
P	✓							
P_1^S	✓		✓	✓	✓	✓	✓	
P_2^S		✓	✓	✓	✓	✓	✓	
P_3^S	✓		✓	✓	✓	✓		✓

3.6.2 Different IP Formulations for Solving Multiple-Portioned (M) Instances

Five different models (including the original P) are represented in this section to solve M problems. All models contain binary valued y variables as the continuous y variables were not as efficient for M problems. Note that the utilization of constraint (3.12) or the modified OF in (3.14) are only performed when we have an M instance.

- P, which is the original P
- P_1^M, which includes constraints (3.9), (3.10), (3.11), and (3.12) and utilizes GA .
- P_2^M, which includes constraints (3.9), (3.10), and (3.11), and (3.12), and utilizes GA and branching on z variables as discussed in Section (3.3.4.1).
- P_3^M, which includes constraints (3.9), (3.10), and (3.11) and OF in (3.14), and utilizes GA and branching on z variables as discussed in Section (3.3.4.1).
- P_4^M, which includes constraints (3.9), (3.10), and (3.11), and (3.12), and utilizes GA and branching on z and y_{j0} variables as discussed in Section (3.3.4.3) with the parameter of 50.

Table 3.4 contains information regarding enhancements included in the 5 models used to solve M instances.

Table 3.4: Implementations to solve M problems

Models	GA	Constraint (3.9)	Constraint (3.10)	Constraint (3.11)	Constraint (3.12)	OF (3.14)	Branch on z	Branch on y and z
P								
P_1^M	✓	✓	✓	✓	✓			
P_2^M	✓	✓	✓	✓	✓		✓	
P_3^M	✓	✓	✓	✓		✓	✓	
P_4^M	✓	✓	✓	✓	✓			✓

Note that only z values taken from the best solution of the GA are fed to the models as an initial solution. We also tested different CPLEX parameters and our findings suggest the following values settings: Effort Level =1 (default), Advance=1 (default), Emphasis = 1 (feasibility over optimality).

3.6.3 Results of Single-Portioned Instances

Out of the 50 S instances, 30 were solved by all the 4 models during the specified time limits. Table 3.5 shows the best OFV, LB, solving time and, OFV of the best solution obtained form GA for each instance. Note that GA took a minimum of 2% and a maximum of 100% of the total the solving times of each model (without considering the instances whose both solving time and GA time are 0.0 seconds). Models P_1^S , P_2^S, and P_3^S spent an average of 40%, 39%, and, 46% of the total solving time in GA, respectively. Details of GA times can be found in Appendix 3.B. The stopping criterion which stopped the GA for most of the 50 S instances was the number of iterations without improvement. It stopped 45, 48, and 44 instances for P_1^S, P_2^S, and P_3^S, respectively. The remaining instances were stopped by the maximum time limit.

The best solving times are highlighted with blue color in Table 3.5. Problems S1-S11 were solved in approximately 0.0 seconds, thus all of the 4 models are highlighted. As expected, many of the smaller instances are solved in shorter amount of time by P. However, P_1^S managed to solve three of the medium sized instances (S22, S25, and S30) quicker than P.

Table 3.5: S instances that were solved in the time limit

Model	P			P_1^S				P_2^S				P_3^S			
Prob #	Best OFV	LB	Time (s)	Best OFV	LB	Time (s)	GA OFV	Best OFV	LB	Time (s)	GA OFV	Best OFV	LB	Time (s)	GA OFV
S1	196	196	**0.0**	196	196	**0.0**	196	196	196	**0.0**	196	196	196	**0.0**	196
S2	165	165	**0.0**	165	165	**0.0**	165	165	165	**0.0**	165	165	165	**0.0**	165
S3	499	499	**0.0**	499	499	**0.0**	499	499	499	**0.0**	499	499	499	**0.0**	499
S4	325	325	**0.0**	325	325	**0.0**	325	325	325	**0.0**	325	325	325	**0.0**	325
S5	1027	1027	**0.0**	1027	1027	**0.0**	1027	1027	1027	**0.0**	1027	1027	1027	**0.0**	1027
S6	721	721	**0.0**	721	721	**0.0**	721	721	721	**0.0**	721	721	721	**0.0**	721
S7	2343	2343	**0.0**	2343	2343	**0.0**	2343	2343	2343	**0.0**	2343	2343	2343	**0.0**	2343
S8	1429	1429	**0.0**	1429	1429	**0.0**	1429	1429	1429	**0.0**	1429	1429	1429	**0.0**	1429
S9	4616	4616	**0.0**	4616	4616	**0.0**	4616	4616	4616	**0.0**	4616	4616	4616	**0.0**	4616
S10	3819	3819	**0.0**	3819	3819	**0.0**	3819	3819	3819	**0.0**	3819	3819	3819	**0.0**	3819
S11	1524	1524	**0.0**	1524	1524	**0.0**	1524	1524	1524	**0.0**	1524	1524	1524	1.0	1524
S12	9384	9384	**0.0**	9384	9384	0.1	9384	9384	9384	0.1	9384	9384	9384	0.1	9503
S13	7588	7588	**0.0**	7588	7588	0.1	7627	7588	7588	0.1	7588	7588	7588	0.1	7588
S14	3543	3543	**0.0**	3543	3543	0.1	3543	3543	3543	1.1	3543	3543	3543	1.1	3543
S15	18365	18365	1.0	18365	18365	**0.2**	18365	18365	18365	**0.2**	18365	18365	18365	**0.2**	18365
S16	14930	14930	2.0	14930	14930	2.2	14930	14930	14930	1.2	15032	14930	14930	3.2	15032
S17	4128	4128	**1.0**	4128	4128	1.1	4128	4128	4128	1.1	4128	4128	4128	2.1	4128
S18	23356	23356	1.0	23356	23356	1.4	23356	23356	23356	**0.7**	23356	23356	23356	**0.7**	23487
S19	18852	18852	5.0	18852	18852	5.4	19030	18852	18852	**4.4**	18892	18852	18852	5.5	18892
S20	7835	7835	**2.0**	7835	7835	3.4	7835	7835	7835	2.7	7835	7835	7835	2.5	7835
S21	47550	47550	**2.0**	47550	47550	3.7	47679	47550	47550	3.1	47550	47550	47550	4.4	47679
S22	36758	36758	32.0	36758	36758	**28.4**	36942	36758	36758	32.3	36758	36758	36758	40.1	37141
S23	8432	8432	**4.0**	8432	8432	8.0	8432	8432	8432	5.2	8432	8432	8432	8.2	8432
S24	95982	95982	**5.0**	95982	95982	7.8	95982	95982	95982	8.1	95982	95982	95982	10.2	95982
S25	72238	72238	140.0	72238	72238	**130.7**	72336	72238	72238	146.5	72238	72238	72238	185.4	72336
S26	15473	15473	**15.0**	15473	15473	18.3	15473	15473	15473	24.3	15473	15473	15473	20.3	15473
S27	169653	169653	**24.0**	169653	169653	55.6	169777	169653	169652	96.6	169653	169653	169653	127.6	169653
S30	49006	49006	407.0	49006	49006	**191.0**	49006	49006	49006	285.7	49006	49006	49006	223.8	49103
S31	242752	242752	**48.0**	242752	242751	158.5	242752	242752	242752	202.3	242752	242752	242752	248.5	242752
S35	43640	43640	**157.0**	43640	43640	295.1	43640	43640	43640	634.6	43750	43640	43640	402.1	43640

In order to compare the other 20 instances which are not solved to optimality in the specified time limits, the best OFVs, LBs, and gaps of all enhanced models are divided by those of P. Since OFVs and gaps are better to be smaller, the associated percentages are preferred to be less than 100% when divided by P's OFVs and gaps. However, the numbers are better to be more than 100% for LBs since a higher LB is desired. The detailed results of each model is presented in Appendix 3.B and 3.C.

Figure 3.2 represents the three percentages for model P_1^S. As shown in the figure, the best OFVs of P_1^S are equal or less than that of P for all the 20 instances. The P_1^S's LBs are at least as low as the LBs of P except for S50. Furthermore, the gaps of P_1^S are always less than the gaps obtained from P for all the 20 S instances. It is concluded that P_1^S outperforms P for large instances.

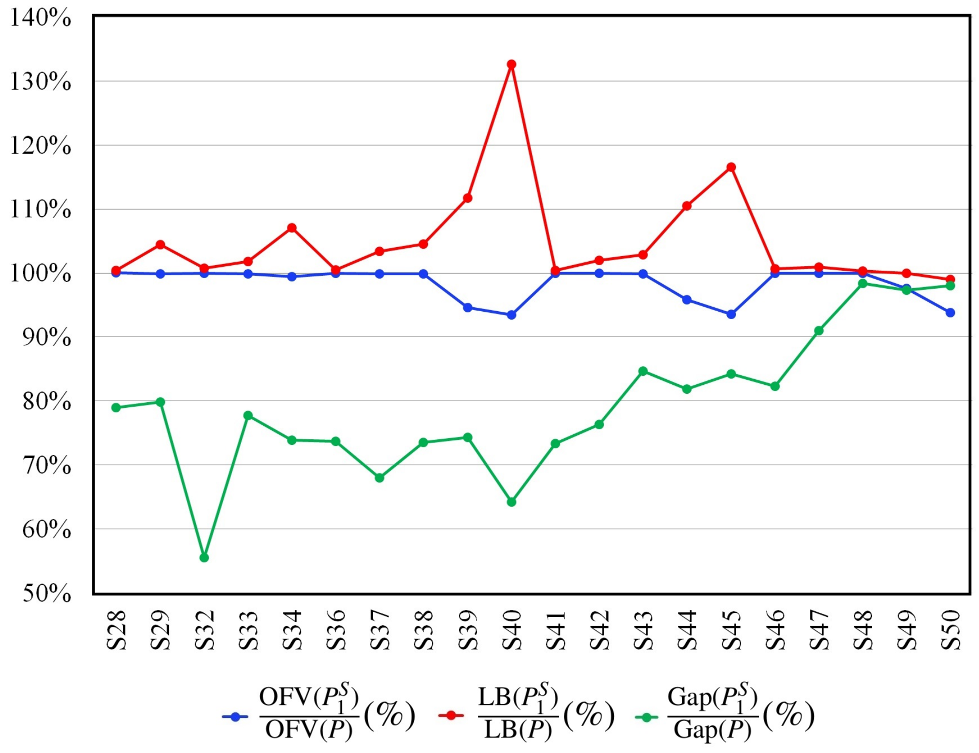

Figure 3.2: Comparison of P_1^S OFV, LB, and gap to P for S instances which were not solved to optimality by the majority of the models

Figure 3.3 compares model P_2^S to P. P_2^S's OFVs are at least as low as the ones obtained from P and the LBs are higher than P's in majority of the instances. Except for one problem (S48), gaps of P_2^S are lower than P, however, they are not as low as the P_1^S.

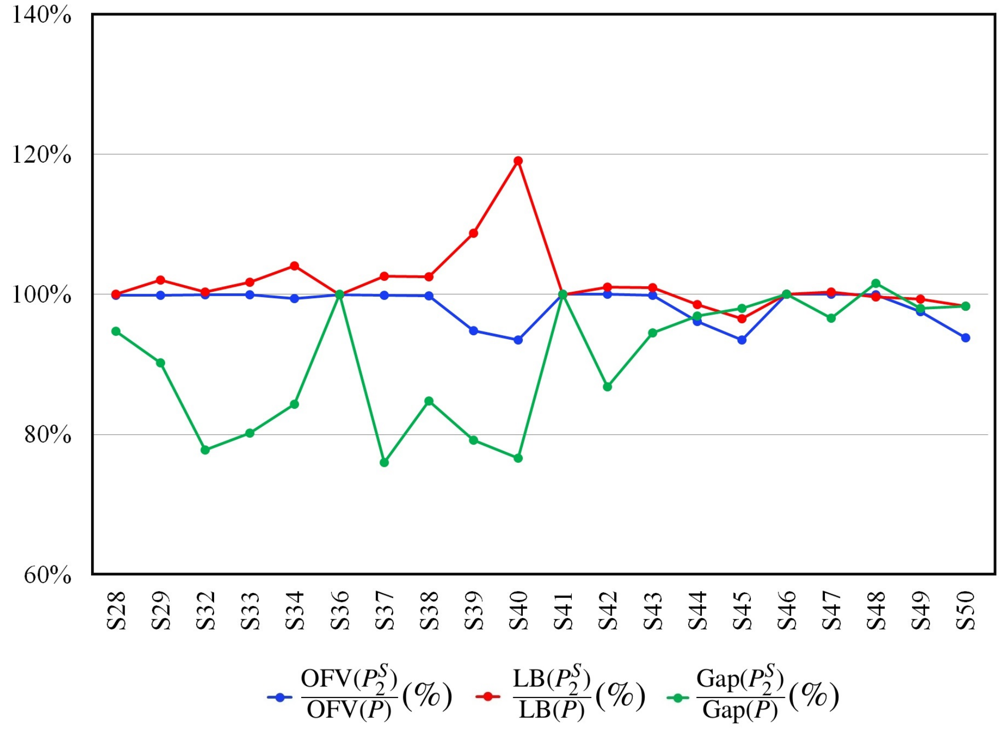

Figure 3.3: Comparison of P_2^S OFV, LB, and gap to P for S instances which were not solved to optimality by the majority of the models

Figure 3.4 compares model P_3^S to P. The difference between the two models (P and P_3^S) are noticeable for relatively smaller sized instances as shown in the figure. Higher LBs assist P to reach to lower gaps compared to P_3^S since the best OFVs are the same. For larger instances, it can be concluded that the best P_3^S can perform is to reach the gap of P. Therefore, P_3^S is not comparable with P, P_1^S, and P_2^S.

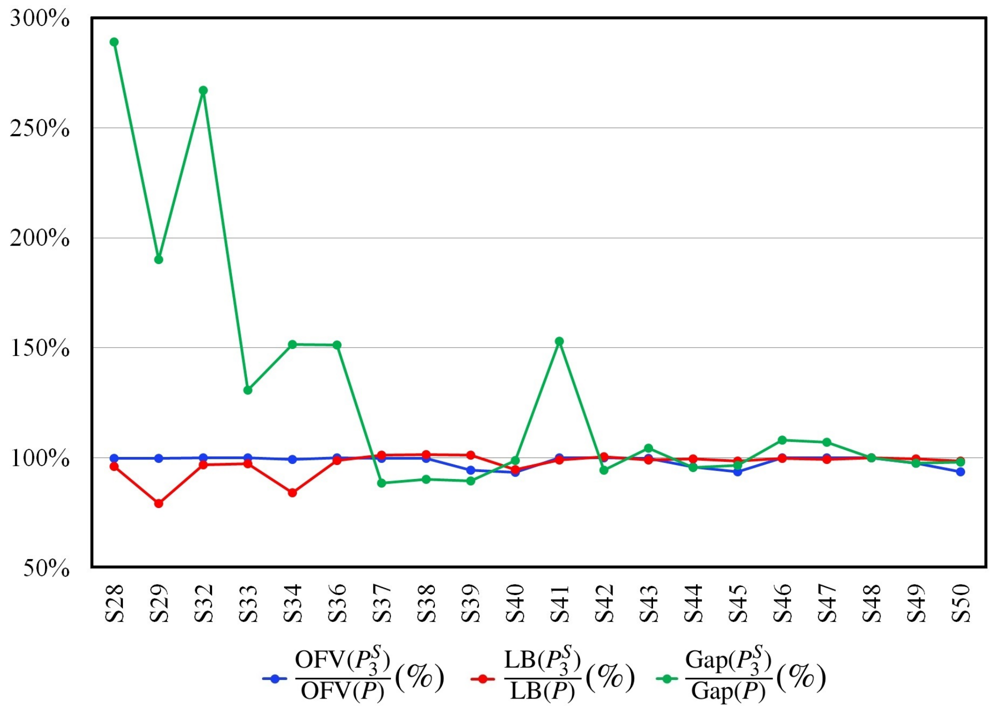

Figure 3.4: Comparison of P_3^S OFV, LB, and gap to P for S instances which were not solved to optimality by the majority of the models

In order to compare the three enhanced models (P_1^S, P_2^S, and P_3^S) simultaneously, the relative gaps (compared to P) are shown in Figure 3.5. As mentioned earlier, P_3^S is not comparable with P, thus the race is between P_1^S and P_2^S since they both outperformed P's gaps. It can be concluded that between P_1^S and P_2^S, P_1^S is capable of reaching to better gaps for relatively large instances. Also, it showed its capability to outperform P for some medium instances (see Table 3.5).

The results show that branching on z variables (in P_1^S and P_2^S) has better performance than when mixed branching in Section 3.3.4.3 occurs with the parameter of 50 (in P_3^S). Other values of the parameter were also tested. For example, 0 showed to be not as efficient as 5 which means branching on y variables are not as helpful as branching on z.

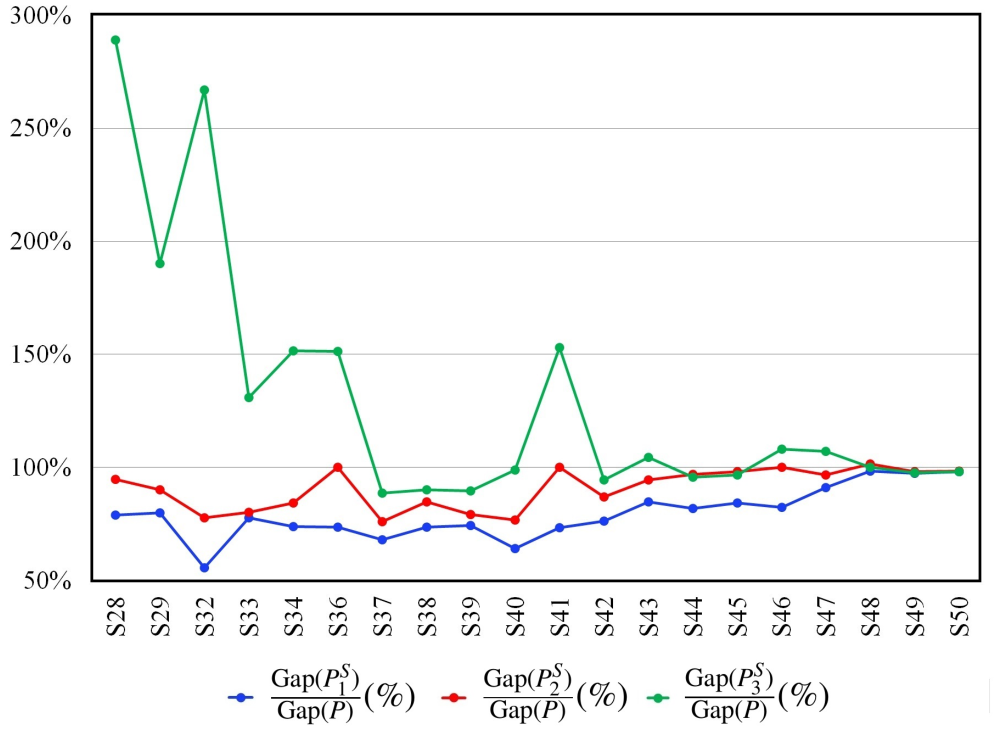

Figure 3.5: Gap comparison among P_1^S , P_2^S , and P_3^S for S instances which were not solved to optimality by the majority of the models

Table 3.6, contains details of the two problems P and P_1^S. Each model's solving time and gap are bold if they are better than the other model. Since each gap is calculated based on the best OFV and LB of its associated model, we also compare the best OFVs and LBs of the models separately. As shown in the table, the better OFV and LB for each instance between the two model are highlighted by blue and violet color, respectively. It can be concluded that model P_1^S can outperform model P in reaching to lower best OFVs and higher LBs as the problem size increases.

Table 3.6: P vs. P_1^S for S instances

Model				P				P_1^S				
Prob #	Content #	Center #	B	Best OFV	LB	Gap (%)	Time (s)	Best OFV	LB	Gap (%)	Time (s)	GA's best OFV
S1	10	3	1	196	196	0.0%	**0.0**	196	196	0.0%	**0.0**	196
S2	10	3	2	165	165	0.0%	**0.0**	165	165	0.0%	**0.0**	165
S3	20	4	1	499	499	0.0%	**0.0**	499	499	0.0%	**0.0**	499
S4	20	4	3	325	325	0.0%	**0.0**	325	325	0.0%	**0.0**	325
S5	50	6	2	1027	1027	0.0%	**0.0**	1027	1027	0.0%	**0.0**	1027
S6	50	6	4	721	721	0.0%	**0.0**	721	721	0.0%	**0.0**	721
S7	100	10	2	2343	2343	0.0%	**0.0**	2343	2343	0.0%	**0.0**	2343
S8	100	10	7	1429	1429	0.0%	**0.0**	1429	1429	0.0%	**0.0**	1429
S9	200	15	3	4616	4616	0.0%	**0.0**	4616	4616	0.0%	**0.0**	4616
S10	200	15	7	3819	3819	0.0%	**0.0**	3819	3819	0.0%	**0.0**	3819
S11	200	15	12	1524	1524	0.0%	**0.0**	1524	1524	0.0%	**0.0**	1524
S12	400	20	4	9384	9384	0.0%	**0.0**	9384	9384	0.0%	0.1	9384
S13	400	20	10	7588	7588	0.0%	**0.0**	7588	7588	0.0%	0.1	7627
S14	400	20	16	3543	3543	0.0%	**0.0**	3543	3543	0.0%	0.1	3543
S15	800	25	5	18365	18365	0.0%	1.0	18365	18365	0.0%	**0.2**	18365
S16	800	25	12	14930	14930	0.0%	**2.0**	14930	14930	0.0%	2.2	14930
S17	800	25	22	4128	4128	0.0%	**1.0**	4128	4128	0.0%	1.1	4128
S18	1000	30	5	23356	23356	0.0%	**1.0**	23356	23356	0.0%	1.4	23356
S19	1000	30	15	18852	18852	0.0%	**5.0**	18852	18852	0.0%	5.4	19030
S20	1000	30	25	7835	7835	0.0%	**2.0**	7835	7835	0.0%	3.4	7835
S21	2000	40	5	47550	47550	0.0%	**2.0**	47550	47550	0.0%	3.7	47679
S22	2000	40	20	36758	36758	0.0%	32.0	36758	36758	0.0%	**28.4**	36942
S23	2000	40	35	8432	8432	0.0%	**4.0**	8432	8432	0.0%	8.0	8432
S24	4000	50	5	95982	95982	0.0%	**5.0**	95982	95982	0.0%	7.8	95982
S25	4000	50	25	72238	72238	0.0%	140.0	72238	72238	0.0%	**130.7**	72336
S26	4000	50	45	15473	15473	0.0%	**15.0**	15473	15473	0.0%	18.3	15473
S27	7000	70	5	169653	169653	0.0%	**24.0**	169653	169653	0.0%	55.6	169777
S28	7000	70	10	167593	164391	1.9%	1809.0	167641	165101	**1.5%**	1807.3	167692
S29	7000	70	35	139789	114102	18.4%	1807.0	139668	119166	**14.7%**	1809.0	139668
S30	7000	70	60	49006	49006	0.0%	407.0	49006	49006	0.0%	**191.0**	49006
S31	10000	100	5	242752	242752	0.0%	**48.0**	242752	242751	0.0%	158.5	242752
S32	10000	100	10	241032	236680	1.8%	3614.0	241026	238533	**1.0%**	3610.5	241026
S33	10000	100	20	236006	216798	8.1%	3624.0	235620	220794	**6.3%**	3614.2	235620
S34	10000	100	50	195746	150719	23.0%	3605.0	194604	161435	**17.0%**	3608.0	194604
S35	10000	100	90	43640	43640	0.0%	**157.0**	43640	43640	0.0%	295.1	43640
S36	15000	150	10	365623	358772	1.9%	3615.0	365527	360439	**1.4%**	3614.1	365527
S37	15000	150	20	363480	326994	10.0%	3613.0	362895	338181	**6.8%**	3613.1	362895
S38	15000	150	30	359894	305602	15.1%	3600.0	359479	319494	**11.1%**	3610.9	359479
S39	15000	150	75	334107	196076	41.3%	3600.0	316156	219033	**30.7%**	3610.8	316156
S40	15000	150	120	174818	80593.2	53.9%	3600.0	163321	106860	**34.6%**	3607.0	163321
S41	20000	200	10	488665	481376	1.5%	7218.0	488646	483349	**1.1%**	7221.4	488647
S42	20000	200	20	487635	450543	7.6%	7200.0	487668	459296	**5.8%**	7214.1	487668
S43	20000	200	40	484903	405859	16.3%	7206.0	484263	417346	**13.8%**	7211.5	484321
S44	20000	200	100	464586	252321	45.7%	7218.0	445402	278758	**37.4%**	7217.0	445402
S45	20000	200	150	330251	128777	61.0%	7200.0	309045	150119	**51.4%**	7213.5	309045
S46	30000	300	15	735313	710255	3.4%	7200.0	735330	714713	**2.8%**	7210.4	735333
S47	30000	300	30	734751	669130	8.9%	7200.0	734672	675123	**8.1%**	7219.1	734727
S48	30000	300	60	733547	596774	18.6%	7200.0	733272	598818	**18.3%**	7213.5	733349
S49	30000	300	150	717367	374263	47.8%	7200.0	700341	374244	**46.6%**	7208.3	700341
S50	30000	300	250	480218	126042	73.8%	7214.0	450350	124763	**72.3%**	7207.3	450350

3.6.4 Results of Multiple-Portioned Instances

Out of the 50 M instances, 25 were solved by all the 4 models during the specified time limits. OFV, LB, solving time and, OFV of the best solution obtained form GA for each of the instances are presented in Table 3.7. The GA took a minimum of 0% and a maximum of 100% of the total the solving times of each model. Models P_1^M , P_2^M, P_3^M, and P_4^S spent an average of 23%, 27%, 29%, and, 23% of the total solving time in the GA, respectively. The number of iterations without improvement criterion stopped the GA for 34, 34, 33, and, 33 instances for P_1^M, P_2^M, P_3^M, and P_4^M models, respectively. The remaining instances were stopped by the maximum time limit criterion. Details of GA times can be found in Appendix 3.C.

As in Table 3.5, the best solving times are highlighted with blue color in Table 3.7. Problems M1-M8 were solved in approximately 0.0 seconds, thus all of the 5 models are highlighted. The majority of medium instances are solved by P in shorter amount of time. However, P_3^M managed to outperform P for three of the medium sized instances (M16, M22, and M24).

Table 3.7: M instances that were solved in the time limit by at least three of the models

Model	P			P_1^M				P_2^M				P_3^M				P_4^M			
Prob #	OFV OFV	Gap (%)	Time (s)	Best OFV	Gap (%)	Time (s)	GA OFV	Best OFV	Gap (%)	Time (s)	GA OFV	Best OFV	Gap (%)	Time	GA OFV	Best OFV	Gap (%)	Time (s)	GA OFV
M1	107	0.0%	**0.0**	107	0.0%	**0.0**	107	107	0.0%	**0.0**	107	107	0.0%	**0.0**	107	107	0.0%	**0.0**	107
M2	48	0.0%	**0.0**	48	0.0%	**0.0**	48	48	0.0%	**0.0**	48	48	0.0%	**0.0**	48	48	0.0%	**0.0**	48
M3	381	0.0%	**0.0**	381	0.0%	**0.0**	381	381	0.0%	**0.0**	381	381	0.0%	**0.0**	381	381	0.0%	**0.0**	381
M4	121	0.0%	**0.0**	121	0.0%	**0.0**	121	121	0.0%	**0.0**	121	121	0.0%	**0.0**	121	121	0.0%	**0.0**	121
M5	801	0.0%	**0.0**	801	0.0%	**0.0**	801	801	0.0%	**0.0**	801	801	0.0%	**0.0**	801	801	0.0%	**0.0**	801
M6	148	0.0%	**0.0**	148	0.0%	**0.0**	148	148	0.0%	**0.0**	148	148	0.0%	**0.0**	148	148	0.0%	**0.0**	148
M7	2013	0.0%	**0.0**	2013	0.0%	**0.0**	2013	2013	0.0%	**0.0**	2013	2013	0.0%	**0.0**	2013	2013	0.0%	**0.0**	2013
M8	13	0.0%	**0.0**	13	0.0%	**0.0**	13	13	0.0%	**0.0**	13	13	0.0%	**0.0**	13	13	0.0%	**0.0**	13
M9	3804	0.0%	**0.0**	3804	0.0%	1.1	3804	3804	0.0%	0.1	3804	3804	0.0%	1.1	3804	3804	0.0%	0.1	3804
M10	1100	0.0%	**0.0**	1100	0.0%	1.1	1100	1100	0.0%	1.1	1100	1100	0.0%	1.1	1100	1100	0.0%	2.1	1100
M11	10	0.0%	**0.0**	10	0.0%	0.1	10	10	0.0%	1.1	10	10	0.0%	0.1	10	10	0.0%	0.1	10
M12	7331	0.0%	**1.0**	7331	0.0%	1.3	7331	7331	0.0%	3.3	7331	7331	0.0%	2.2	7331	7331	0.0%	3.3	7331
M13	2300	0.0%	**4.0**	2300	0.0%	6.2	2300	2300	0.0%	6.2	2300	2300	0.0%	4.4	2300	2300	0.0%	102.4	2300
M14	137	0.0%	**1.0**	137	0.0%	2.1	143	137	0.0%	2.2	137	137	0.0%	1.1	137	137	0.0%	5.2	137
M15	15309	0.0%	**9.0**	15309	0.0%	17.6	15309	15309	0.0%	16.6	15351	15309	0.0%	10.8	15309	15309	0.0%	39.7	15351
M16	5399	0.0%	30.0	5399	0.0%	35.6	5495	5399	0.0%	29.6	5495	5399	0.0%	**20.8**	5577	5399	25.6%	3600.8	5399
M17	0	0.0%	**1.0**	0	0.0%	5.0	0	0	0.0%	3.0	0	0	0.0%	3.0	0	0	0.0%	4.1	0
M18	19768	0.0%	**14.0**	19768	0.0%	20.9	19768	19768	0.0%	20.7	19768	19768	0.0%	15.6	19768	19768	0.0%	22.1	19768
M19	6984	0.0%	**97.0**	6984	0.0%	126.8	6984	6984	0.0%	117.5	6984	6984	0.0%	102.1	6984	6984	73.2%	3600.2	6984
M20	64	0.0%	**4.0**	64	0.0%	13.8	64	64	0.0%	15.9	64	64	0.0%	5.0	64	64	0.0%	17.3	64
M21	42029	0.0%	**31.0**	42029 9	0.0%	93.6	42029	42029	0.0%	60.2	42029	42029	0.0%	51.9	42029	42029	0.0%	105.0	42029
M22	8963	0.0%	420.0	8963	0.0%	655.2	8963	8963	0.0%	527.7	8963	8963	0.0%	**350.9**	8963	2073	76.9%	3605.9	8963
M23	0	0.0%	**6.0**	0	0.0%	14.2	0	0	0.0%	17.2	0	0	0.0%	7.7	20	0	0.0%	40.1	20
M24	89390	0.0%	304.0	89390	0.0%	586.1	89390	89390	0.0%	425.1	89390	89390	0.0%	**286.5**	89390	89390	0.0%	1881.0	89390
M26	0	0.0%	17.0	0	0.0%	17.4	0	0	0.0%	15.6	0	0	0.0%	33.1	0	0	0.0%	**13.7**	0

In order to compare the other 25 instances that were not solved to optimality by the majority of the models in the time limits, the relative best OFVs, LBs, and gaps are the base of our comparison. The values of each model (P_1^M, P_2^M, and P_3^M) are divided to the same values obtained from the P model and the percentages are represented in Figures 3.6-3.9.

Figure 3.6 shows that the best OFVs of model P_1^M are always better than P's best OFVs.

The LBs of P_1^M are lower than P model for medium sized instances, however, they get better as the instance size increases. This causes the P_1^M's gaps to have a similar trend. Note that the percentage of gap for problem M27 is 525.2% which is outside the range of the chart. Although the improvement is not extreme compared to P's gaps, it can be concluded that P_1^M's gaps are lower than P's for larger instances.

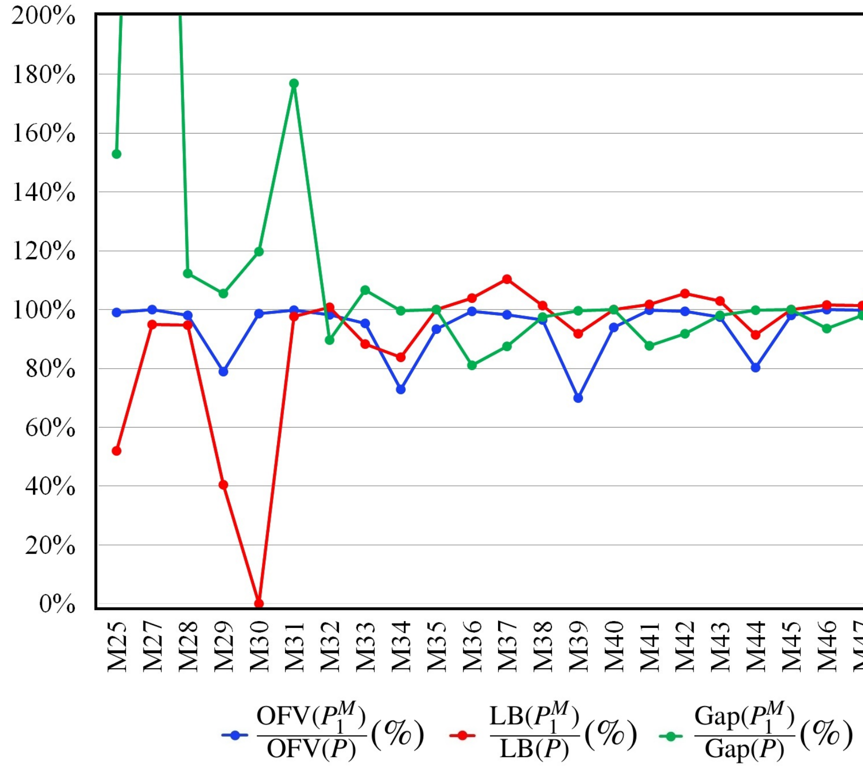

Figure 3.6: Comparison of P_1^M OFV, LB, and gap to P for M instances which were not solved to optimality by the majority of the models

Results for P_2^M are depicted in Figure 3.7. Except for problem M35, P_2^M's best OFVs are better than P for the remainder of 24 instances. Aside from problem M47, whose relative gap value is 227.4%, it can be concluded that P_2^M's LBs and gaps improve when the size of the problem increases, though not significantly.

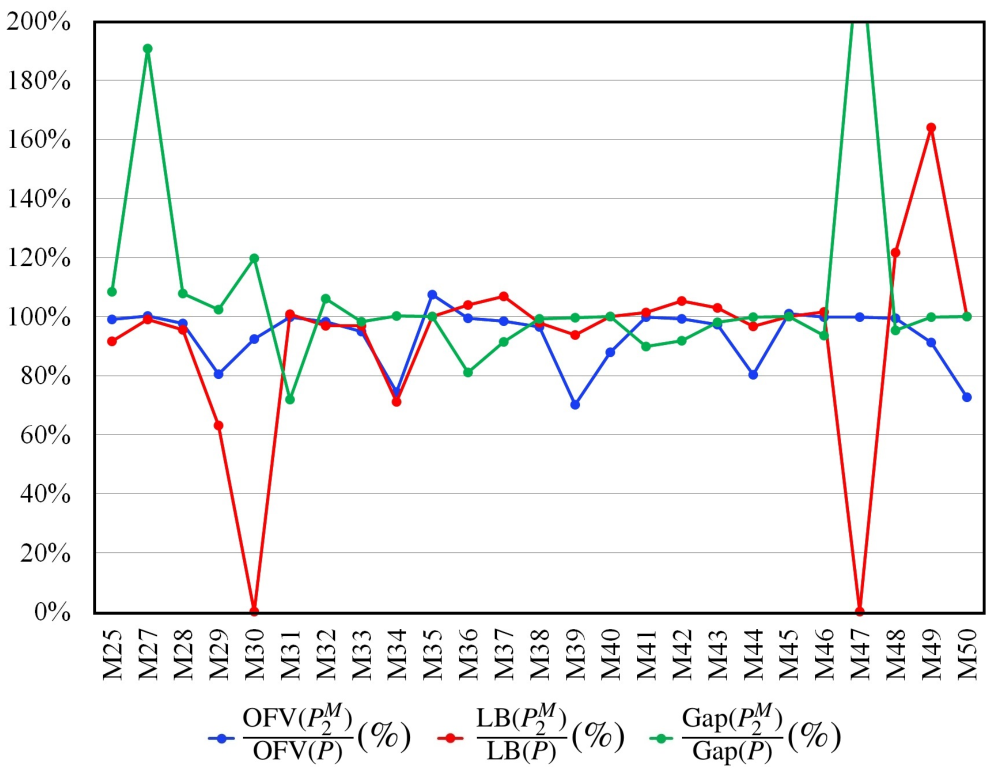

Figure 3.7: Comparison of P_2^M OFV, LB, and gap to P for M instances which were not solved to optimality by the majority of the models

Figure 3.8 shows the results of model P_3^M compared to P. Note that gap of instances M30 is 521.9% of gap of P model. Since the LBs of M35 is 0 for all models except for P_3^M which has a LB of 67, a large value (1000%) has been to chosen to represent superiority of P_3^M over other models for this instance.

OFVs of P_3^M are always better than P. P_3^M's LBs does not improve by increasing the size of the problems, however, gaps are better than P's gaps for medium sized instances. Both models, P and P_3^M, act almost similarly for larger instances, however, due to to GA usage, the best OFV of model P_3^M is lower than P.

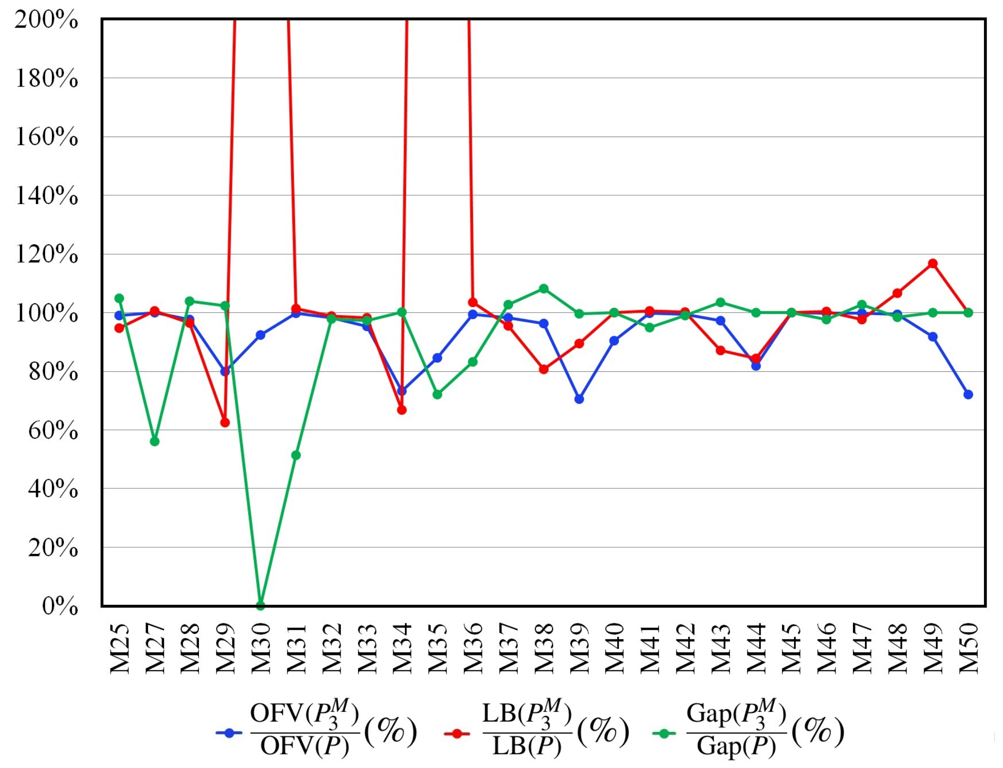

Figure 3.8: Comparison of P_3^M OFV, LB, and gap to P for M instances which were not solved to optimality by the majority of the models

P_4^M's results are shown in Figure 3.9. The best OFVs are always lower for P_4^M compared to P. P's LBs and gaps are better for medium sized instances, however, with the exception of M47, increasing the size of the problem results in even more significant improvements.

Since Model P_1^M showed slightly better performance than the other three models (i.e., P_2^M, P_3^M, and P_4^M) compared to P, Table 3.8 contains the detail of the two models of P and P_1^M. As in Table 3.6, solving times and gaps are bold if they are less than the other model. Note that if gap is equal to 100% (i.e., LB=0), then none of them are highlighted.

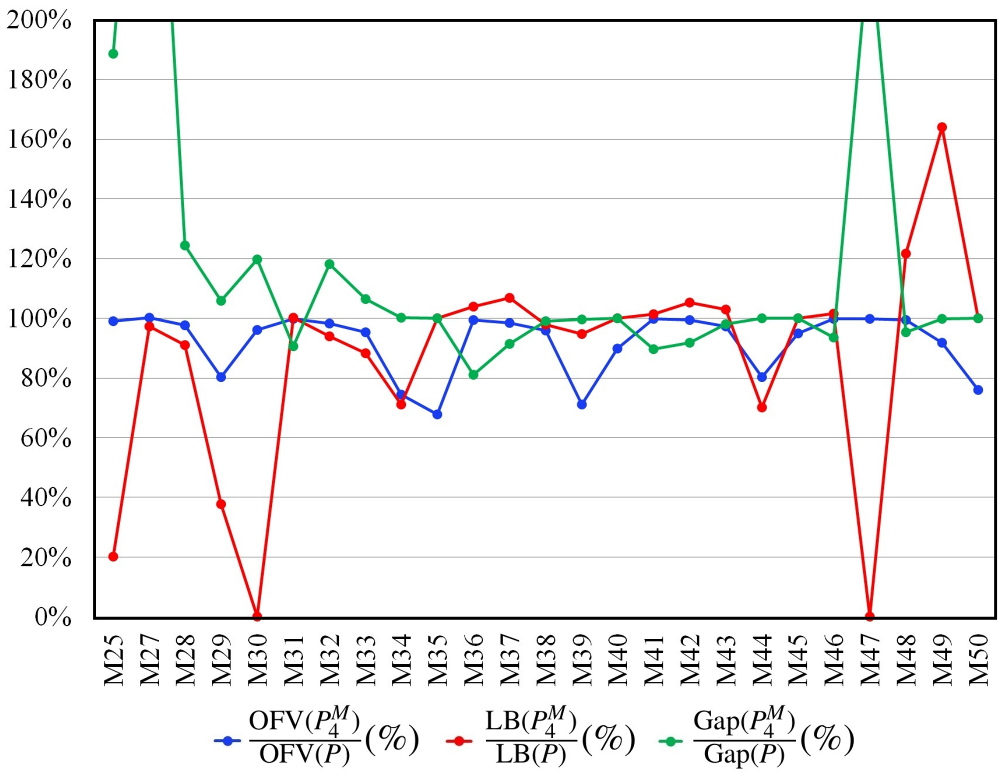

Figure 3.9: Comparison of P_4^M OFV, LB, and gap to P for M instances which were not solved to optimality by the majority of the models

The smaller instances were always solved quicker by model P. Some of the medium instances that were not solved to optimality have better gaps for model P (e.g., M27-M31). However, in order to do a better comparison, the best OFVs and LBs are compared separately and highlighted by blue and violet color, respectively, if they are better. Model P_1^M has at least as good best OFVs compared to P for all 50 instances and it also obtained better LBs for larger instances. Therefore, it can be concluded that model P_1^M can outperform model P for a majority of larger instances, however this improvement is not as high as the improvement seen for model P_1^S when solving S instances.

Table 3.8: P vs. P_1^M for M instances

Model				P				P_1^M				
Prob #	Content #	Center #	B	Best OFV	LB	Gap (%)	Time (s)	Best OFV	LB	Gap (%)	Time (s)	GA's best OFV
M1	10	3	1	107	107	0.0%	**0.0**	107	107	0.0%	**0.0**	107
M2	10	3	2	48	48	0.0%	**0.0**	48	48	0.0%	**0.0**	48
M3	20	4	1	381	381	0.0%	**0.0**	381	381	0.0%	**0.0**	381
M4	20	4	3	121	121	0.0%	**0.0**	121	121	0.0%	**0.0**	121
M5	50	6	2	801	801	0.0%	**0.0**	801	801	0.0%	**0.0**	801
M6	50	6	4	148	148	0.0%	**0.0**	148	148	0.0%	**0.0**	148
M7	100	10	2	2013	2013	0.0%	**0.0**	2013	2013	0.0%	**0.0**	2013
M8	100	10	7	13	13	0.0%	**0.0**	13	13	0.0%	**0.0**	13
M9	200	15	3	3804	3804	0.0%	**0.0**	3804	3804	0.0%	1.1	3804
M10	200	15	7	1100	1100	0.0%	**0.0**	1100	1100	0.0%	1.1	1100
M11	200	15	12	10	10	0.0%	**0.0**	10	10	0.0%	0.1	10
M12	400	20	4	7331	7331	0.0%	**1.0**	7331	7331	0.0%	1.3	7331
M13	400	20	10	2300	2300	0.0%	**4.0**	2300	2300	0.0%	6.2	2300
M14	400	20	16	137	137	0.0%	**1.0**	137	137	0.0%	2.1	143
M15	800	25	5	15309	15309	0.0%	**9.0**	15309	15309	0.0%	17.6	15309
M16	800	25	12	5399	5399	0.0%	**30.0**	5399	5399	0.0%	35.6	5495
M17	800	25	22	0	0	0.0%	**1.0**	0	0	0.0%	5.0	0
M18	1000	30	5	19768	19768	0.0%	**14.0**	19768	19768	0.0%	20.9	19768
M19	1000	30	15	6984	6984	0.0%	**97.0**	6984	6984	0.0%	126.8	6984
M20	1000	30	25	64	64	0.0%	**4.0**	64	64	0.0%	13.8	64
M21	2000	40	5	42029	42029	0.0%	**31.0**	42029	42029	0.0%	93.6	42029
M22	2000	40	20	8963	8963	0.0%	**420.0**	8963	8963	0.0%	655.2	8963
M23	2000	40	35	0	0	0.0%	**6.0**	0	0	0.0%	14.2	0
M24	4000	50	5	89390	89390	0.0%	**304.0**	89390	89390	0.0%	586.1	89390
M25	4000	50	25	23437	12342	**47.3%**	3600.0	23215	6412	72.4%	3600.6	23215
M26	4000	50	45	0	0	0.0%	**17.0**	0	0	0.0%	17.4	0
M27	7000	70	5	164162	162214	**1.2%**	3600.0	164162	153928	6.2%	3600.0	164273
M28	7000	70	10	157340	123093	**21.8%**	3600.0	154373	116654	24.4%	3599.6	154373
M29	7000	70	35	77737	7829	**89.9%**	3600.0	61318	3162	94.8%	3600.6	61318
M30	7000	70	60	763	126	**83.6%**	3600.0	753	0	100.0%	3600.0	753
M31	10000	100	5	239146	232475	**2.8%**	7200.0	238913	227120	4.9%	7200.1	238913
M32	10000	100	10	234648	188814	19.5%	7200.0	230771	190369	**17.5%**	7200.6	230771
M33	10000	100	20	222949	104281	**53.2%**	7200.0	212700	92037	56.7%	7201.2	212700
M34	10000	100	50	142095	4326	97.0%	7200.0	103425	3621	**96.5%**	7199.9	103425
M35	10000	100	90	283	0	100.0%	7200.0	264	0	100.0%	7200.4	264
M36	15000	150	10	363227	292309	19.5%	7200.0	361092	303931	**15.8%**	7199.6	361092
M37	15000	150	20	358395	180316	49.7%	7201.0	352011	198842	**43.5%**	7313.9	352011
M38	15000	150	30	351160	117566	66.5%	7201.0	339161	119161	**64.9%**	7371.6	339161
M39	15000	150	75	256589	3016	98.8%	7201.0	179657	2770	**98.5%**	7202.7	179657
M40	15000	150	120	12308	0	100.0%	7200.0	11560	0	100.0%	7200.8	11560
M41	20000	200	10	488207	421162	13.7%	10800.0	486866	428252	**12.0%**	10800.5	486866
M42	20000	200	20	486577	280578	42.3%	10800.0	483746	295709	**38.9%**	10806.1	483746
M43	20000	200	40	479935	121318	74.7%	10878.0	467799	124835	**73.3%**	10909.6	467799
M44	20000	200	100	380772	2996	99.2%	10827.0	306088	2737	**99.1%**	10803.9	306088
M45	20000	200	150	63802	0	100.0%	10801.0	62518	0	100.0%	10801.3	62518
M46	30000	300	15	733306	586825	20.0%	10801.0	732687	595876	**18.7%**	10801.2	732687
M47	30000	300	30	732201	410219	44.0%	10801.0	730705	415626	**43.1%**	10802.8	730705
M48	30000	300	60	729558	126573	82.7%	10801.0	725532	154006	**78.8%**	10860.8	725532
M49	30000	300	150	661937	858	99.9%	10801.0	611566	1529	**99.8%**	10801.6	611566
M50	30000	300	250	115350	0	100.0%	10800.0	86258	0	100.0%	10802.1	86258

The results for model P_1^S indicates the efficiency of GA, and the additional enhancements (e.g., constraints (3.9), (3.10), and (3.11), and the custom branching on z variables). Also, the results of larger instances for P_1^M shows how much GA and other enhancements such as constraints (3.9), (3.10), (3.11), and (3.12) can assist model *P*.

3.7 Conclusion and Future Work

In this chapter, we introduced the Clustered Content Interdiction Problem (CCIP) which considers groups of content dispersed across a collection of centers. Different content is assigned to the centers to ensure availability. Given a content assignment across a collection of available centers, an interdictor's goal is to determine which centers to interdict to minimize the content availability. An integer program was formulated to model the problem which can have single-portion (S) or multiple-portion (M) content.

The problem is proven to be NP-complete. Therefore, several modified formulations were tested to solve larger problems more efficiently. Multiple enhancements (e.g., symmetry breaking and other valid inequality constraints, and custom branchings) were offered to be added to the formulations. Each modified formulation contains a combination of the enhancements and also exploits a genetic algorithm as a method to generate a quality solution efficiently.

After testing the modified formulations for 100 S and M instances, the two best ones were selected to be compared to the original model *P*. The two models showed to be more efficient for solving larger instances. The GA exploitation is shown to be always helpful to reaching smaller best OFVs in the time limits compared to *P* formulation. Constraint (3.9), (3.10), and (3.11) showed to be helpful to solve both S and M instances. The custom branching on z variables and constraint (3.12) showed to be helpful for solving S and M instances, respectively.

For future study, we can name exploring generalizations of the matrix interdiction methodologies/approaches to allow for multiple content. Also, in cybersecurity context, a bilevel setting of the problem, which allows interdictors decisions to be made in the inner problem and the defenders assignment decisions in the outer problem, can be explored.

Acknowledgment

This material is based upon work supported by Arkansas High Performance Computing Center which is funded through multiple National Science Foundation grants and the Arkansas Economic Development Commission.

Bibliography

Altner, D. S., Ergun, Ö., and Uhan, N. A. (2010). The maximum flow network interdiction problem: valid inequalities, integrality gaps, and approximability. *Operations Research Letters*, 38(1):33–38.

Assimakopoulos, N. (1987). A network interdiction model for hospital infection control. *Computers in biology and medicine*, 17(6):413–422.

Benzel, T. (2011). The science of cyber security experimentation: the deter project. In *Proceedings of the 27th Annual Computer Security Applications Conference*, pages 137–148. ACM.

Fulkerson, D. R. and Harding, G. C. (1977). Maximizing the minimum source-sink path subject to a budget constraint. *Mathematical Programming*, 13(1):116–118.

Ghare, P., Montgomery, D. C., and Turner, W. (1971). Optimal interdiction policy for a flow network. *Naval Research Logistics (NRL)*, 18(1):37–45.

Infosecurity Magazine (2013). The top five it security cyber threats are... https://www.infosecurity-magazine.com/news/the-top-five-it-security-cyber-threats-are/. Accessed 2017.01.22.

Israeli, E. and Wood, R. K. (2002). Shortest-path network interdiction. *Networks*, 40(2):97–111.

Karp, R. M. (1972). Reducibility among combinatorial problems. In *Complexity of computer computations*, pages 85–103. Springer.

L. Columbus. Gartner predicts infrastructure services will accelerate cloud computing growth. http://www.forbes.com/sites/louiscolumbus/2013/02/19/gartner-predicts-infrastructure-services-will-accelerate-cloud-computing-growth/#57cb2d5c788c. Accessed 2017.01.22.

Malaviya, A., Rainwater, C., and Sharkey, T. (2012). Multi-period network interdiction problems with applications to city-level drug enforcement. *IIE Transactions*, 44(5):368–380.

McMasters, A. W. and Mustin, T. M. (1970). Optimal interdiction of a supply network. *Naval Research Logistics (NRL)*, 17(3):261–268.

Memon, N. and Larsen, H. (2006). Practical algorithms for destabilizing terrorist networks. *Intelligence and Security Informatics*, pages 389–400.

Morton, D. P., Pan, F., and Saeger, K. J. (2007). Models for nuclear smuggling interdiction. *IIE Transactions*, 39(1):3–14.

Pan, F. and Kasiviswanathan, S. (2010). Matrix interdiction problem. Technical report, Los Alamos National Laboratory (LANL).

Phillips, C. A. (1993). The network inhibition problem. In *Proceedings of the twenty-fifth annual ACM symposium on Theory of computing*, pages 776–785. ACM.

Pourbohloul, B., Meyers, L. A., Skowronski, D. M., Krajden, M., Patrick, D. M., and Brunham, R. C. (2005). Modeling control strategies of respiratory pathogens. *Emerging infectious diseases*, 11(8):1249.

Sherali, H. D. and Adams, W. P. (1998). *A reformulation-linearization technique for solving discrete and continuous nonconvex problems*, volume 31. Springer.

Von Solms, R. and Van Niekerk, J. (2013). From information security to cyber security. *Computers & Security*, 38:97–102.

Wood, R. K. (1993). Deterministic network interdiction. *Mathematical and Computer Modelling*, 17(2):1–18.

Appendix

3.A Relaxed z variables

Theorem 3 *If y_j^k are required to be binary and interdiction decisions are relaxed (i.e., $z_i \in [0,1]$), then a binary solution to P still exists.*

Proof. To establish this result, we define problem P' as P, but relaxing $z_i \in \{0,1\}$ as $z_i \in [0,1]$, $\forall i \in I$. Let $OFV(P)$ denote the optimal OFV of problem P. To demonstrate that $OFV(P) = OFV(P')$, let (y^*, z^*) be any optimal solution to P'. We construct a solution (y^*, z) to P' with binary valued z and the same objective value as (y^*, z^*). To this end, observe that when $y = y^*$ is fixed, the constraints (3.2) reduce to

$$z_i \geq y_j^{*k}, \qquad \forall j \in J,\ k \in \{1,\ldots,n_j\},\ \text{where } x_{jk}^i = 1 \tag{3.19}$$

Also, constraints (3.4) forces the summation of z_i variables to be equal to B. There are three values that each z_i can have in z^*: 0, a fractional value between 0 and 1, and 1. In order to construct the solution with binary z_i, we keep the z_is with values of 0 and 1 and arbitrarily select $B - |i \in I : z_i = 1|$ of the ones with fractional values and force them to be equal to 1. The remainder of the fractional z_i-values then will be forced to 0. Note that this action will still keep the summation of z_i-variables equal to B, hence not violating constraint (3.4). This also does not violate constraint (3.19) since y-variables are all binary valued. Now, all the new z_i-variables are binary establishing the binary solution of (y^*, z) and since z_i coefficients in the OF are 0, $OFV(P) = OFV(P')$.

□

3.B Single-Portioned Instances' Results

Table 3.B.1: Single-portioned instances results derived from *P* model

Prob #	OFV	LB	gap (%)	solving time (s)
S1	196	196	0.0%	0.0
S2	165	165	0.0%	0.0
S3	499	499	0.0%	0.0
S4	325	325	0.0%	0.0
S5	1027	1027	0.0%	0.0
S6	721	721	0.0%	0.0
S7	2343	2343	0.0%	0.0
S8	1429	1429	0.0%	0.0
S9	4616	4616	0.0%	0.0
S10	3819	3819	0.0%	0.0
S11	1524	1524	0.0%	0.0
S12	9384	9384	0.0%	0.0
S13	7588	7588	0.0%	0.0
S14	3543	3543	0.0%	0.0
S15	18365	18365	0.0%	1.0
S16	14930	14930	0.0%	2.0
S17	4128	4128	0.0%	1.0
S18	23356	23356	0.0%	1.0
S19	18852	18852	0.0%	5.0
S20	7835	7835	0.0%	2.0
S21	47550	47550	0.0%	2.0
S22	36758	36758	0.0%	32.0
S23	8432	8432	0.0%	4.0
S24	95982	95982	0.0%	5.0
S25	72238	72238	0.0%	140.0
S26	15473	15473	0.0%	15.0
S27	169653	169653	0.0%	24.0
S28	167593	164391	1.9%	1809.0
S29	139789	114102	18.4%	1807.0
S30	49006	49006	0.0%	407.0
S31	242752	242752	0.0%	48.0
S32	241032	236680	1.8%	3614.0
S33	236006	216798	8.1%	3624.0
S34	195746	150719	23.0%	3605.0
S35	43640	43640	0.0%	157.0
S36	365623	358772	1.9%	3615.0
S37	363480	326994	10.0%	3613.0
S38	359894	305602	15.1%	3600.0
S39	334107	196076	41.3%	3600.0
S40	174818	80593	53.9%	3600.0
S41	488665	481376	1.5%	7218.0
S42	487635	450543	7.6%	7200.0
S43	484903	405859	16.3%	7206.0
S44	464586	252321	45.7%	7218.0
S45	330251	128777	61.0%	7200.0
S46	735313	710255	3.4%	7200.0
S47	734751	669130	8.9%	7200.0
S48	733547	596774	18.6%	7200.0
S49	717367	374263	47.8%	7200.0
S50	480218	126042	73.8%	7214.0

Table 3.B.2: Single-portioned instances results derived from P_1^S model

Prob #	OFV	LB	gap (%)	solving time (s)	GA best OFV	GA time (s)
S1	196	196	0.0%	0.0	196	0.0
S2	165	165	0.0%	0.0	165	0.0
S3	499	499	0.0%	0.0	499	0.0
S4	325	325	0.0%	0.0	325	0.0
S5	1027	1027	0.0%	0.0	1027	0.0
S6	721	721	0.0%	0.0	721	0.0
S7	2343	2343	0.0%	0.0	2343	0.0
S8	1429	1429	0.0%	0.0	1429	0.0
S9	4616	4616	0.0%	0.0	4616	0.0
S10	3819	3819	0.0%	0.0	3819	0.0
S11	1524	1524	0.0%	0.0	1524	0.0
S12	9384	9384	0.0%	0.1	9384	0.1
S13	7588	7588	0.0%	0.1	7627	0.1
S14	3543	3543	0.0%	0.1	3543	0.1
S15	18365	18365	0.0%	0.2	18365	0.2
S16	14930	14930	0.0%	2.2	14930	0.2
S17	4128	4128	0.0%	1.1	4128	0.1
S18	23356	23356	0.0%	1.4	23356	0.4
S19	18852	18852	0.0%	5.4	19030	0.4
S20	7835	7835	0.0%	3.4	7835	0.4
S21	47550	47550	0.0%	3.7	47679	1.7
S22	36758	36758	0.0%	28.4	36942	2.4
S23	8432	8432	0.0%	8.0	8432	1.0
S24	95982	95982	0.0%	7.8	95982	2.8
S25	72238	72238	0.0%	130.7	72336	6.7
S26	15473	15473	0.0%	18.3	15473	3.3
S27	169653	169653	0.0%	55.6	169777	26.6
S28	167641	165101	1.5%	1807.3	167692	62.3
S29	139668	119166	14.7%	1809.0	139668	122.0
S30	49006	49006	0.0%	191.0	49006	36.0
S31	242752	242751	0.0%	158.5	242752	128.5
S32	241026	238533	1.0%	3610.5	241026	311.5
S33	235620	220794	6.3%	3614.2	235620	219.2
S34	194604	161435	17.0%	3608.0	194604	254.0
S35	43640	43640	0.0%	295.1	43640	78.1
S36	365527	360439	1.4%	3614.1	365527	234.1
S37	362895	338181	6.8%	3613.1	362895	548.1
S38	359479	319494	11.1%	3610.9	359479	397.9
S39	316156	219033	30.7%	3610.8	316156	504.8
S40	163321	106860	34.6%	3607.0	163321	513.0
S41	488646	483349	1.1%	7221.4	488647	553.4
S42	487668	459296	5.8%	7214.1	487668	561.1
S43	484263	417346	13.8%	7211.5	484321	584.5
S44	445402	278758	37.4%	7217.0	445402	1093.0
S45	309045	150119	51.4%	7213.5	309045	879.5
S46	735330	714713	2.8%	7210.4	735333	1200.4
S47	734672	675123	8.1%	7219.1	734727	1200.1
S48	733272	598818	18.3%	7213.5	733349	1200.5
S49	700341	374244	46.6%	7208.3	700341	1200.3
S50	450350	124763	72.3%	7207.3	450350	1202.3

Table 3.B.3: Single-portioned instances results derived from P_2^S model

Prob #	OFV	LB	gap (%)	solving time (s)	GA best OFV	GA time (s)
S1	196	196	0.0%	0.0	196	0.0
S2	165	165	0.0%	0.0	165	0.0
S3	499	499	0.0%	0.0	499	0.0
S4	325	325	0.0%	0.0	325	0.0
S5	1027	1027	0.0%	0.0	1027	0.0
S6	721	721	0.0%	0.0	721	0.0
S7	2343	2343	0.0%	0.0	2343	0.0
S8	1429	1429	0.0%	0.0	1429	0.0
S9	4616	4616	0.0%	0.0	4616	0.0
S10	3819	3819	0.0%	0.0	3819	0.0
S11	1524	1524	0.0%	0.0	1524	0.0
S12	9384	9384	0.0%	0.1	9384	0.1
S13	7588	7588	0.0%	0.1	7588	0.1
S14	3543	3543	0.0%	1.1	3543	0.1
S15	18365	18365	0.0%	0.2	18365	0.2
S16	14930	14930	0.0%	1.2	15032	0.2
S17	4128	4128	0.0%	1.1	4128	0.1
S18	23356	23356	0.0%	0.7	23356	0.7
S19	18852	18852	0.0%	4.4	18892	0.4
S20	7835	7835	0.0%	2.7	7835	0.7
S21	47550	47550	0.0%	3.1	47550	2.1
S22	36758	36758	0.0%	32.3	36758	2.3
S23	8432	8432	0.0%	5.2	8432	1.2
S24	95982	95982	0.0%	8.1	95982	3.1
S25	72238	72238	0.0%	146.5	72238	6.5
S26	15473	15473	0.0%	24.3	15473	2.3
S27	169653	169652	0.0%	96.6	169653	39.6
S28	167363	164419	1.8%	1799.5	167363	44.5
S29	139672	116424	16.6%	1806.6	139672	85.6
S30	49006	49006	0.0%	285.7	49006	44.7
S31	242752	242752	0.0%	202.3	242752	105.3
S32	241015	237536	1.4%	3604.5	241015	141.5
S33	235959	220628	6.5%	3610.5	235959	126.5
S34	194604	156881	19.4%	3599.6	194604	232.6
S35	43640	43640	0.0%	634.6	43750	120.6
S36	365528	358720	1.9%	3600.1	365528	207.1
S37	362911	335462	7.6%	3600.1	362911	547.1
S38	359166	313299	12.8%	3599.7	359166	385.7
S39	316714	213266	32.7%	3600.1	316714	509.1
S40	163526	95968	41.3%	3600.0	163526	296.0
S41	488670	481145	1.5%	7200.2	488689	555.2
S42	487623	455307	6.6%	7200.4	487623	564.4
S43	484406	409648	15.4%	7199.4	484406	587.4
S44	446665	248587	44.3%	7200.2	446665	1082.2
S45	308820	124297	59.8%	7200.3	308820	884.3
S46	735309	710648	3.4%	7199.5	735309	940.5
S47	734739	671367	8.6%	7200.2	734739	959.2
S48	733335	594767	18.9%	7200.5	733408	1013.5
S49	699891	371724	46.9%	7200.5	699891	1200.5
S50	450583	123916	72.5%	7200.3	450583	1201.3

Table 3.B.4: Single-portioned instances results derived from P_3^S model

Prob #	OFV	LB	gap (%)	solving time (s)	GA best OFV	GA time (s)
S1	196	196	0.0%	0.0	196	0.0
S2	165	165	0.0%	0.0	165	0.0
S3	499	499	0.0%	0.0	499	0.0
S4	325	325	0.0%	0.0	325	0.0
S5	1027	1027	0.0%	0.0	1027	0.0
S6	721	721	0.0%	0.0	721	0.0
S7	2343	2343	0.0%	0.0	2343	0.0
S8	1429	1429	0.0%	0.0	1429	0.0
S9	4616	4616	0.0%	0.0	4616	0.0
S10	3819	3819	0.0%	0.0	3819	0.0
S11	1524	1524	0.0%	1.0	1524	0.0
S12	9384	9384	0.0%	0.1	9503	0.1
S13	7588	7588	0.0%	0.1	7588	0.1
S14	3543	3543	0.0%	1.1	3543	0.1
S15	18365	18365	0.0%	0.2	18365	0.2
S16	14930	14930	0.0%	3.2	15032	0.2
S17	4128	4128	0.0%	2.1	4128	0.1
S18	23356	23356	0.0%	0.7	23487	0.7
S19	18852	18852	0.0%	5.5	18892	0.5
S20	7835	7835	0.0%	2.5	7835	0.5
S21	47550	47550	0.0%	4.4	47679	1.4
S22	36758	36758	0.0%	40.1	37141	1.1
S23	8432	8432	0.0%	8.2	8432	1.2
S24	95982	95982	0.0%	10.2	95982	4.2
S25	72238	72238	0.0%	185.4	72336	7.4
S26	15473	15473	0.0%	20.3	15473	3.3
S27	169653	169653	0.0%	127.6	169653	35.6
S28	167363	158171	5.5%	1800.1	167363	48.1
S29	139408	90620	35.0%	1811.0	139408	50.0
S30	49006	49006	0.0%	223.8	49103	45.8
S31	242752	242752	0.0%	248.5	242752	128.5
S32	240973	229392	4.8%	3601.3	240973	208.3
S33	235896	210884	10.6%	3613.3	235896	144.3
S34	194636	126823	34.8%	3610.9	194636	363.9
S35	43640	43640	0.0%	402.1	43640	153.1
S36	365528	355011	2.9%	3600.6	365528	252.6
S37	362939	330769	8.9%	3601.5	362939	497.5
S38	359283	310359	13.6%	3601.0	359283	391.0
S39	315399	198704	37.0%	3603.5	315399	600.5
S40	163405	76362	53.3%	3601.6	163405	600.6
S41	488664	477449	2.3%	7201.8	488688	788.8
S42	487625	452625	7.2%	7216.2	487631	427.2
S43	484033	401704	17.0%	7232.5	484033	591.5
S44	445976	251065	43.7%	7215.3	445976	1087.3
S45	309082	126809	59.0%	7213.8	309082	887.8
S46	735312	708280	3.7%	7205.4	735320	1200.4
S47	734703	664678	9.5%	7204.3	734762	957.3
S48	733075	596799	18.6%	7236.3	733252	1200.3
S49	700306	372980	46.7%	7215.3	700306	1200.3
S50	450024	124342	72.4%	7204.9	450024	1200.9

3.C Multiple-Portioned Instances' Results

Table 3.C.1: Multiple-portioned instances results derived from *P* model

Prob #	OFV	LB	gap (%)	solving time (s)
M1	107	107	0.0%	0.0
M2	48	48	0.0%	0.0
M3	381	381	0.0%	0.0
M4	121	121	0.0%	0.0
M5	801	801	0.0%	0.0
M6	148	148	0.0%	0.0
M7	2013	2013	0.0%	0.0
M8	13	13	0.0%	0.0
M9	3804	3804	0.0%	0.0
M10	1100	1100	0.0%	0.0
M11	10	10	0.0%	0.0
M12	7331	7331	0.0%	1.0
M13	2300	2300	0.0%	4.0
M14	137	137	0.0%	1.0
M15	15309	15309	0.0%	9.0
M16	5399	5399	0.0%	30.0
M17	0	0	0.0%	1.0
M18	19768	19768	0.0%	14.0
M19	6984	6984	0.0%	97.0
M20	64	64	0.0%	4.0
M21	42029	42029	0.0%	31.0
M22	8963	8963	0.0%	420.0
M23	0	0	0.0%	6.0
M24	89390	89390	0.0%	304.0
M25	23437	12342	47.3%	3600.0
M26	0	0	0.0%	17.0
M27	164162	162214	1.2%	3600.0
M28	157340	123093	21.8%	3600.0
M29	77737	7829	89.9%	3600.0
M30	763	126	83.6%	3600.0
M31	239146	232475	2.8%	7200.0
M32	234648	188814	19.5%	7200.0
M33	222949	104281	53.2%	7200.0
M34	142095	4326	97.0%	7200.0
M35	283	0	100.0%	7200.0
M36	363227	292309	19.5%	7200.0
M37	358395	180316	49.7%	7201.0
M38	351160	117566	66.5%	7201.0
M39	256589	3016	98.8%	7201.0
M40	12308	0	100.0%	7200.0
M41	488207	421162	13.7%	10800.0
M42	486577	280578	42.3%	10800.0
M43	479935	121318	74.7%	10878.0
M44	380772	2996	99.2%	10827.0
M45	63802	0	100.0%	10801.0
M46	733306	586825	20.0%	10801.0
M47	732201	410219	44.0%	10801.0
M48	729558	126573	82.7%	10801.0
M49	661937	858	99.9%	10801.0
M50	115350	0	100.0%	10800.0

Table 3.C.2: Multiple-portioned instances results derived from P_1^M model

Prob #	OFV	LB	gap (%)	solving time (s)	GA best OFV	GA time (s)
M1	107	107	0.0%	0.0	107	0.0
M2	48	48	0.0%	0.0	48	0.0
M3	381	381	0.0%	0.0	381	0.0
M4	121	121	0.0%	0.0	121	0.0
M5	801	801	0.0%	0.0	801	0.0
M6	148	148	0.0%	0.0	148	0.0
M7	2013	2013	0.0%	0.0	2013	0.0
M8	13	13	0.0%	0.0	13	0.0
M9	3804	3804	0.0%	1.1	3804	0.1
M10	1100	1100	0.0%	1.1	1100	0.1
M11	10	10	0.0%	0.1	10	0.1
M12	7331	7331	0.0%	1.3	7331	0.3
M13	2300	2300	0.0%	6.2	2300	0.2
M14	137	137	0.0%	2.1	143	0.1
M15	15309	15309	0.0%	17.6	15309	0.6
M16	5399	5399	0.0%	35.6	5495	0.6
M17	0	0	0.0%	5.0	0	0.0
M18	19768	19768	0.0%	20.9	19768	1.9
M19	6984	6984	0.0%	126.8	6984	1.8
M20	64	64	0.0%	13.8	64	0.8
M21	42029	42029	0.0%	93.6	42029	4.6
M22	8963	8963	0.0%	655.2	8963	5.2
M23	0	0	0.0%	14.2	0	0.2
M24	89390	89390	0.0%	586.1	89390	17.1
M25	23215	6412	72.4%	3600.6	23215	23.6
M26	0	0	0.0%	17.4	0	1.4
M27	164162	153928	6.2%	3600.0	164273	211.0
M28	154373	116654	24.4%	3599.6	154373	212.6
M29	61318	3162	94.8%	3600.6	61318	181.6
M30	753	0	100.0%	3600.0	753	52.0
M31	238913	227120	4.9%	7200.1	238913	472.1
M32	230771	190369	17.5%	7200.6	230771	369.6
M33	212700	92037	56.7%	7201.2	212700	600.2
M34	103425	3621	96.5%	7199.9	103425	583.9
M35	264	0	100.0%	7200.4	264	227.4
M36	361092	303931	15.8%	7199.6	361092	600.6
M37	352011	198842	43.5%	7313.9	352011	600.9
M38	339161	119161	64.9%	7371.6	339161	600.6
M39	179657	2770	98.5%	7202.7	179657	600.7
M40	11560	0	100.0%	7200.8	11560	600.8
M41	486866	428252	12.0%	10800.5	486866	1200.5
M42	483746	295709	38.9%	10806.1	483746	1202.1
M43	467799	124835	73.3%	10909.6	467799	1201.6
M44	306088	2737	99.1%	10803.9	306088	1202.9
M45	62518	0	100.0%	10801.3	62518	1202.4
M46	732687	595876	18.7%	10801.2	732687	1202.2
M47	730705	415626	43.1%	10802.8	730705	1202.8
M48	725532	154006	78.8%	10860.8	725532	1203.8
M49	611566	1529	99.8%	10801.6	611566	1201.6
M50	86258	0	100.0%	10802.1	86258	1201.1

Table 3.C.3: Multiple-portioned instances results derived from P_2^M model

Prob #	OFV	LB	gap (%)	solving time (s)	GA best OFV	GA time (s)
M1	107	107	0.0%	0.0	107	0.0
M2	48	48	0.0%	0.0	48	0.0
M3	381	381	0.0%	0.0	381	0.0
M4	121	121	0.0%	0.0	121	0.0
M5	801	801	0.0%	0.0	801	0.0
M6	148	148	0.0%	0.0	148	0.0
M7	2013	2013	0.0%	0.0	2013	0.0
M8	13	13	0.0%	0.0	13	0.0
M9	3804	3804	0.0%	0.1	3804	0.1
M10	1100	1100	0.0%	1.1	1100	0.1
M11	10	10	0.0%	1.1	10	0.1
M12	7331	7331	0.0%	3.3	7331	0.3
M13	2300	2300	0.0%	6.2	2300	0.2
M14	137	137	0.0%	2.2	137	0.2
M15	15309	15309	0.0%	16.6	15351	0.6
M16	5399	5399	0.0%	29.6	5495	0.6
M17	0	0	0.0%	3.0	0	0.0
M18	19768	19768	0.0%	20.7	19768	1.7
M19	6984	6984	0.0%	117.5	6984	1.5
M20	64	64	0.0%	15.9	64	0.9
M21	42029	42029	0.0%	60.2	42029	4.2
M22	8963	8963	0.0%	527.7	8963	4.7
M23	0	0	0.0%	17.2	0	1.2
M24	89390	89390	0.0%	425.1	89390	16.1
M25	23215	11299	51.3%	3600.0	23215	22.0
M26	0	0	0.0%	15.6	0	2.6
M27	164437	160713	2.3%	3599.5	164437	185.5
M28	153669	117592	23.5%	3599.8	153669	126.8
M29	62545	4938	92.1%	3600.3	62545	287.3
M30	705	0	100.0%	3600.2	705	76.2
M31	238913	234116	2.0%	7202.5	238913	268.5
M32	230771	182924	20.7%	7200.5	230771	377.5
M33	211594	100990	52.3%	7200.5	211594	600.5
M34	105801	3077	97.1%	7200.5	105801	556.5
M35	304	0	100.0%	7200.4	304	133.4
M36	361003	303794	15.8%	7200.7	361003	600.7
M37	352715	192517	45.4%	7339.4	352715	600.4
M38	338596	114971	66.0%	7200.9	338596	600.9
M39	179811	2830	98.4%	7200.2	179811	601.2
M40	10809	0	100.0%	7201.1	10809	600.1
M41	487248	427064	12.4%	10800.7	487248	1201.7
M42	482981	295363	38.8%	10801.9	482981	1200.9
M43	466737	124834	73.3%	11160.4	466737	1200.4
M44	305921	2896	99.1%	10799.7	305921	1202.7
M45	64408	0	100.0%	10800.3	64408	1201.4
M46	732609	595817	18.7%	10996.2	732609	1201.2
M47	730704	0	100.0%	10808.4	730704	1202.4
M48	725160	154006	78.8%	11031.0	725160	1204.0
M49	603563	1407	99.8%	10801.5	603563	1201.5
M50	83748	0	100.0%	10802.3	83748	1201.3

Table 3.C.4: Multiple-portioned instances results derived from P_3^M model

Prob #	OFV	LB	gap (%)	solving time (s)	GA best OFV	GA time (s)
M1	107	107	0.0%	0.0	107	0.0
M2	48	48	0.0%	0.0	48	0.0
M3	381	381	0.0%	0.0	381	0.0
M4	121	121	0.0%	0.0	121	0.0
M5	801	801	0.0%	0.0	801	0.0
M6	148	148	0.0%	0.0	148	0.0
M7	2013	2013	0.0%	0.0	2013	0.0
M8	13	13	0.0%	0.0	13	0.0
M9	3804	3804	0.0%	1.1	3804	0.1
M10	1100	1100	0.0%	1.1	1100	0.1
M11	10	10	0.0%	0.1	10	0.1
M12	7331	7331	0.0%	2.2	7331	0.2
M13	2300	2300	0.0%	4.4	2300	0.4
M14	137	137	0.0%	1.1	137	0.1
M15	15309	15309	0.0%	10.8	15309	0.8
M16	5399	5399	0.0%	20.8	5577	0.8
M17	0	0	0.0%	3.0	0	0.0
M18	19768	19768	0.0%	15.6	19768	1.6
M19	6984	6984	0.0%	102.1	6984	2.1
M20	64	64	0.0%	5.0	64	1.0
M21	42029	42029	0.0%	51.9	42029	4.9
M22	8963	8963	0.0%	350.9	8963	5.9
M23	0	0	0.0%	7.7	20	1.7
M24	89390	89390	0.0%	286.5	89390	26.5
M25	23215	11695	49.6%	3599.4	23215	24.4
M26	0	0	0.0%	33.1	0	3.1
M27	164273	163178	0.7%	3600.2	164437	163.2
M28	153588	118827	22.6%	3600.2	153588	129.2
M29	62063	4900	92.1%	3600.2	62063	267.2
M30	705	705	0.0%	3325.1	772	61.1
M31	238913	235485	1.4%	7213.1	238913	318.1
M32	230771	186620	19.1%	7200.1	230771	496.1
M33	212526	102479	51.8%	7199.4	212526	600.4
M34	104053	2891	97.2%	7199.7	104053	600.7
M35	239	67	72.0%	7199.8	239	230.8
M36	361020	302346	16.3%	7200.4	361020	601.4
M37	351877	172263	51.0%	7201.0	351877	600.0
M38	337989	94755	72.0%	7200.2	337989	601.2
M39	181196	2701	98.5%	7200.3	181196	600.3
M40	11125	0	100.0%	7200.5	11125	600.5
M41	487059	423548	13.0%	10800.3	487059	1201.3
M42	483660	281031	41.9%	10801.2	483660	1201.2
M43	467276	105785	77.4%	10799.9	467276	1200.9
M44	311967	2531	99.2%	10799.9	311967	1200.9
M45	63789	0	100.0%	10801.1	63789	1202.1
M46	732608	589678	19.5%	10829.2	732608	1200.3
M47	730853	400895	45.1%	10966.0	730853	1202.0
M48	725016	134869	81.4%	11056.8	725016	1203.9
M49	607925	1002	99.8%	10800.1	607925	1201.1
M50	83229	0	100.0%	10801.1	83229	1203.1

Table 3.C.5: Multiple-portioned instances results derived from P_4^M model

Prob #	OFV	LB	gap (%)	solving time (s)	GA best OFV	GA time (s)
M1	107	107	0.0%	0.0	107	0.0
M2	48	48	0.0%	0.0	48	0.0
M3	381	381	0.0%	0.0	381	0.0
M4	121	121	0.0%	0.0	121	0.0
M5	801	801	0.0%	0.0	801	0.0
M6	148	148	0.0%	0.0	148	0.0
M7	2013	2013	0.0%	0.0	2013	0.0
M8	13	13	0.0%	0.0	13	0.0
M9	3804	3804	0.0%	0.1	3804	0.1
M10	1100	1100	0.0%	2.1	1100	0.1
M11	10	10	0.0%	0.1	10	0.1
M12	7331	7331	0.0%	3.3	7331	0.3
M13	2300	2300	0.0%	102.4	2300	0.4
M14	137	137	0.0%	5.2	137	0.2
M15	15309	15309	0.0%	39.7	15351	0.7
M16	5399	4016	25.6%	3600.8	5399	0.8
M17	0	0	0.0%	4.1	0	0.1
M18	19768	19768	0.0%	22.1	19768	2.1
M19	6984	1875	73.2%	3600.2	6984	1.2
M20	64	64	0.0%	17.3	64	1.3
M21	42029	42029	0.0%	105.0	42029	4.0
M22	8963	2073	76.9%	3605.9	8963	5.9
M23	0	0	0.0%	40.1	20	2.1
M24	89390	89390	0.0%	1881.0	89390	19.0
M25	23215	2492	89.3%	3599.9	23215	27.9
M26	0	0	0.0%	13.7	0	0.7
M27	164437	157926	4.0%	3602.3	164437	235.3
M28	153588	112021	27.1%	3599.8	153588	207.8
M29	62402	2953	95.3%	3600.2	62402	300.2
M30	733	0	100.0%	3600.3	733	57.3
M31	238913	232872	2.5%	7216.1	238913	229.1
M32	230771	177519	23.1%	7200.2	230771	431.2
M33	212406	92055	56.7%	7201.1	212406	542.1
M34	105828	3074	97.1%	7201.3	105828	600.3
M35	192	0	100.0%	7200.1	192	271.1
M36	360935	303794	15.8%	7201.5	360935	600.5
M37	352756	192517	45.4%	7305.2	352756	600.2
M38	336993	114971	65.9%	7201.3	336993	600.3
M39	182744	2857	98.4%	7200.2	182744	601.2
M40	11062	0	100.0%	7201.4	11062	600.4
M41	487066	427064	12.3%	10801.8	487066	1192.8
M42	483485	295363	38.9%	10803.2	483485	1200.2
M43	467159	124834	73.3%	11188.5	467159	1201.5
M44	305912	2103	99.3%	10912.3	305912	1202.3
M45	60602	0	100.0%	10804.5	60602	1200.5
M46	732605	595817	18.7%	10964.0	732605	1201.0
M47	730993	0	100.0%	10810.9	730993	1200.9
M48	725217	154006	78.8%	11074.7	725217	1200.7
M49	607768	1407	99.8%	10805.4	607768	1200.4
M50	87612	0	100.0%	10804.2	87612	1203.3

3.D Certification of Student Work

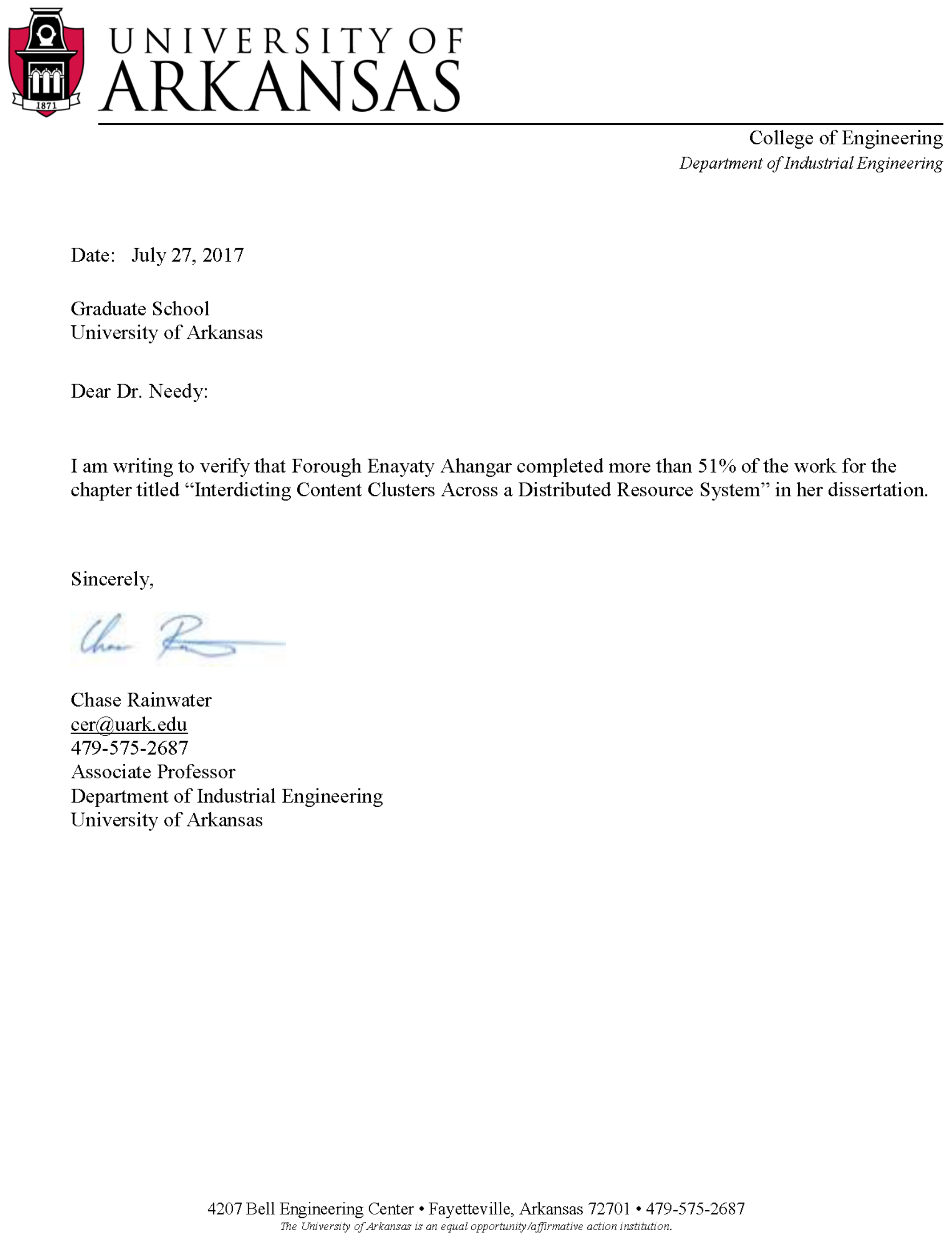

UNIVERSITY OF ARKANSAS

College of Engineering
Department of Industrial Engineering

Date: July 27, 2017

Graduate School
University of Arkansas

Dear Dr. Needy:

I am writing to verify that Forough Enayaty Ahangar completed more than 51% of the work for the chapter titled "Interdicting Content Clusters Across a Distributed Resource System" in her dissertation.

Sincerely,

[illegible]

Chase Rainwater
cer@uark.edu
479-575-2687
Associate Professor
Department of Industrial Engineering
University of Arkansas

4207 Bell Engineering Center • Fayetteville, Arkansas 72701 • 479-575-2687
The University of Arkansas is an equal opportunity/affirmative action institution.

4. Risk Assessment of *Salmonella* Contamination in Chinese Poultry Production and Delivery

4.1 Introduction

Salmonella is one of the foodborne pathogens that can be transmitted to human by consuming pork, chicken meat, etc. Foodborne *Salmonellosis*, the disease caused by *Salmonella*, has been a great concern to many countries including China in the past years. Also, according to interviews with experts in China risks of antibiotics and pesticides in Chinese poultry has been under investigation recently. They believe that microbial risk assessment is necessary as it will be a requirement for preparation for the next set of challenges they face in food safety.

Salmonella particularly draws attentions because its infection can pose serious threats to human health and this can result in enormous economic loss (Li et al., 2016). *Salmonellosis*' symptoms start 8-72 hours after infection and last 4-7 days. They include fever, abdominal cramps, and diarrhea (Bollaerts et al., 2008). It can also lead to hospitalization and result in blood infection which can be fatal.

According to China National Center for Food Safety Risk Assessment (2015), each year more than 9 million people get sick because of consuming *Salmonella* and 800 of them die. It is estimated that 3 million person-times cases in a year caused by *Salmonella* were because of consuming chickens and nearly half of them are caused by cross-contamination (CC) with raw chicken. This number can be reduced to 1 million cases if preparing raw chicken and cooking occur using different utensil or to 1.2 million if all the utensil used to prepare the raw chicken be washed by detergent before the cooking.

Salmonella is known to be the cause of approximately 70-80% of foodborne bacterial infection in China (Yang et al. 2010 and World Health Organization and others 2000) and based on a survey conducted in 2011 in six provinces, about 40% of retail raw chickens in China are contaminated by *Salmonella* which is relatively close to the rate of the other countries. However, the rate is estimated to be higher in summers (China National Center for Food Safety Risk Assessment, 2015). This costs poultry related companies enormously every year, thus, more efforts are required to take place in order to control *Salmonella*'s raw chicken CC as it is continuously being done in other countries. The United States managed to drop this number to only 2 percent of chicken parts from the suppliers by defining new supplier requirements in June 2016 (Carol Beach, 2016).

Due to being perceived as healthier, pork is being substituted by poultry in China (Zhijian, 2013). In 2011, China was the second largest producer of poultry meat and eggs (Mulder, 2011) in the world. There are different breeds of chickens for different purposes, however, for simplicity they can be placed into three categories (Nutrena, 2017):

– Laying breeds, which produce eggs
– Broilers or meat-producing breeds, which are the source of poultry meat
– Dual-purpose breeds

Among all types of chickens, broilers are the main kind that is consumed in many countries and a large percentage of it is colonized by *Salmonella* since their skin and meat of carcasses can be contaminated during slaughter and processing (World Health Organization, 2002). There are three types of poultry meat-producing breeds that dominates China's poultry market: 1- broilers ($\approx$ 50%), 2- spent hens ($\approx$ 20%), and 3- waterfowl ($\approx$ 30%). In all, chicken makes up almost 70% of the poultry market in China. There are two known types of broilers in the first category, white and yellow feathered chickens. White-feathered chickens, introduced by foreigners to China, are replacing the domestic yellow-feathered breeds due to shorter growing periods and having higher gain of weight in shorter amount of time (Pan, 2013).

As food safety has become an important factor in every food industry, bacterial infection in poultry market has also attracted great attentions to all poultry industries including the ones in China (Li et al., 2016). Applying different control methods for reducing the *Salmonellosis* infections in food industry is now necessary for such industry in a country with more than 1.3 billion population (Worldometers, 2017).

In Section 4.2, risk assessment and our proposed model will be explained. In Section 4.3 results will be discussed followed by conclusion and future work in Section 4.4.

4.2 Risk Assessment (RA)

According to Lammerding and Fazil (2000) a hazard can be referred to "a biological agent, that is, the microorganism and/or its toxin(s), that has the potential to cause an adverse health effect" while risk is "the probability of a specific adverse outcome per exposure to the food." To assess risk in the poultry supply chain, first we need to identify which food and pathogen are leading a particular foodborne illness and its magnitude (Lammerding and Fazil, 2000). In this research, the pathogens are various strains of *Salmonella* that may cause infection to the consumer of the meat and the objective is to develop a quantitative model to assess its risk. In order to assess the risk, we first need to divide the pathway into multiple operation units (e.g., slaughtering, scalding, defeathering, evisceration, etc) so at each stage possible changes to *Salmonella* is individually studied.

Risk assessment (RA) is "a process that provides an estimate of the probability and impact of adverse health effects attributable to potentially contaminated foods" (Lammerding and Fazil, 2000). As shown in Figure 4.1, RA includes four steps (Lammerding and Fazil, 2000):

1- **Hazard Identification**, which determines what agents the food of concern contains that have the capability to cause adverse health effect.

2- **Exposure Assessment**, which is related to calculating the likelihood of the food consumption.

3- **Hazard Characterization**, which specifies the nature of the adverse health effect. There are DR models used in this step that will be discussed later.

4- **Risk Characterization**, which is the integration of the last two steps and outputs the risk estimate.

The completion of the four steps results in a risk estimate which is the probability of illness caused by the food and can be expressed as the number of infected people per year in a country or a number of infected people per 10,000 population (Lammerding and Fazil, 2000). Lammerding

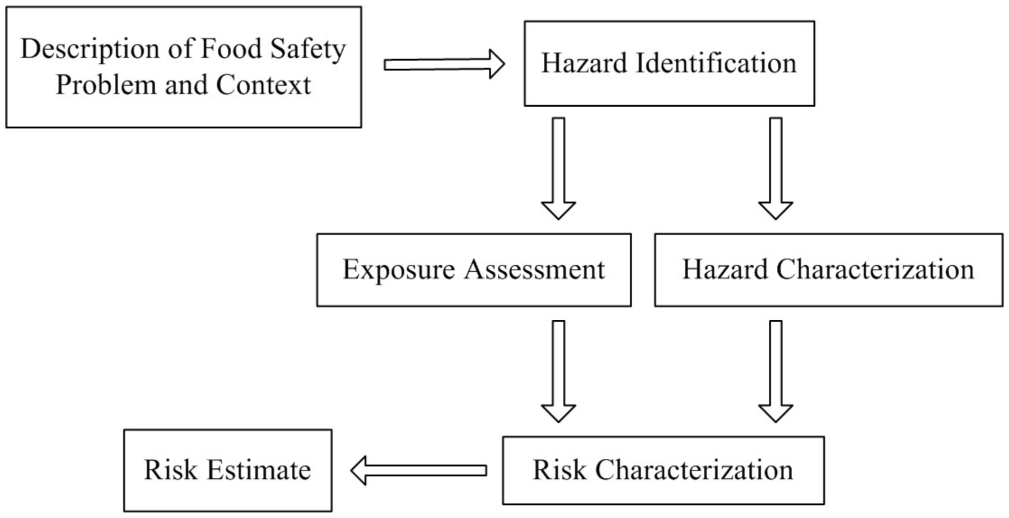

Figure 4.1: Steps of microbial food safety risk assessment (Lammerding and Fazil, 2000)

and Fazil (2000) define risk estimate a "measure of the magnitude of risk based on current scientific knowledge and understanding".

Since the hazard, *Salmonella*, is already specified, Step 1 is completed. We next consider the Exposure Assessment in Step 2 and determine the risk for whoever consumes the potentially contaminated meat. In order to do that, we create a comprehensive QRAM that includes the production operations and distribution before the retail, transportation, preparation and serving, and consuming that are done in the literature. In order to do Step 3, Hazard Characterization, we need to identify a DR model which suits our assessment in accordance to food, host, and pathogen which are all known (poultry meat, human, *Salmonella* strains). The main focus of our research lies in Step 4, Risk Characterization, which will result in the risk estimate.

Each province in China has its own development levels of poultry processing industry which will affect on *Salmonella* contamination Li et al. (2016). The supply chain of chickens in the companies includes multiple stages as shown in Figure 4.2. Each broiler chicken transported in coops (cages to confine the chickens) initially go through the slaughtering stage and the carcass will be wetted and hanged to complete bleeding. Then each carcass goes into a hot water pool to be scalded for easier defeathering. After less than a minute scalding, fast operations of defeathering and rinsing are performed. Then operators complete evisceration manually and all birds go into a pool for a thorax cleaning. A precooling pool accept carcasses afterward to lower their temperature below 10 °C and then they go into a second chilling pool with the temperature of 0-2 °C for half an hour before going to storage.

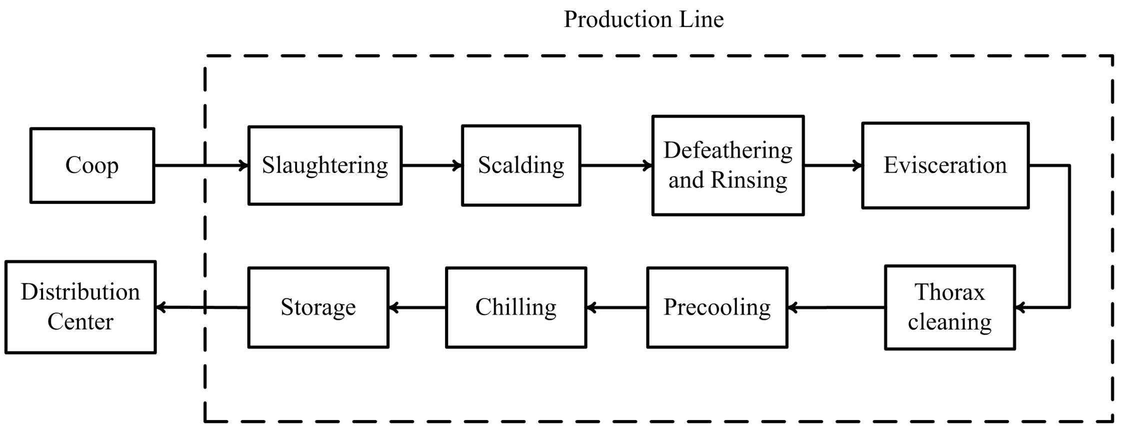

Figure 4.2: The studied pathway including all the production line operations

After production, birds are transported to a distributor. The distributor will then package the carcasses which may include carcasses from other companies. This serves as a post-processing source of CC that has received little attention in the literature due to the deviation in distribution between Asia and North America.

According to field interviews with Chinese biological engineerings, two of the stages in Figure 4.2 are assumed to have the potentials for *Salmonellosis* CC, precooling and chilling. However, we added thorax cleaning stage to the list since all of these stages include pools in which numerous carcasses soak for an extended period of time. These pools are the only places where birds come into contact with one another and this increases possibility of CC. Due to the slim chance of contact between the birds in all the other stages, CC is not considered in the remainder of the production line. Note that the possibility of CC at two stages of slaughtering and evisceration would only be due to poor tool sanitation which is not considered in this effort.

In order to enhance the food safety of poultry products, our Chinese representative companies (names redacted to respect confidentiality agreements) in conjunction with veterinary scientists from South China Agricultral University have collected data on the contamination of foodborne pathogens since October 2016. Every 2-3 weeks, samples from various stages of the process were taken. The results specify the positivity or negativity of the bird contamination by each *Salmonella* strain. These results are used in our proposed QRAM as input data or data for validation of the model's output. However, to better estimate different distributions used in the model, other tests are required to be done in the next 6-12 months. For that reason, in this research, the lack of data is compensated by the published data in multiple papers from the literature.

Table 4.1 summarizes the combined data for 5 rounds of the tests performed in three production lines from October 2016 to May 2017. At different points throughout the production, samples of size 3-109 were collected and tested different parts of the birds (anal, swab, and chicken carcass) or water samples for contamination. The data provided contains each test's sample size and positive rate which indicates the percentage of prevalence. The prevalence incidence indicates the percentage of the infected chickens. The first two tests that are samples on the chicken are ”Before the slaughter” and ”After opening the chamber”. Based on the average of the two positive rates (8.6% and 29.7%), we use 20% as our initial prevalence rate.

Table 4.1: Data from the Chinese partner company

Samples' Times	Sample type	Sample size	Positive number	Positive rate (%)
Coop	Contact area	10	1	10.0 %
Before the slaughter	Anal	245	21	**8.6** %
After beating the hair	Swab	258	66	25.6 %
After opening the chamber	Carcass	246	73	**29.7** %
After cleaning	Carcass	120	13	10.8 %
Thorax cleaning	Water	27	6	22.2 %
Before the precooling pool	Water	62	12	19.4 %
During the precooling pool	Water	21	3	14.3 %
After the precooling pool	Water	80	4	5.0 %
After Precooling	Carcass	270	42	15.6 %
Before the cold storage	Carcass	321	42	13.1 %
Food samples	Contact area	110	20	18.2 %
Total		1770	303	17.1 %

4.2.1 Enumeration Methods

In order to describe the model, first we need to define the units of the pathogen. There are two different ways to enumerate a microorganism (Whittemore, 1993):

1- Quantitative procedures, by which the number of microorganisms is counted.

2- Semiquantitative, which is done by one of the standard culture procedures such as the standard plate counting (SPC) that counts the colony forming unit (CFU) of the microorganisms or one of the most probable number (MPN) procedures.

A CFU is defined to be a tissue culture infectious dose of a particular pathogen (World Health Organization, 2003). Oblinger and Koburger (1975) define the MPN method as the statistics directly related to the frequency of occurrence of positive results that are most likely to happen when a given number of bacteria exist in a sample. Therefore, MPN can be defined as the most probable number of CFU in a particular sample volume. According to Dickson (1989) the MPN method is used to present the extent of contamination for most food products. The data regarding extent of contamination is currently being collected, therefore, we will only use the prevalence data from the tests' results and use the data from the literature for the extent of contaminations and CCs. As done in Oscar (1998) and Oscar (2004b), throughout this research we will use MPN method based on different distributions that we define and the extent unit will be the logarithmic form of CFU/chicken to represent the extent of *Salmonella* contamination except for the last two stages (serving and consumption) in which MPN will be used.

4.2.2 Previous Quantitative Risk Assessment Models

There are multiple QRAMs in the literature for different combinations of pathogen, host, food, and pathway. Cassin et al. (1998) established a model for *Escherichia Coli O157:H7* in ground beef hamburgers in which the pathway includes the production of the food through processing, handling, and consumption and the exposure prediction at the end. A Monte Carlo was applied to simulate the created risk model. Initial data for this paper was based on the data in the literature and they applied a histogram of the data instead of a fitted distribution. Our model also considers different stages of the production line but there are great gaps between the their paper and ours such as the studied pathogen and the animal carrying the bacteria.

Rosenquist et al. (2003) developed a model for chickens and a pathogen called Campylobacter. They too consider the production line in the slaughterhouse (including scalding, defeathering, evisceration, and wash+chill) and handling in their model. Lack of data forced them to simplify several details of the process (the production line and the kitchen). They show that CC from positive to negative flocks in the production line has almost no impact on the final human cases compared to the effect that smaller number of prevalence or lower contamination dose for the positive flocks at the beginning of the process can have. The pathway, the host, and the food are similar to ours but the different pathogen distinguishes our research from theirs.

Whiting and Buchanan (1997) applied a stochastic simulation approach to predict growth or inactivation of Sallmonella *Enteritidis* in eggs which will be used to produce mayonnaise. They broke down the pathway of farm-to-table into different units of operation and applied Monte Carlo for their simulation. Various distributions or variations were simulated to see their reflect on the output (final probability of infection). Even though their studied pathogen is one of the strains of *Salmonella*, but the fact that the food of study is egg with a completely different processing line makes this research different than ours.

Oscar (1998) simulated a model to assess the number of *Salmonellosis* cases out of 1000 chickens. The pathway started right after the processing plant exit and continued until the consumption. A valid input setting was not defined in the paper, therefore, in 2004, he modified the model and filled out most of the input gaps in his 1998's paper (Oscar, 1998).

Oscar (2004b) developed a QRAM for a whole chicken and *Salmonella* considering a pathway of retail-to-table. He divided the pathway into multiple unit operations: retail, consumer transportation, cooking, serving and applied a DR model for the consumption part. Based on the data taken from the literature, he proposed different probability distributions for the initial amount of *Salmonella* in the retail section and its growth in the other sections. First he developed a QRAM and used @Risk simulate 10,000 iterations (representing 10,000 chickens) to describe his model, and then, he simulated 4 different scenarios with different random seeds to simulate 1,000,000 chickens and predicted there are 0.44 cases of *Salmonellosis* per 100,000 consumers of chicken meat and a mean of 17.8 *Salmonella* cases per 1,000,000 chickens Oscar (2004b). To the best of our knowledge, this paper is the closest one in the literature to our research as it considers *Salmonellosis* cases in human by chicken consumption. The main difference between our research and his paper lies in the defined pathway of the pathogen. His pathway starts after the retail and does not consider the previous stages. We focus on each stage of the production line, transportation and distribution before retail and all stages following the retail. In the next section modeling and simulation details of the model for each stage of the pathway are discussed.

4.2.3 Quantitative Risk Assessment Model (QRAM)

Due to having a long pathway we will discuss each component of the process modeled individually. Modeling each stage in the pathway includes determining prevalence incidence, the extent of contamination, log growth or reduction of the pathogen and CC for each broiler. The prevalence incidence indicates whether or not the chicken is contaminated while the extent of contamination represents the log CFU/chicken if the chicken is contaminated. The prevalence incidence and the extent of contamination appear both as inputs at the beginning of the stage and outputs at the end of the stage. Each will not change if no growth/reduction or CC occurs during that stage. However, at multiple stages, there is a chance of growth or reduction of the existed number of the pathogen. This will be represented as log growth or log reduction which represents the amount of increase or decrease of the pathogen in logarithmic scale (except for the last two stages). Also, CC may occur for a negative chicken at some stages turning it to a positive one for the next stage.

Note that *Salmonella* must be treated as a discrete entity, thus we need to force each contamination extent unit to represent an integer value of *Salmonella*. To have a discrete value, we take the floor of those whose unit is MPN. If a value x has a unit of CFU/chicken, we take the log of the floor of 10^x to keep the unit and have an integer value of *Salmonella*.

4.2.3.1 Initial Contamination

As shown in Table 4.1, there are two sets of tests on the birds at early stages: “Before the slaughter” and “After opening the chamber”. Out of 491 (245+246) samples, 94 (21+73) were positive which gives a positive rate of 19.1%. Therefore, as our initial prevalence, we use the value of 20%. Not that we will use other values for our sensitivity analysis in Section 4.3.

As our colleagues in China continue work on the ongoing tests for contamination and CC extents throughout the production line stages, we use published data for multiple parts of our model regarding these parameters. For that reason, the extent of contamination will be taken from three different papers shown in Table 4.2. Oscar (2004b) used 6 different papers to estimate the interval of the contamination, however only three of them (Waldroup 1996, Whittemore 1993, and Surkiewics et al. 1969) studied the contamination extent for the processing plant and not the retail. The three papers’ values are shown in Table 4.2.

Table 4.2: MPN of *Salmonella* per chicken at processing plant

Reference	Minimum	Most likely	Maximum
Surkiewics et al. (1969)	1	30^{-}	300^{+}
Waldroup (1996)	-	6^{-}	-
Whittemore (1993)	-	7	-
Maximum	1	30	300

$^{-}$ Less than
$^{+}$ More than

Most of our inputs or outputs are considered to have PERT distributions. It is known to be flexible since it vary from a normal distribution to a lognormal one that is skewed to the left or right (Oscar, 2004b). It requires three values, minimum, most likely (mean or median), and maximum to be defined. To be conservative, we use the extreme values, 1 for the minimum, 30 for the mean, and 300 for the maximum, from Table 4.2. Note that the PERT distribution throughout this chapter is shown as follows: PERT(minimum,mean,maximum).

Table 4.3 represents the input/output data for the first stage considered in the process, Initial Contamination. The input (incidence) representing the prevalence indicates whether or not the simulated chicken is contaminated. It has a Bernoulli distribution with the probability of 0.2. The extent of contamination has a distribution of PERT(0,1.5,2.5). Note that the three values are equal to log(1), ≈log(30), and ≈log(300), respectively, due to using log CFU/chicken as our unit of contamination extent. Since no operation takes place at this stage, both outputs are the same as the inputs. Also, if a chicken is not contaminated (i.e., $i_{in}^{IC} = 0$), the associated extent output will be equal to 0 in (4.4).

Table 4.3: Initial Contamination

Description	Distribution/Formula	
Input (incidence)	$^{*}i_{in}^{IC} = Binomial(1, 0.2)$	(4.1)
Input (extent)	$^{**}e_{in}^{IC} = Pert(0, 1.15, 2.5)$	(4.2)
Output (incidence)	$i_{out}^{IC} = i_{in}^{IC}$	(4.3)
Output (extent)	$e_{out}^{IC} = e_{in}^{IC} * i_{in}^{IC}$	(4.4)

* Reference: retrieved from real data
** Reference: Surkiewics et al. (1969)

4.2.3.2 Slaughtering

The second stage of the pathway is slaughtering which contains slaughtering, wetting, hanging, and bleeding. Table 4.4 represent all the information in our model regarding this stage. The first two input values in the table are equal to the two outputs of the previous stage in Table 4.3. As each stage can have a positive or negative effect on the number of the pathogen on each contaminated chicken, we must specify some functions to model the log growth/reduction of the possibly existed pathogens. Note that for some stages these log growth/reduction will be equal to 0, but they are still in the model to be updated in case any changes occur.

There are multiple factors that can cause a growth or reduction of the extent of contamination in a contaminated chicken. Two of the most common ones are temperature and time which are required to always be considered, especially when the temperature is in the interval where *Salmonella* can grow or get inactivated. According to United States Department of Agriculture

Agricultural Research Service (2017), the minimum, optimum, and maximum temperatures of growth for *Salmonella* serotypes are 5.2°C, 35-43°C, and 46.2 °C, respectively. Temperatures above the maximum will reduce the number of the pathogen. There are papers that studied the effect of various temperature ranges on different *Salmonella* serotypes (Oscar 2003, Oscar 2006 Juneja et al. 2007, Oscar 2009, and Oscar 2011), however, they all considered the temperatures above 4°C which is less than the minimum temperature of the growth interval. Richard Lawley (2013) claims that reports suggesting the growth of *Salmonella* are not universally accepted, however *Salmonella* can survive in chilled or frozen foods. Therefore, we assume *Salmonella* cannot grow but will survive when temperature is below 4°C.

Throughout the model, we use the data provided in the literature and present simplifying assumptions if there is no information regarding the growth/reduction of the pathogen. The temperature in the slaughterhouse is the same as the outdoor, which is 18°C in the winter, 25°C in the spring and the fall, and 33°C in the summer. Thus, a discrete distribution, as shown in Table 4.4, is considered to model the temperature. Since 25° occurs twice as much as the other two temperatures it has the probability of 0.5. Each chicken stays in this stage between 20 and 60 minutes with a mean of 40 minutes, hence the distribution is PERT(20,40,60).

There are two papers that we use to convert time and temperature to log growth/reduction distributions at each stage. Murphy et al. (2002) considers the thermal inactivation for the temperature between 55-70°C and Oscar (2002) considers the growth for the interval of 8-48°. Note that the number of *Salmonella* instantly start to reduce when encounters heat but it requires a specific amount of time, called lag time, before it can start growing. As all the lag times for temperatures between 18-33 are more than 1.4 hours (Oscar, 2002), it can be concluded that there will be no growth at this stage, hence log growth is equal to 0 in (4.9). All the output are equal to the input ones plus any possible changes that occur during the stage. Since the unit of the contamination extent is log CFU/chicken, the changes during the process need to be added or deducted from the input extent value. Note that at each stage, a change in contamination extent occurs only when it was already contaminated or it got cross-contaminated during the stage. Therefore, *d* is added to or deducted from the initial contamination (i.e., e_{in}^{Sl}) only when $i_{in}^{Sl} = 1$ as done in (4.11).

Table 4.4: Slaughtering

Description	Distribution/Formula	
Input (incidence)	$i_{in}^{Sl} = i_{out}^{IC}$	(4.5)
Input (extent)	$e_{in}^{Sl} = e_{out}^{IC}$	(4.6)
Input (temperature)	$^{*}Discrete(\{18,25,33\},\{0.25,0.5,0.25\})$	(4.7)
Input (time)	$^{*}PERT(20,40,60)$	(4.8)
Input (extent log growth)	$d = 0$	(4.9)
Output (incidence)	$i_{out}^{Sl} = i_{in}^{Sl}$	(4.10)
Output (extent)	$e_{out}^{Sl} = e_{in}^{Sl} + d * i_{in}^{Sl}$	(4.11)

* Reference: retrieved from real data

4.2.3.3 Scalding

In the scalding stage, chickens stay in a pool of hot water with a temperature between 50-65°C for 10-40 seconds modeled as the two PERT distributions in Table 4.5. Note that the time unit in the model is a minute. Since the temperature is above the growth interval, we use the data in Murphy et al. (2002) to model a log reduction. Note that log reduction (growth) is equal to the logarithmic value of any reduction (increase) that occurs to the number of pathogen. Although the temperatures of study are 55-70°C in Murphy et al. (2002), it will give us a very good estimate of the log reduction in our scenario. We use the data for chicken tenders in the paper which has an intercept of 8.6599 and slope of -0.1314. So the output of extent in (4.18) is going to be $e_{out}^{Sc} = e_{in}^{Sc} - d$ if the chicken is contaminated; otherwise it will have the value of e_{in}^{Sc} which is 0.

Table 4.5: Scalding

Description	Distribution/Formula	
Input (incidence)	$i_{in}^{Sc} = i_{out}^{Sl}$	(4.12)
Input (extent)	$e_{in}^{Sc} = e_{out}^{Sl}$	(4.13)
Input (temperature)	$^{*}t_1 = PERT(50, 57.5, 65)$	(4.14)
Input (time)	$^{*}t_2 = PERT(0.2, 0.4, 0.7)$	(4.15)
Input (extent log reduction)	$^{**}d = t_2/10^{-0.1314 * t_1 + 8.6599}$	(4.16)
Output (incidence)	$i_{out}^{Sc} = i_{in}^{Sc}$	(4.17)
Output (extent)	$e_{out}^{Sc} = e_{in}^{Sc} - d * i_{in}^{Sc}$	(4.18)

* Reference: retrieved from real data
** Reference: Murphy et al. (2002)

4.2.3.4 Defeathering and Rinsing

After scalding, a very quick process of defeathering occurs that is followed by rinsing. Both of these operations take less than a minute (modeled in (4.22) of Table 4.6) at a temperature between 10-20°C (4.21). Since the lag time for these temperatures are more than 3 hours (Oscar, 2002), the amount of log growth is negligible, hence $d = 0$, meaning no considerable changes occur on the contamination extent.

Table 4.6: Defeathering and Rinsing

Description	Distribution/Formula	
Input (incidence)	$i_{in}^{DR} = i_{out}^{Sc}$	(4.19)
Input (extent)	$e_{in}^{DR} = e_{out}^{Sc}$	(4.20)
Input (temperature)	$^{*}t_1 = PERT(10, 15, 20)$	(4.21)
Input (time)	$^{*}t_2 = PERT(0.2, 0.4, 1)$	(4.22)
Input (extent log growth)	$d = 0$	(4.23)
Output (incidence)	$i_{out}^{DR} = i_{in}^{DR}$	(4.24)
Output (extent)	$e_{out}^{DR} = e_{in}^{DR} + d * i_{in}^{DR}$	(4.25)

* Reference: retrieved from real data

4.2.3.5 Evisceration

Evisceration can be operated automatically or manually. In all the three production lines, there are operators who manually eviscerate each chicken in one motion. Each carcass stays in the evisceration room between 1-2 minutes. The room temperature is relatively cold (10-20°C) as shown in (4.28) in Table 4.7. The lag time for this temperature is more than 3 hours (Oscar, 2002) so there will not be enough time for the pathogen to start growing, hence, $d = 0$.

Table 4.7: Evisceration

Description	Distribution/Formula	
Input (incidence)	$i_{in}^{Ev} = i_{out}^{DR}$	(4.26)
Input (extent)	$e_{in}^{Ev} = e_{out}^{DR}$	(4.27)
Input (temperature)	$^{*}t_1 = PERT(10, 15, 20)$	(4.28)
Input (time)	$^{*}t_2 = PERT(1, 1.5, 2)$	(4.29)
Input (extent log growth)	$d = 0$	(4.30)
Output (incidence)	$i_{out}^{Ev} = i_{in}^{Ev}$	(4.31)
Output (extent)	$e_{out}^{Ev} = e_{in}^{Ev} + d * i_{in}^{Ev}$	(4.32)

* Reference: retrieved from real data

4.2.3.6 Thorax Cleaning

After evisceration, the thorax of the carcass is cleaned. This process takes 15-30 minutes or less than a minute in a pool with a temperature of 5-15°C which has a lag time more than 6 hours for growth (Oscar, 2002), so the log growth is equal to 0 in (4.37) of Table 4.8. Note that the maximum cumulative time of all of these stages has not exceeded any of the lag time after scalding when the heat led to a reduction of the pathogen, therefore, no growth can still be added to the model.

Up to this stage, the chance of CC has been considered negligible due to lack of contact between the carcasses. This stage is the first stage in the pathway that carcasses have direct contact with each other since they pass through the same pool. To be conservative, we assume a negative carcass can be contaminated with a 20% probability in (4.38) and the extent of contamination has a distribution similar to the initial contamination extent in (4.1). The output (4.41) then will be different from the previous ones since there is a chance that a 0 incidence input changes to a 1 depending on the value of i_{CC}. If a carcass was initially contaminated (i.e., $i_{in}^{TC} = 1$), then its output extent of contamination is equal to $e_{in}^{TC} - d$; otherwise it is equal to $i_{CC} * e_{CC}$ which is the value of

CC extent if CC occurred.

Table 4.8: Thorax Cleaning

Description	Distribution/Formula	
Input (incidence)	$i_{in}^{TC} = i_{out}^{Ev}$	(4.33)
Input (extent)	$e_{in}^{TC} = e_{out}^{Ev}$	(4.34)
Input (temperature)	$^{*}t_1 = PERT(5, 10, 15)$	(4.35)
Input (time)	$^{*}t_2 = PERT(0.2, 0.5, 0.8)$	(4.36)
Input (extent log reduction)	$d = 0$	(4.37)
Input (CC incidence)	$^{**}i_{CC} = Bernoulli(0.2)$	(4.38)
Input (CC extent)	$^{**}e_{CC} = PERT(0, 1.5, 2.5)$	(4.39)
Output (incidence)	$i_{out}^{TC} = max\{i_{in}^{TC}, i_{CC}\}$	(4.40)
Output (extent)	$e_{out}^{TC} = i_{in}^{TC} * (e_{in}^{TC} - d) + (1 - i_{in}^{TC}) * i_{CC} * e_{CC}$	(4.41)

* Reference: retrieved from real data
** Reference: based on estimate

4.2.3.7 Precooling

After cleaning, the carcasses' temperature needs to reach to 0°C to be ready for storage. This happens in two stages, precooling and chilling. Both of these stages contain pools through which each carcass passes. The temperature of the first pool is 6-8°C. The data regarding the time estimated based on field observation is considered to be approximately 5-10 minutes as shown in Table 4.9. The minimum temperature considered in Oscar (2002) is 8°C which has a lag time more than 40 hours. Thus, it is safe to assume that no growth can occur in this pool (i.e., $d = 0$). However, due to the extent of contact that each carcass has with other carcasses and the water, CC must be taken into account. We assumed each negative carcass has a chance of 25% to be contaminated in this stage to an extent modeled in (4.48). Although the temperature in this stage is lower that the previous stage, the chance of CC is considered to be higher due to the larger amount of time spent in this pool. The two outputs are then calculated similarly to the previous stage.

Table 4.9: Precooling

Description	Distribution/Formula	
Input (incidence)	$i_{in}^{Pr} = i_{out}^{TC}$	(4.42)
Input (extent)	$e_{in}^{Pr} = e_{out}^{TC}$	(4.43)
Input (temperature)	$^{*}t_1 = PERT(6,7,8)$	(4.44)
Input (time)	$^{**}t_2 = PERT(5,7,10)$	(4.45)
Input (extent log reduction)	$d = 0$	(4.46)
Input (CC incidence)	$^{**}i_{CC} = Bernoulli(0.2)$	(4.47)
Input (CC extent)	$^{**}e_{CC} = PERT(0,1.5,2.5)$	(4.48)
Output (incidence)	$i_{out}^{Pr} = max\{i_{in}^{Pr}, i_{CC}\}$	(4.49)
Output (extent)	$e_{out}^{Pr} = i_{in}^{Pr} * (e_{in}^{Pr} - d) + (1 - i_{in}^{Pr}) * i_{CC} * e_{CC}$	(4.50)

* Reference: retrieved from real data
* Reference: based on estimate

4.2.3.8 Chilling

The water in the second pool has a temperature between 0-2°C and the carcasses stay in it approximately 5-10 minutes. This part of the process is simulated by a PERT distribution as shown in Table 4.10. Since the highest temperature in this stage is less than the interval for which *Salmonella* can grow it is safe to assume that no growth can occur at this stage.

In order to clean the carcasses the water contains chlorine. Since the pathogen may be present in the meat of the chicken and not its skin, we introduce a Bernoulli distribution in (4.56) with the probability of 50% that indicates whether or not the chlorine in water can affect the existed *Salmonella*. The density of the chlorine in the water is determined to have a Uniform distribution between 20 and 70 ppm. Stopforth et al. (2008) tested the effect of washing spinach and lettuce with water containing 50-200 ppm chlorine on *Escherichia coli O157:H7*, *Salmonella* and showed that it has a reduction of 2.1-2.8 log CFU/g for fresh greens that initially had an extent of 6 log CFU/g. Since the density of chlorine in the paper is more than the pool, we use the first value for the maximum of our PERT distribution to represent the log reduction for our model as done in (4.57). Also, we use 0 as our minimum and 0.3 as our median for the PERT distribution. 0.3 log reduction means the chlorine can inactivate 50% ($10^{-0.3} \approx 0.5$) of the pathogens on the skin of a contaminated bird. The probability of CC incidence is equal to 20% which is less than the previous stage due to lower temperature.

Table 4.10: Chilling

Description	Distribution/Formula	
Input (incidence)	$i_{in}^{Ch} = i_{out}^{Pr}$ 0	(4.51)
Input (extent)	$e_{in}^{Ch} = e_{out}^{Pr}$	(4.52)
Input (temperature)	$^{*}t_1 = PERT(0,1,2)$	(4.53)
Input (time)	$^{*}t_2 = PERT(25,30,35)$	(4.54)
Input (chlorine density in ppm)	$^{*}ch = Uniform(20,70)$	(4.55)
Input (skin contamination incident)	$^{***}s = Bernoulli(0.5)$	(4.56)
Input (extent log reduction)	$^{**}d = PERT(0,0.3,2.1)$	(4.57)
Input (CC incidence)	$^{***}i_{CC} = Bernoulli(0.2)$	(4.58)
Input (CC extent)	$^{***}e_{CC} = PERT(0,1.5,2.5)$	(4.59)
Output (incidence)	$i_{out}^{Ch} = max\{i_{in}^{Ch}, i_{CC}\}$	(4.60)
Output (extent)	$e_{out}^{Ch} = i_{in}^{Ch} * (e_{in}^{Ch} - d) + (1 - i_{in}^{Ch}) * i_{CC} * e_{CC}$	(4.61)

* Reference: retrieved from real data
** Reference: based on estimate and Stopforth et al. (2008)
*** Reference: based on estimate

4.2.3.9 Storage

When the temperature of the carcasses are as low as 0°C they will be stored and depending on their destinations will be sent to their distributors. As shown in Table 4.11, the time in the storage room is modeled as a PERT distribution with minimum and maximum of 1 hour and two days (2880 minutes) and a mean of 10 hours (600 minutes). The temperature is also assumed to have a PERT distribution with the three values of -2, 0, and 2°C . The precise data regarding any log reduction for the temperatures below 4°C requires further tests, however, for now, we just consider no reduction can occur at this stage ($d = 0$).

Table 4.11: Storage

Description	Distribution/Formula	
Input (incidence)	$i_{in}^{St} = i_{out}^{Ch}$	(4.62)
Input (extent)	$e_{in}^{St} = e_{out}^{Ch}$	(4.63)
Input (temperature)	$^{*}t_1 = PERT(-2,0,2)$	(4.64)
Input (time)	$^{*}t_2 = PERT(60,600,2880)$	(4.65)
Input (extent log reduction)	$d = 0$	(4.66)
Output (incidence)	$i_{out}^{St} = i_{in}^{St}$	(4.67)
Output (extent)	$e_{out}^{St} = e_{in}^{St} - d * i_{in}^{St}$	(4.68)

* Reference: based on estimate

4.2.3.10 Transportation and Distribution

It is assumed that no temperature abuse occurs during any part of the transportation to the distributor, at the distribution center, and the transportation to the retail afterward since all the containers of the chickens have a specific temperature range. This range is modeled as a PERT(-2,0,2°C) shown in (4.71) of Table 4.12. The data regarding the time of the total transportations is modeled as a PERT distribution with the values of 5 hours, 10 hours, and 2 days as shown in (4.72). However, due to low values of the temperature, it is safe to assume that log reduction is equal to 0 (i.e., $d = 0$).

One important aspect of this stage is that the distributor combines carcasses from multiple companies and package them together which means there is a high chance of CC for a negative chicken. The CC incidence is modeled in (4.74) which indicate negative chickens might be contaminated with a probability of 0.25 during the packaging. The dose of contamination is assumed to be similar to the other CCs (4.75) . The outputs, similar to other stages, are calculated based on the input data and any possible changes in the stage.

Table 4.12: Transportation and Distribution

Description	Distribution/Formula	
Input (incidence)	$i_{in}^{TD} = i_{out}^{St}$	(4.69)
Input (extent)	$e_{in}^{TD} = e_{out}^{St}$	(4.70)
Input (temperature)	$^*t_1 = PERT(-2, 0, 2)$	(4.71)
Input (time)	$^*t_2 = PERT(300, 600, 2880)$	(4.72)
Input (extent log reduction)	$d = 0$	(4.73)
Input (CC incidence)	$^*i_{CC} = Bernoulli(0.25)$	(4.74)
Input (CC extent)	$^*e_{CC} = PERT(0, 1.5, 2.5)$	(4.75)
Output (incidence)	$i_{out}^{TD} = max\{i_{in}^{TD}, i_{CC}\}$	(4.76)
Output (extent)	$e_{out}^{TD} = i_{in}^{TD} * (e_{in}^{TD} - d) + (1 - i_{in}^{TD}) * i_{CC} * e_{CC}$	(4.77)

* Reference: based on estimate

4.2.3.11 Retail

Retail is the first stage considered in Oscar (2004b) that includes the initial contamination input data as his pathway starts from the retail. In our model, we consider this stage as a middle stage that does not affect the prevalence and the contamination. Therefore, in Table 4.13, the output is exactly the same as the input which is taken from the previous stage. Although, further investigation of any temperature abuse that my lead to pathogen's growth can be considered for this stage. Currently, it is assumed that the situation of each chicken remains the same at the retail stage. Note that from this stage forward, we will apply the model used in Oscar (2004b).

Table 4.13: Retail

Description	Distribution/Formula	
Input (incidence)	$i_{in}^{Re} = i_{out}^{TD}$	(4.78)
Input (extent)	$e_{in}^{Re} = i_{out}^{TD}$	(4.79)
Output (incidence)	$i_{out}^{Re} = i_{in}^{Re}$	(4.80)
Output (extent)	$e_{out}^{Re} = e_{in}^{Re}$	(4.81)

4.2.3.12 Consumer Transportation

Oscar (2004b) modeled consumer transportation with two distributions shown in Table 4.14. Based on a survey used by him, this stage takes between 0.2 hours to 6.3 hours with a mean of 1 hour. Also, the temperature is from -3.9 to 21.1°C with the mean of 7.8°C. Both of them are modeled as PERT distributions. Applying simulation by the data (lag time and growth rate) in Oscar (2002), he calculated that the predicted incidence of potential growth events is as low as 0.02% and the relatively small growth of contamination can be modeled as a PERT distribution shown in (4.85) of Table 4.14.

Note that the data regarding this stage can be improved by taking a survey specifically for Chinese consumers, however, the small values of the existed data in Oscar (2004b) indicates that no high impact this stage can have on the growth of the pathogen unless the average transportation time is much higher than one hour.

Table 4.14: Consumer Transportation

Description	Distribution/Formula	
Input (incidence)	$i_{in}^{CT} = i_{out}^{Re}$	(4.82)
Input (extent)	$e_{in}^{CT} = i_{out}^{Re}$	(4.83)
Input (thermal abuse incidence)	$^{*}T = Bernoulli(0.02)$	(4.84)
Input (extent log growth)	$^{*}d = PERT(0.0005, 0.04, 0.15)$	(4.85)
Output (incidence)	$i_{out}^{CT} = i_{in}^{CT}$	(4.86)
Output (extent)	$e_{out}^{CT} = e_{in}^{CT} + d * T$	(4.87)

* Reference: Oscar (2004b)

4.2.3.13 Cooking

Thermal inactivation during cooking can depend on multiple factors (Oscar, 2004b) such as time and temperature (Murphy et al., 2002), methods of cooking (Brown et al., 1998), products' shape and size and strains of *Salmonella* (Murphy et al., 1999), etc. Based on the data used in Oscar (2004b) and the data for chicken tenders in (Murphy et al., 2002), the distribution shown in (4.90) of Table 4.15 can be used to predict the extent log reduction of the pathogen during the cooking.

Table 4.15: Cooking

Description	Distribution/Formula	
Input (incidence)	$i_{in}^{Co} = i_{out}^{CT}$	(4.88)
Input (extent)	$e_{in}^{Co} = i_{out}^{CT}$	(4.89)
Input (extent log reduction)	$^{*}d = PERT(0.83, 0.81, 96)$	(4.90)
Output (incidence)	$i_{out}^{Co} = i_{in}^{Co}$	(4.91)
Output (extent)	$e_{out}^{Co} = e_{in}^{Co} - d$	(4.92)

* Reference: Oscar (2004b)

4.2.3.14 Serving

There is a chance that before the thermal inactivation during cooking some CC occurs during the food preparation that can cause some pathogens to survive. Percentage of the mishandled chicken that can survive at this stage will be called the CC incidence and be simulated in (4.95) of Table 4.16. There are multiple surveys in the literature about mishandling raw chickens that can lead the pathogen to stay on hands or other surfaces of the kitchen that can be consumed by the person who prepares or serves the food. Oscar (2004b) summarizes the published data in the literature and concluded that a CC incidence rate of 28% can occur in this stage with 0.021, 0.057, and 0.24 as the minimum, mean, and maximum transfer rates, respectively.

Note that the input data, (4.93)-(4.94), are taken from the consumer transportation stage and not the previous stage as mishandling the food occurs before or during cooking. The output's unit of this stage differs from the previous ones as (4.96) indicates the rate and not log reduction. Therefore, we need to calculate the MPN/chicken (not log CFU/chicken) of the pathogens that survived during cooking and also serving.

If mishandling occurs, the extent of the pathogen is going to be the summation of the pathogens survived from cooking and serving. Note that MPN cannot take a fractional value, thus we need to round down the numbers. If no mishandling occur during the cooking (e.g., $i_{CC} = 0$), then the only pathogens that will survive are the ones that could survive the cooking stage.

Table 4.16: Serving

Description	Distribution/Formula	
Input (incidence)	$i_{in}^{Se} = i_{out}^{CT}$	(4.93)
Input (extent)	$e_{in}^{Se} = e_{out}^{CT}$	(4.94)
Input (CC incidence)	$^{*}i_{CC} = Bernoulli(0.28)$	(4.95)
Input (CC extent rate)	$^{*}R_{CC} = PERT(0.021, 0.057, 0.24)$	(4.96)
Output (incidence)	$i_{out}^{Se} = max\{i_{in}^{Se}, i_{CC}\}$	(4.97)
Output (extent in MPN)	$e_{out}^{Se} = i_{CC} * \lfloor 10^{e_{in}^{Se}} * R_{CC} \rfloor + \lfloor 10^{e_{out}^{CT}} \rfloor$	(4.98)

* Reference: Oscar (2004b)

4.2.3.15 Consumption

As discussed in Section 4.2.1, a DR model will be applied in Step 3 of RA, hazard characterization (Figure 4.1). A DR is the relationship between the number of microbial organisms digested by a consumer and a specific outcome (e.g., infection, illness, or mortality). The degree of the sickness caused by *Salmonella* depends on the consumer's health status, which differs for individuals who are infants, elderly, pregnant, or immunocompromised, and the virulence of *Salmonella* ingested (Bollaerts et al., 2008). According to Bollaerts et al. (2008), human feeding trials and epidemiological data taken from outbreak studies can be used to model the DR relationships. Each of these methods has disadvantages, for instance, human trials do not include all the variability that there is in real life and they mostly take place for healthy young volunteers who are not good representatives of the total population. On the other hand, epidemiological data taken from outbreak studies are more subjected to uncertainty.

There have been different studies to model the DR relationships of human *Salmonellosis* in the literature. Holcomb et al. (1999) compared six different DR models from the literature to determine which one fit more to all the available data sets. Oscar (2004a) fits the data for 13 strains of *Salmonella* to a three-phase linear model to define Pert distribution in a computer simulation model while Bollaerts et al. (2008) modeled the DR relationship of 20 *Salmonella* outbreaks as discussed by *World Health Organization*. Teunis et al. (2010) also fitted a DR models for infection and illness using a multi-level statistical framework and outbreak data collected from the literature.

Based on the published data (feeding trials and the existed outbreak studies), (Oscar, 2004b) simulated the illness dose of a consumer of *Salmonella* with a PERT distribution with values of 1, 3, and 7 (log CFU) as its minimum, mean, and maximum, respectively. For simplification, he assumes each chicken is consumed by 4 people, one of which consumes all the survived *Salmonella*. Then, for each chicken in an iteration, a value representing the illness dose will be simulated as in (4.101) of Table 4.17. Note that there is a high chance that all pathogens in a contaminated chicken get inactivated in cooking and no CC occurs at preparation and serving, thus the input data for this stage is conditional on the number of survived pathogens (4.99). Finally, for an illness to occur, the dose of consumed *Salmonella* need to exceed the illness dose (4.102).

Table 4.17: Consumption

Description	Distribution/Formula	
Input (incidence)	$i_{in}^{C} = 1$, if $e_{out}^{Se} > 0$, 0, otherwise	(4.99)
Input (extent)	$e_{in}^{C} = e_{out}^{Se}$	(4.100)
Input (Illness dose)	${}^{*}D = 10^{PERT(0,3,7)}$	(4.101)
Output (Illness Occurrence)	$IO = 1 \text{ if } e_{in}^{C} > D, \text{ 0 otherwise}$	(4.102)

* Reference: Oscar (2004b)

4.3 Results

Oscar (2004b) simulated 10,000 iterations to describe his model. He did not have any *Salmonellosis* cases in the 10,000 iterations and increased the number of iterations to 1,000,000. Oscar (2004b) repeated the simulation for four different random seeds. The average over the four simulation runs were computed divided by 40 (4*10) to estimate the *Salmonellosis* cases per 100,000 consumers. These values were taken because it is assumed in this previous work that each chicken is consumed by four people and 10 is derived from 1,000,000/100,000. Most importantly, note that the number of *Salmonellosis* cases per 100,000 consumers is 0.44 in Oscar (2004b).

@RISK is a software that uses Monte Carlo simulation in a Microsoft Excel spreadsheet to perform risk analysis. Based on the defined distributions for a model's inputs, it shows the possible outcomes and tells their occurrence likelihood (Palisade Corporation, 2017). Our model, described in the Tables (4.3)-(4.17), was simulated using @Risk 7.5 with sampling type *Monte Carlo* and a randomly chosen initial seed.

Since we desire to compare the final output to that of Oscar (2004b) and the number of cases of bacterial infection, hospitalization, and death by *Salmonella* in the United States (CDC. Foodborne Diseases Active Surveillance Network (FoodNet), 2014) which represents incidence rate per 100,000 people, we follow the same method. Four rounds of 1,000,000 chickens were simulated by @Risk. The four simulation runs produced results of 68, 73, 64, and 67 *Salmonellosis* cases with an average of 68. This means the number of *Salmonellosis* cases per 100,000 consumers is 1.70. This value is almost four times more than the value of 0.44 in Oscar (2004b).

According to CDC. Foodborne Diseases Active Surveillance Network (FoodNet) (2014), 15.29 incidence per 100,000 people occurred in the United States. Chicken meat is the cause of 4.4% of the *Salmonellosis* cases (Bryan and Doyle, 1995). This means approximately 0.67 (15.29*0.044) *Salmonellosis* cases occur in the United Sates per 100,000 people.

Table 4.1 represents three (7, 68037, and 628831) out of the 1,000,000 simulated chickens for illustrative purposes. Iteration 7 represents a chicken that was not initially contaminated and did not get infected because of CC in any of the stages with possibility of CC (e.g., thorax cleaning and precooling). The consumer of chicken 7 has an illness dose of 1842 MPN which is greater than the MPN of *Salmonella* consumed (0), thus the consumer did not get infected.

Separately, the chicken at iteration 68037 was initially contaminated with a contamination extent of 2.38 CFU which is equal to $240 = 10^{2.38}$ MPN. As discussed in Section 4.2.3, at each iteration the contamination extent (in CFU/chicken unit) gets modified so the total number of *Salmonella* has an integer value. The extent of contamination gets reduced to 2.32 CFU (209 MPN) at scalding because of the thermal inactivation of the hot water in which it comes into contact. Then, none of the other stages changes the number of pathogens until it is bought by the consumer. No thermal abuse occur during the consumer transportation. The total number of *Salmonella* survived after the cooking is 17, however, because of mishandling during preparation and serving another 16 *Salmonella* survive and makes the total number of consumed *Salmonella* equal to 33. The illness dose is 20 for the consumer which means an illness occurs.

Iteration 628830 represents a chicken which was not initially contaminated and did not get infected during the stages before chilling. In the chilling stage, a CC occurs and makes the contamination extent of the chicken 2.40 CFU (252 MPN). This value does not change until bought by the consumer. No thermal abuse occurs during the consumer transportation, but all the *Salmonella* in the chicken gets inactivated during cooking. However, mishandling during preparation and serving of food keep 22 of the pathogens active. Therefore, with an illness dose of 16 an infection occurs.

Table 4.1: Three iterations out of the 1,000,000 iterations

Stage	Output	Reference	Iter. 7	Iter. 68037	Iter. 628831
Initial Contamination	Contaminated?	(4.3)	No	Yes	No
	Contamination extent? (CFU)	(4.4)	0	2.38	0
Slaughtering	Contamination extent? (CFU)	(4.11)	0	2.32	0
Scalding	Contamination extent? (CFU)	(4.18)	0	2.32	0
Defeathering	Contamination extent? (CFU)	(4.25)	0	2.32	0
Evisceration	Contamination extent? (CFU)	(4.32)	0	2.32	0
Thorax Cleaning	CC occurred?	(4.38)	No	-*	No
	CC extent? (CFU)	(4.39)	0	-	0
	Contaminated?	(4.40)	No	Yes	No
	Contamination extent? (CFU)	(4.41)	0	2.32	0
Precooling	CC occurred?	(4.47)	No	-	No
	CC extent? (CFU)	(4.48)	0	-	0
	Contaminated?	(4.49)	No	Yes	No
	Contamination extent? (CFU)	(4.50)	0	2.32	0
Chilling	CC occurred?	(4.58)	No	-	Yes
	CC extent? (CFU)	(4.59)	0	-	2.40
	Contaminated?	(4.60)	No	Yes	Yes
	Contamination extent? (CFU)	(4.61)	0	2.32	2.40
Storage	Contamination extent? (CFU)	(4.68)	0	2.32	2.40
Transportation and Distribution	CC occurred?	(4.74)	No	-	-
	CC extent? (CFU)	(4.75)	0	-	-
	Contaminated?	(4.76)	No	Yes	Yes
	Contamination extent? (CFU)	(4.77)	0	2.32	2.40
Retail	Contamination extent?	(4.81)	0	2.32	2.40
Consumer Transportation	Thermal abused?	(4.84)	No	No	No
	Contamination extent? (CFU)	(4.77)	0	2.32	2.40
Cooking	Contaminated?	(4.91)	No	Yes	Yes
	Survived # of *Salmonella*? (MPN)	(4.90)	0	17	0
Preparation and Serving	Mishandling occurred?	(4.95)	0	1	1
	Survived # of *Salmonella*? (MPN)	(4.94)-(4.96)	0	16	22
	Consumed # of *Salmonella*? (MPN)	(4.98)	0	33	22
	Illness Dose (MPN)	(4.101)	1842	20	16
	Illness Occurrence	(4.102)	No	Yes	Yes

* If a chicken is already contaminated, there is no need for CC outputs

Prevalences of *Salmonella* isolated from chickens sampled at supermarket in 7 different regions in China are shown in Table 4.2. The prevalence percentages have a minimum of 63% (Haizhu District) and a maximum of 82% (Yuexiu District) and the average of 72%.

Table 4.2: Prevalence of *Salmonella* isolated from chicken at supermarkets

Region	Sample Size	Positive number	Positive Rate
Tiana District	13	9	69%
Bayiun District	19	14	74%
Haizhu District	16	10	**63%**
Yuexiu District	11	9	**82%**
liwan District	10	8	80%
nanshan District	12	8	67%
Futian District	4	3	75%
Total	85	61	**72%**

In order to validate the results from the simulations, we need to calculate how many chickens are contaminated at retail stage and compare it to the prevalence average percentage at the supermarkets. The data regarding the prevalence numbers and percentages of chickens obtained from the first 1,000,000 iterations are presented in Table 4.3. 199,971 or 20% of the chickens are initially contaminated. The percentage decreases to 19.95% in scalding stage and then increases in Thorax cleaning to 35.42%. The increase continues at transportation and distribution but remains the same at retail for which the percentage is 65.66%. Given that the average value from the supermarket prevalence is 72% in Table 4.2, 65.66% is a reasonable estimate.

Table 4.3: Contaminated chickens at different stages

Total contaminated chicken	# of contaminated chickens out of 1,000,000	% of contaminated chickens
Initial contaminated	199971	20.00%
Scalding	195341	19.53%
Thorax cleaning	354179	35.42%
Precooling	513715	51.37%
Chilling	561330	56.13%
Transportation and Distribution	656609	65.66%
Retail	656609	65.66%

Sensitivity Analysis

The consumption dose is between 0 and 47 MPN for the first round of 1,000,000 iterations and the average consumption dose among the 68 *Salmonellosis* cases is 21.8 MPN. A comparison between the 68 infected consumer shows that only 3 (4.4%) of cases are infected solely because of the direct consumption of the chicken and not by mishandling it during preparation and serving. The average consumption dose for these three consumers is only 5.3 MPN while it is 22.58 MPN for the other 65 (95.6%) infected consumers. Out of the 22.58 MPN *Salmonella*, 21.11 MPN is obtained from the mishandling during the preparation and serving. This means the number of *Salmonellosis* cases can decrease dramatically if consumers learn to have less handling mistakes during preparation and serving.

The results also shows that 14 out of the 68 *Salmonellosis* cases are from the initially infected chickens and 14 of them are from the chickens contaminated during the transportation and distribution stage by CC. The rest of them got contaminated from CC during the production stages (thorax cleaning, precooling, and chilling). This means these stages require to be considered in order to identify the most effective parameters that can be improved.

In order to reduce the number of infected chickens and the number of *Salmonella* in each chicken, we need to identify which factors have the most impact on the final value of illness occurrence. Figure 4.1, derived from @Risk sensitivity analysis, represents the most effective factors on the mean of illness occurrence. These factors are ranked based on regression coefficients which are calculated by stepwise multiple regression in @Risk. These coefficient represent the relationship between each of the factors and the mean of the output (illness occurrence) and they can be between -1 to $+1$. Value 0 indicates no correlation between the input and output exists while any positive correlation is shown by a positive value. Figure 4.1 represents all the non-zero correlations which are all positive (less than 0.001).

The most important factors are the consumer's illness dose, consumer transportation, and preparation and serving. Chilling, initial contamination, thorax cleaning, transportation and distribution, and precooling are the next inputs which are not controlled by the consumer, hence they can be improved. In the next few tables we demonstrate how changing each of these inputs' parameters affect the final *Salmonellosis* cases.

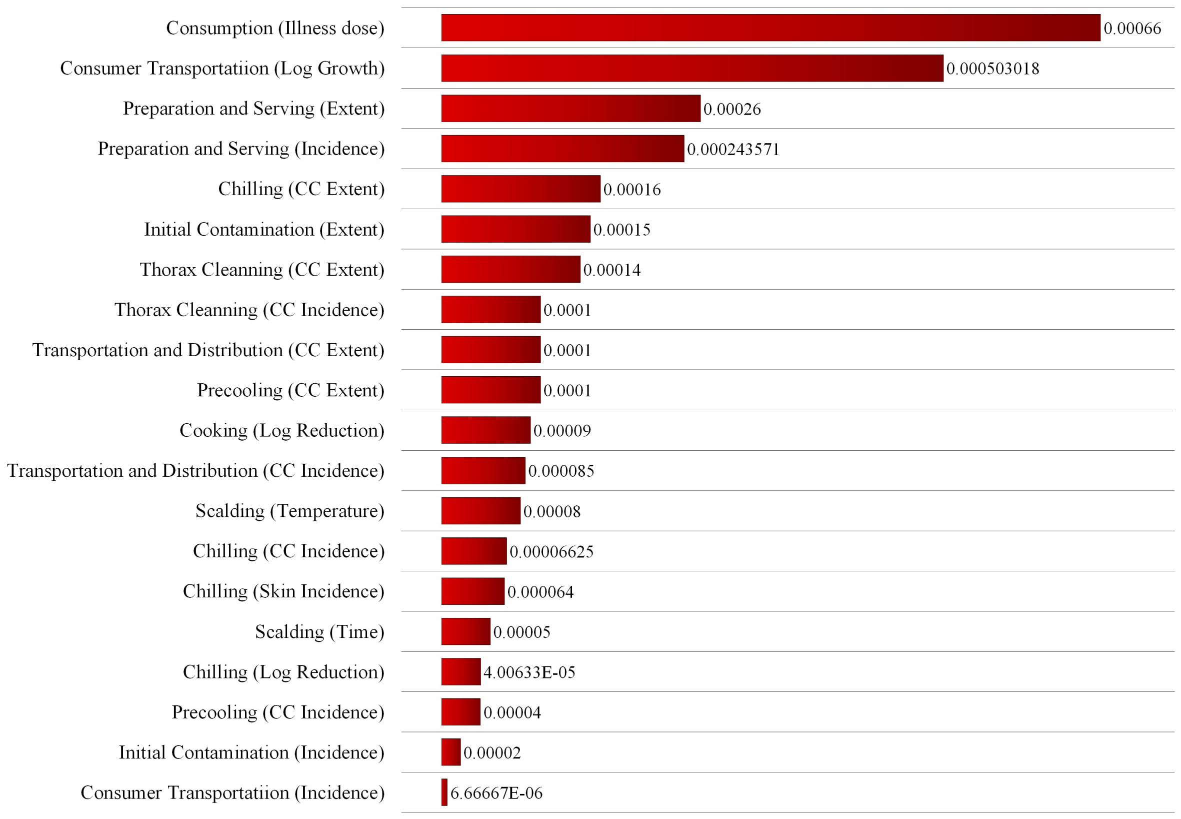

Figure 4.1: Input ranked by effect on the mean of illness occurrence

In Table 4.4, we begin by testing different values of initial contamination incidence probability. Since 10,000 or even 100,000 are too small to represent enough *Salmonellosis* cases we need to simulate 1,000,000 iterations for each scenario that can be effective for our comparisons. As the values in Table 4.4 do not differ much we can conclude that the initial contamination probability does not have a large effect of the total number of illness occurrence.

Table 4.4: Influence of initial incidence probability on the illness occurrence

Probability of initial incidence used in (4.1)	*Salmonellosis* cases in 1,000,000 iterations
0	66
0.2	68
0.4	59
0.6	48
0.8	52
1	57

As discussed in Section 4.2.3.8, chlorine is used in the chilling pool to reduce the number of *Salmonella*. A probability of 0.5 was used to model the skin contamination incident. However, if this value varies, the total number of illness occurrence might change. Table 4.5 has the data regarding different values for this probability. Based on the fact that the *Salmonellosis* cases' values do not vary much, we can conclude that with the current log reduction of chlorine in (4.57), the probability used in (4.56) does not affect the final illness occurrence tremendously.

Table 4.5: Influence of skin contamination incidence (4.56) on the illness occurrence

Probability of skin contamination incidence used in 4.56	*Salmonellosis* cases in 1,000,000 iterations
0.0	86
0.25	63
0.50	68
0.75	53
1.0	31

Thorax cleaning, precooling, chilling, and transportation and distribution are the four stages before retail that are assumed to have potentials for CC. CC incidence rates are 0.2, 0.25, 0.2, and 0.25 for these stages, respectively. In Table 4.6, 4 multipliers (0.5, 1, 2, and 4), are tested to see the influence of CC incidence rates. As shown in the table, the total illness occurrence values does not increase by increasing the CC incidence rate. This indicates the low impact that these values have on the final *Salmonellosis* cases.

Table 4.6: Influence of CC incidence probabilities on the illness occurrence

Ratio compared to original values (0.2, 0.25, 0.2, 0.25)	Probability of CC incidence in (4.38), (4.47), (4.58), (4.74)	*Salmonellosis* cases in 1,000,000 iterations
0.5	0.1, 0.125, 0.1, 0.125	53
1	0.2, 0.25, 0.2, 0.25	68
2	0.4, 0.5, 0.4, 0.5	61
4	0.8, 1, 0.8, 1	58

Table 4.7 represents the illness numbers in 10,000 iteration for 5 different scenarios for the initial contamination and CC extents' parameters. By multiplying the mean and maximum of the CC

extent parameters by 5 different multipliers, we can see that the total illness occurrence changes. The reduction from 68 to 28 indicates that if the average and maximum of the initial contamination and CC extent get cut in half, the total number of *Salmonellosis* cases decreases by more than 50%. Comparisons among all the values in Table 4.7 shows that the initial contamination and CC extent have a great influence on the final number of illness occurrence.

Table 4.7: Influence of initial contamination and CC extent on the illness occurrence

Ratio compared to the original MPN values (0,1.5,2.5)	Initial contamination and CC extent parameters (min, mean, max) in (4.2), (4.39), (4.48), (4.59), (4.75)	*Salmonellosis* cases in 1,000,000 iterations
0.03	(0, 1, 2) CFU/chicken = $(1, 1, 10)$ MPN/chicken	0
0.5	(0, 1.2, 2.2) CFU/chicken $\approx (1, 15, 150)$ MPN/chicken	28
1	(0, 1.5, 2.5) CFU/chicken $\approx (1, 30, 300)$ MPN/chicken	68
2	(0, 1.8, 2.8) CFU/chicken $\approx (1, 60, 600)$ MPN/chicken	408
3	(0, 2, 3) CFU/chicken = $(1, 100, 1000)$ MPN/chicken	960

4.4 Conclusion and Future Work

This chapter details the creation of a Quantitative Risk Assessment Model (QRAM) that attempts to assess the risk of *Salmonellosis* cases caused by contaminated chicken broiler produced in Chinese companies. The work was done in collaboration with researchers in biological engineering, poultry science, and numerous companies and universities throughout China.

To our knowledge, all the previous QRAMs regarding *Salmonella* in chicken, targeted for human consumption, consider a pathway at retail and after it is purchased by a consumer, but our model considered all the unit operations of the production and distribution. The QRAM is informed by data collected from Chinese poultry producers since Fall 2016, published data, and predictive models for growth/reduction of *Salmonella* at each stage. The model made use of @Risk that is used to simulate 1,000,000 iterations representing 1,000,000 chickens and aimed to estimate the final *Salmonella* extent in each chicken. The illness occurrence was then determined by applying a dose-response model defined by Oscar (2004b).

Results shows that the number of *Salmonellosis* cases per 100,000 consumers is 1.70 which is 4 times more than the value obtained in Oscar (2004b). Although, 95.6% of the *Salmonellosis* cases are caused by consumers mishandling during the chicken preparation and serving, sensitivity analysis demonstrated that by improving the production operations and the transportation and distribution parameters regarding the extent of contamination, final number of *Salmonellosis* cases can be reduced.

Furthermore, to evaluate the quality of the proposed model, a comparison between prevalence incidence of contaminated chickens at retail in our model and the real data derived from samples taken from multiple supermarkets in 6 regions in China was performed. A close estimate of the prevalence at retail was obtained, however, most of the input data regarding the extent of contamination/cross-contamination are still required to be updated for a better risk assessment.

As the first step of the future study, we can name updating all the data regarding contamination extent, CC incidence and extent for a better risk assessment. Also, new surveys representing Chinese consumers' behavior and a specific DR model for Chinese people can assist the model to better estimate the final *Salmonellosis* cases.

Although this model is designed specifically for the supply chain in Chinese companies, it is flexible to model other supply chains as well. To this end, all the input data is required to be specifically defined for the new pathway. Furthermore, this research is a good starting point for developing a more comprehensive QRAM for *Salmonella* in chicken for a *farm-to-fork* pathway.

Bibliography

Bollaerts, K., Aerts, M., Faes, C., Grijspeerdt, K., Dewulf, J., and Mintiens, K. (2008). Human salmonellosis: Estimation of dose-illness from outbreak data. *Risk Analysis*, 28(2):427–440.

Brown, M. H., Davies, K. W., BILLON, C. M.-P., Adair, C., and McCLURE, P. J. (1998). Quantitative microbiological risk assessment: principles applied to determining the comparative risk of salmonellosis from chicken products. *Journal of Food Protection*, 61(11):1446–1453.

Bryan, F. L. and Doyle, M. P. (1995). Health risks and consequences of salmonella and campylobacter jejuni in raw poultry. *Journal of Food Protection*, 58(3):326–344.

Carol Beach (2016). Wal-Marts chicken safety program shows significant results.

Cassin, M. H., Lammerding, A. M., Todd, E. C., Ross, W., and McColl, R. S. (1998). Quantitative risk assessment for escherichia coli o157: H7 in ground beef hamburgers. *International journal of food microbiology*, 41(1):21–44.

CDC. Foodborne Diseases Active Surveillance Network (FoodNet) (2014). Foodnet surveillance report for 2014 (final report). *U.S. Department of Health and Human Services*.

China National Center for Food Safety Risk Assessment (2015). Choose the chicken, pay attention to health, prevention of Salmonella food poisoning.

Dickson, J. S. (1989). Enumeration of salmonellae by most-probable-number using the salmonella 1–2 test. *Journal of Food Protection*, 52(6):388–391.

Holcomb, D. L., Smith, M. A., Ware, G. O., Hung, Y.-C., Brackett, R. E., and Doyle, M. P. (1999). Comparison of six dose-response models for use with food-borne pathogens. *Risk Analysis*, 19(6):1091–1100.

Juneja, V. K., Melendres, M. V., Huang, L., Gumudavelli, V., Subbiah, J., and Thippareddi, H. (2007). Modeling the effect of temperature on growth of salmonella in chicken. *Food microbiology*, 24(4):328–335.

Lammerding, A. M. and Fazil, A. (2000). Hazard identification and exposure assessment for microbial food safety risk assessment. *International journal of food microbiology*, 58(3):147–157.

Li, Y., Kidd, M., Kent, J., Raiwater, C., Liao, M., Ding, H., Ying, Y., Wang, M., and Qiao, X. (July 2016). Poultry excellence in china: In-field tests and risk assessment of salmonella contamination and fluoroquinolones residue for poultry supply chains. *University of Arkansas Technical Paper*.

Mulder, N.-d. (2011). Crossroads for growth: The international poultry sector towards 2020. *Utrecht: Rabobank*.

Murphy, R., Duncan, L., Johnson, E., Davis, M., and Smith, J. (2002). Thermal inactivation d- and z-values of salmonella serotypes and listeria innocua in chicken patties, chicken tenders, franks, beef patties, and blended beef and turkey patties. *Journal of food protection*, 65(1):53–60.

Murphy, R., Marks, B., Johnson, E., and Johnson, M. (1999). Inactivation of salmonella and listeria in ground chicken breast meat during thermal processing. *Journal of Food Protection*, 62(9):980–985.

Nutrena (2017). Types of Poultry.

Oblinger, J. and Koburger, J. (1975). Understanding and teaching the most probable number technique 1. *Journal of Milk and Food technology*, 38(9):540–545.

Oscar, T. (1998). The development of a risk assessment model for use in the poultry industry. *Journal of food safety*, 18(4):371–381.

Oscar, T. (2003). Comparison of predictive models for growth of parent and green fluorescent protein–producing strains of salmonella. *Journal of food protection*, 66(2):200–207.

Oscar, T. (2004a). Dose-response model for 13 strains of salmonella. *Risk Analysis*, 24(1):41–49.

Oscar, T. (2006). Validation of a tertiary model for predicting variation of salmonella typhimurium dt104 (atcc 700408) growth from a low initial density on ground chicken breast meat with a competitive microflora. *Journal of food protection*, 69(9):2048–2057.

Oscar, T. P. (2002). Development and validation of a tertiary simulation model for predicting the potential growth of salmonella typhimurium on cooked chicken. *International Journal of Food Microbiology*, 76(3):177–190.

Oscar, T. P. (2004b). A quantitative risk assessment model for salmonella and whole chickens. *International journal of food microbiology*, 93(2):231–247.

Oscar, T. P. (2009). General regression neural network and monte carlo simulation model for survival and growth of salmonella on raw chicken skin as a function of serotype, temperature, and time for use in risk assessment. *Journal of food protection*, 72(10):2078–2087.

Oscar, T. P. (2011). Development and validation of a predictive microbiology model for survival and growth of salmonella on chicken stored at 4 to 12 c. *Journal of food protection*, 74(2):279–284.

Palisade Corporation (2017). @RISK 5.x Tutorials.

Pan, C. (2013). Can chinas poultry move out of porks shadow. *Still on the Road to Industrialization,(Utrecht: Rabobank, 2013)*, 5.

Richard Lawley (2013). Salmonella.

Rosenquist, H., Nielsen, N. L., Sommer, H. M., Nørrung, B., and Christensen, B. B. (2003). Quantitative risk assessment of human campylobacteriosis associated with thermophilic campylobacter species in chickens. *International journal of food microbiology*, 83(1):87–103.

Stopforth, J., Mai, T., Kottapalli, B., and Samadpour, M. (2008). Effect of acidified sodium chlorite, chlorine, and acidic electrolyzed water on escherichia coli o157: H7, salmonella, and listeria monocytogenes inoculated onto leafy greens. *Journal of food protection*, 71(3):625–628.

Surkiewics, B., Johnston, R., Moran, A., and GW, K. (1969). A bacteriological survey of chicken eviscerating plants. *Food Technol*, pages 80–85.

Teunis, P. F., Kasuga, F., Fazil, A., Ogden, I. D., Rotariu, O., and Strachan, N. J. (2010). Dose–response modeling of salmonella using outbreak data. *International journal of food microbiology*, 144(2):243–249.

United States Department of Agriculture Agricultural Research Service (2017). Growth factors for selected bateria.

Waldroup, A. (1996). Contamination of raw poultry with pathogens1. *World's Poultry Science Journal*, 52(1):7–25.

Whiting, R. C. and Buchanan, R. L. (1997). Development of a quantitative risk assessment model for salmonella enteritidis in pasteurized liquid eggs. *International Journal of Food Microbiology*, 36(2-3):111–125.

Whittemore, A. (1993). Research note: a modified most probable number technique to enumerate total aerobes, enterobacteriaceae, and salmonella on poultry carcasses after the whole carcass rinse procedure. *Poultry science*, 72(12):2353–2357.

World Health Organization (2002). *Risk assessments of Salmonella in eggs and broiler chickens*, volume 2. Food & Agriculture Org.

World Health Organization (2003). *Hazard characterization for pathogens in food and water: guidelines*. Number 3. Food & Agriculture Org.

World Health Organization and others (2000). Overcoming antimicrobial resistance. *Overcoming antimicrobial resistance.*

Worldometers (2017). Countries in the world by population.

Yang, B., Qu, D., and Shen, Jinling, e. (2010). Resistance to salmonella and related genes in food-borne in shaanxi province. *Journal of Biology*, (6):788–796.

Zhijian, C. (2013). Shengnong development depth report: the amount of price increases, profit cycle reversed. *Wuhan: Changjiang Securities*, 3(38).

Appendix

4.A Quantitative Risk Assessment Model Information

Table 4.A.1: Quantitative Risk Assessment Model

Description	Distribution/Formula
Initial Contamination	
Input (incidence)	$i_{in}^{IC} = Binomial(1, 0.2)$
Input (extent)	$e_{in}^{IC} = Pert(0, 1.15, 2.5)$
Output (incidence)	$i_{out}^{IC} = i_{in}^{IC}$
Output (extent)	$e_{out}^{IC} = e_{in}^{IC} * i_{in}^{IC}$
Slaughtering	
Input (incidence)	$i_{in}^{Sl} = i_{out}^{IC}$
Input (extent)	$e_{in}^{Sl} = e_{out}^{IC}$
Input (temperature)	$Discrete(\{18, 25, 33\}, \{0.25, 0.5, 0.25\})$
Input (time)	$PERT(20, 40, 60)$
Input (extent log growth)	$d = 0$
Output (incidence)	$i_{out}^{Sl} = i_{in}^{Sl}$
Output (extent)	$e_{out}^{Sl} = e_{in}^{Sl} + d * i_{in}^{Sl}$
Scalding	
Input (incidence)	$i_{in}^{Sc} = i_{out}^{Sl}$
Input (extent)	$e_{in}^{Sc} = e_{out}^{Sl}$
Input (temperature)	$t_1 = PERT(50, 57.5, 65)$
Input (time)	$t_2 = PERT(0.2, 0.4, 0.7)$
Input (extent log reduction)	$d = t_2 / 10^{-0.1314 * t_1 + 8.6599}$
Output (incidence)	$i_{out}^{Sc} = i_{in}^{Sc}$
Output (extent)	$e_{out}^{Sc} = e_{in}^{Sc} - d * i_{in}^{Sc}$
Defeathering and Rinsing	
Input (incidence)	$i_{in}^{DR} = i_{out}^{Sc}$
Input (extent)	$e_{in}^{DR} = e_{out}^{Sc}$
Input (temperature)	$t_1 = PERT(10, 15, 20)$
Input (time)	$t_2 = PERT(0.2, 0.4, 1)$
Input (extent log growth)	$d = 0$
Output (incidence)	$i_{out}^{DR} = i_{in}^{DR}$
Output (extent)	$e_{out}^{DR} = e_{in}^{DR} + d * i_{in}^{DR}$

Table 4.A.2: Quantitative Risk Assessment Model (continued)

Description	Distribution/Formula
Evisceration	
Input (incidence)	$i_{in}^{Ev} = i_{out}^{DR}$
Input (extent)	$e_{in}^{Ev} = e_{out}^{DR}$
Input (temperature)	$t_1 = PERT(10, 15, 20)$
Input (time)	$t_2 = PERT(1, 1.5, 2)$
Input (extent log growth)	$d = 0$
Output (incidence)	$i_{out}^{Ev} = i_{in}^{Ev}$
Output (extent)	$e_{out}^{Ev} = e_{in}^{Ev} + d * i_{in}^{Ev}$
Thorax Cleaning	
Input (incidence)	$i_{in}^{TC} = i_{out}^{Ev}$
Input (extent)	$e_{in}^{TC} = e_{out}^{Ev}$
Input (temperature)	$t_1 = PERT(5, 10, 15)$
Input (time)	$t_2 = PERT(0.2, 0.5, 0.8)$
Input (extent log reduction)	$d = 0$
Input (CC incidence)	$i_{CC} = Bernoulli(0.2)$
Input (CC extent)	$e_{CC} = PERT(0, 1.5, 2.5)$
Output (incidence)	$i_{out}^{TC} = max\{i_{in}^{TC}, i_{CC}\}$
Output (extent)	$e_{out}^{TC} = i_{in}^{TC} * (e_{in}^{TC} - d) + (1 - i_{in}^{TC}) * i_{CC} * e_{CC}$
Precooling	
Input (incidence)	$i_{in}^{Pr} = i_{out}^{TC}$
Input (extent)	$e_{in}^{Pr} = e_{out}^{TC}$
Input (temperature)	$t_1 = PERT(6, 7, 8)$
Input (time)	$t_2 = PERT(5, 7, 10)$
Input (extent log reduction)	$d = 0$
Input (CC incidence)	$i_{CC} = Bernoulli(0.2)$
Input (CC extent)	$e_{CC} = PERT(0, 1.5, 2.5)$
Output (incidence)	$i_{out}^{Pr} = max\{i_{in}^{Pr}, i_{CC}\}$
Output (extent)	$e_{out}^{Pr} = i_{in}^{Pr} * (e_{in}^{Pr} - d) + (1 - i_{in}^{Pr}) * i_{CC} * e_{CC}$

Table 4.A.3: Quantitative Risk Assessment Model (continued)

Description	Distribution/Formula
Chilling	
Input (incidence)	$i_{in}^{Ch} = i_{out}^{Pr}$
Input (extent)	$e_{in}^{Ch} = e_{out}^{Pr}$
Input (temperature)	$t_1 = PERT(0,1,2)$
Input (time)	$t_2 = PERT(25,30,35)$
Input (chlorine density in ppm)	$ch = Uniform(20,70)$
Input (skin contamination incident)	$s = Bernoulli(0.5)$
Input (extent log reduction)	$d = PERT(0,0.3,2.1)$
Input (CC incidence)	$i_{CC} = Bernoulli(0.2)$
Input (CC extent)	$e_{CC} = PERT(0,1.5,2.5)$
Output (incidence)	$i_{out}^{Ch} = max\{i_{in}^{Ch}, i_{CC}\}$
Output (extent)	$e_{out}^{Ch} = i_{in}^{Ch} * (e_{in}^{Ch} - d) + (1 - i_{in}^{Ch}) * i_{CC} * e_{CC}$
Storage	
Input (incidence)	$i_{in}^{St} = i_{out}^{Ch}$
Input (extent)	$e_{in}^{St} = e_{out}^{Ch}$
Input (temperature)	$t_1 = PERT(-2,0,2)$
Input (time)	$t_2 = PERT(60,600,2880)$
Input (extent log reduction)	$d = 0$
Output (incidence)	$i_{out}^{St} = i_{in}^{St}$
Output (extent)	$e_{out}^{St} = e_{in}^{St} - d * i_{in}^{St}$
Transportation and Distribution	
Input (incidence)	$i_{in}^{TD} = i_{out}^{St}$
Input (extent)	$e_{in}^{TD} = e_{out}^{St}$
Input (temperature)	$t_1 = PERT(-2,0,2)$
Input (time)	$t_2 = PERT(300,600,2880)$
Input (extent log reduction)	$d = 0$
Input (CC incidence)	$i_{CC} = Bernoulli(0.25)$
Input (CC extent)	$e_{CC} = PERT(0,1.5,2.5)$
Output (incidence)	$i_{out}^{TD} = max\{i_{in}^{TD}, i_{CC}\}$
Output (extent)	$e_{out}^{TD} = i_{in}^{TD} * (e_{in}^{TD} - d) + (1 - i_{in}^{TD}) * i_{CC} * e_{CC}$

Table 4.A.4: Quantitative Risk Assessment Model (continued)

Description	Distribution/Formula
Retail	
Retail Input (incidence)	$i_{in}^{Re} = i_{out}^{TD}$
Input (extent)	$e_{in}^{Re} = i_{out}^{TD}$
Output (incidence)	$i_{out}^{Re} = i_{in}^{Re}$
Output (extent)	$e_{out}^{Re} = e_{in}^{Re}$
Consumer Transportation	
Input (incidence)	$i_{in}^{CT} = i_{out}^{Re}$
Input (extent)	$e_{in}^{CT} = i_{out}^{Re}$
Input (thermal abuse incidence)	$T = Bernoulli(0.02)$
Input (extent log growth)	$d = PERT(0.0005, 0.04, 0.15)$
Output (incidence)	$i_{out}^{CT} = i_{in}^{CT}$
Output (extent)	$e_{out}^{CT} = e_{in}^{CT} + d * T$
Cooking	
Input (incidence)	$i_{in}^{Co} = i_{out}^{CT}$
Input (extent)	$e_{in}^{Co} = i_{out}^{CT}$
Input (extent log reduction)	$d = PERT(0.83, 0.81, 96)$
Output (incidence)	$i_{out}^{Co} = i_{in}^{Co}$
Output (extent)	$e_{out}^{Co} = e_{in}^{Co} - d$
Serving	
Input (incidence)	$i_{in}^{Se} = i_{out}^{CT}$
Input (extent)	$e_{in}^{Se} = e_{out}^{CT}$
Input (CC incidence)	$i_{CC} = Bernoulli(0.28)$
Input (CC extent rate)	$R_{CC} = PERT(0.021, 0.057, 0.24)$
Output (incidence)	$i_{out}^{Se} = max\{i_{in}^{Se}, i_{CC}\}$
Output (extent in MPN)	$e_{out}^{Se} = i_{CC} * \lfloor 10^{e_{in}^{Se}} * R_{CC} \rfloor + \lfloor 10^{e_{out}^{CT}} \rfloor$
Consumption	
Input (incidence)	$i_{in}^{C} = 1$, if $e_{out}^{Se} > 0$, 0, otherwise
Input (extent)	$e_{in}^{C} = e_{out}^{Se}$
Input (Illness dose)	$D = 10^{PERT(0,3,7)}$
Output (Illness Occurrence)	$IO = 1$ if $e_{in}^{C} > D$, 0 otherwise

4.B Certification of Student Work

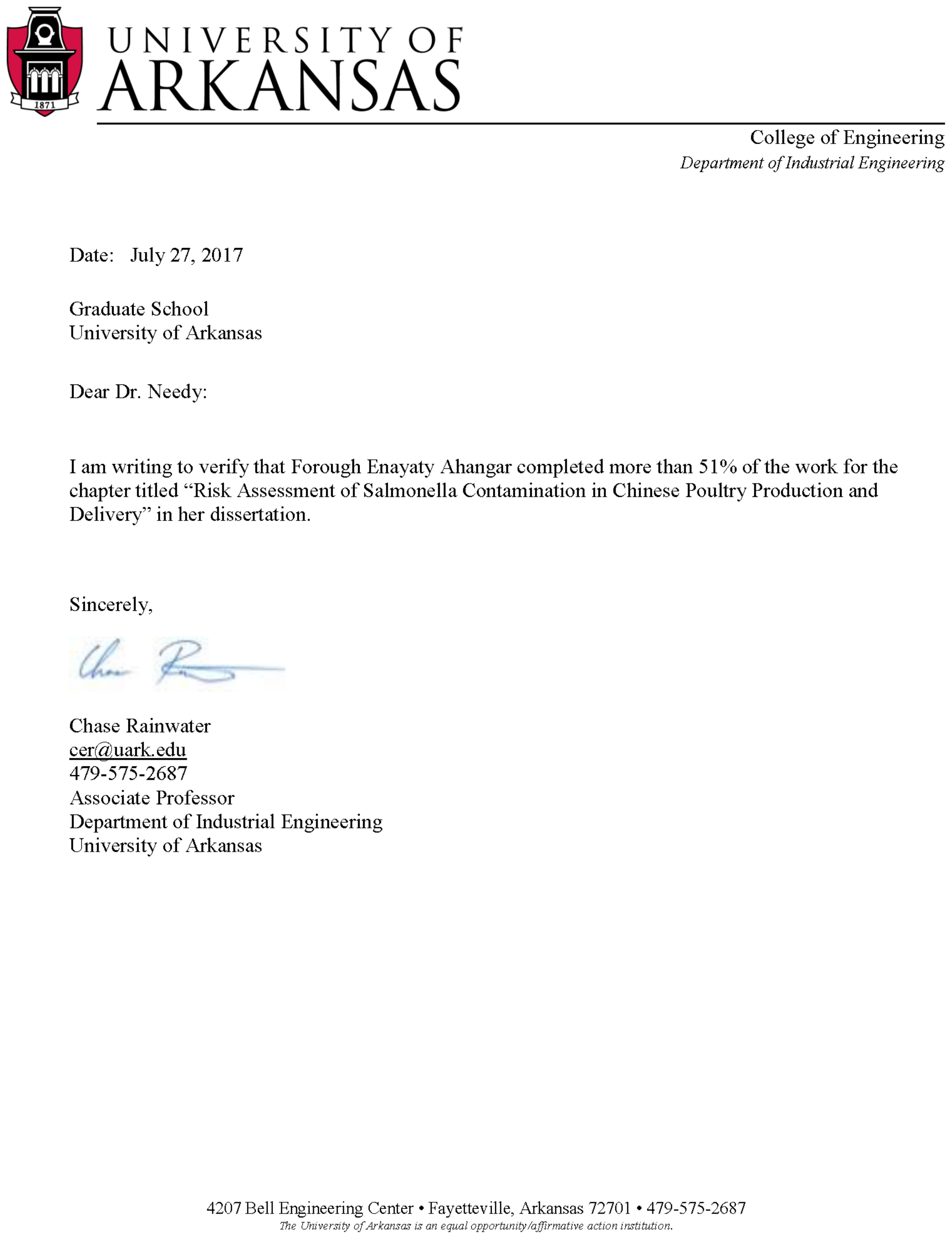

UNIVERSITY OF ARKANSAS

College of Engineering
Department of Industrial Engineering

Date: July 27, 2017

Graduate School
University of Arkansas

Dear Dr. Needy:

I am writing to verify that Forough Enayaty Ahangar completed more than 51% of the work for the chapter titled "Risk Assessment of Salmonella Contamination in Chinese Poultry Production and Delivery" in her dissertation.

Sincerely,

[illegible]

Chase Rainwater
cer@uark.edu
479-575-2687
Associate Professor
Department of Industrial Engineering
University of Arkansas

4207 Bell Engineering Center • Fayetteville, Arkansas 72701 • 479-575-2687
The University of Arkansas is an equal opportunity/affirmative action institution.

5. Conclusion and Future Work

In this dissertation, three different security scenarios were modeled and solution methodologies were proposed to address each problem. Chapter 2 presented a logic-based decomposition (LBD) approach for a class of dynamic maximum flow network interdiction problems in which interdiction activities must be scheduled in order to minimize the cumulative maximum flow over a finite time horizon. The approach utilized a mixed integer formulation and a constraint programming formulation to form our hybrid decomposition framework. Constraint programming was utilized since it showed to be more efficient to formulate the scheduling aspects of the problem. LBD and traditional mixed-integer programming approach got tested on various small and large instances that were generated based on real data parameters and compared with each other. Computational results suggested that LBD is more efficient in finding solutions for medium to large problem instances when presolver if on and when presolver is off, LBD outperformed MIP for all size of instances. In general it can be concluded that, LBD is comparable to MIP for smaller instances but consistently outperform MIP for large instances.

One of the directions to which this work can be extended is to initialize LBD with a given feasible solution. This solution can be generated by forcing LBD to just remove the first level actors. While this chapter's proposed approach offers better performance for solving large instances, there remain applications for which even larger instances must be solved which makes large-scale heuristics an appropriate avenue of study.

In Chapter 3, we introduced the Clustered Content Interdiction Problem (CCIP) which considers groups of content dispersed across a collection of centers. In this problem, different content is assigned to the centers to ensure availability. Given a content assignment across a collection of available centers, an interdictor attempts to determine which centers to interdict in order to minimize the content availability. An integer program P was formulated to model the problem, which is proven to be NP-complete. Several modified formulations were developed by adding symmetry breaking and other valid inequality constraints, and custom branchings to solve larger problems more efficiently. They also exploit a genetic algorithm as a method to generate a quality solution efficiently. The two best ones were selected for 100 S and M instances to be compared to the original model *P*. The two models showed more efficiency for solving larger instances, however, the improvement is more for S instances.

For future study, a bilevel setting of the problem in cybersecurity context and also generalizations of the matrix interdiction methodologies/approaches to allow for multiple content can be explored.

In Chapter 4, we proposed a novel Quantitative Risk Assessment Model (QRAM) that attempts to quantify the risk of microbial poultry contamination across the food supply chain in China. This work was done in collaboration with biological engineering, poultry science and numerous companies and universities throughout China. While all the previous QRAMs regarding *Salmonella* in chicken, considered a pathway after it is purchased by a consumer, our model considered an extensive pathway in the supply chain that starts from the beginning of production line and finishes by food consumption. It aimed to assess the risk of *Salmonellosis* human case per 100,000 consumers. The model made use of @Risk that was used to simulate 1,000,000 iterations representing chickens. The illness occurrence was then determined by applying a does-response model. Results showed that 1.70 cases of *Salmonellosis* occur in per 100,000 consumers which can be reduced to less than 1. Analysis of the results indicated that 95.6% of the *Salmonellosis* cases are caused by consumers mishandling during the chicken preparation and serving. However, sensitivity analysis demonstrated that by improving the production operations and the transportation and distribution parameters regarding the extent of the contamination and cross-contamination, final number of *Salmonellosis* cases can be noticeably reduced.

For future study we can incorporate lab-generated cross-contamination extent and incidence data for an improved risk assessment. Furthermore, new surveys representing consumers' behavior and a specific DR model for Chinese people can lead to a more precise model. This model was designed specifically for the supply chain in Chinese companies, however, it is flexible to model other supply chains. To achieve this goal, all the input data is required to be specifically defined for the new pathway. Furthermore, this research can be seen as a good starting point for developing a more comprehensive QRAM for a *farm-to-fork* pathway.